

Project no.:

608608

Project acronym:

MiReCOL

Project title:

Mitigation and remediation of leakage from geological storage

Collaborative Project

Start date of project: 2014-03-01

Duration: 3 years

D3.4

Brine/water injection as flow diversion option in CO₂ storage operations

Status: definitive

Organisation name of lead contractor for this deliverable:

SINTEF Petroleum

Project co-funded by the European Commission within the Seventh Framework Programme		
Dissemination Level		
PU	Public	X
PP	Restricted to other programme participants (including the Commission Services)	
RE	Restricted to a group specified by the consortium (including the Commission Services)	
CO	Confidential , only for members of the consortium (including the Commission Services)	

Deliverable number:	D3.4
Deliverable name:	Brine/water injection as flow diversion option in CO ₂ storage operations
Work package:	WP3: CO ₂ flow diversion and mobility control within the reservoir
Lead contractor:	SINTEF Petroleum

Status of deliverable		
Action	By	Date
Submitted (Author(s))	Robert Drysdale	21 June 2016
	Sevket Durucan	22 Sept 2016
	Anna Korre	22 Sept 2016
	Bernd Wiese	27 Nov 2016
	Daniel Loeve	02 Dec 2016
Verified (WP-leader)	Robert Drysdale	16 Dec 2016
Approved (Coordinator)	Holger Cremer	17 Jan 2017

Author(s)		
Name	Organisation	E-mail
Robert Drysdale	Sintef Petroleum	robert.drysdale@sintef.no
Sevket Durucan	Imperial College	s.durucan@imperial.ac.uk
Anna Korre	Imperial College	a.korre@imperial.ac.uk
Bernd Wiese	GFZ	wiese@gfz-potsdam.de
Daniel Loeve	TNO	daniel.loeve@tno.nl

Public abstract
<p>This report is part of the research project MiReCOL (Mitigation and Remediation of CO₂ leakage) funded by the EU FP7 programme. Research activities aim at developing a handbook of corrective measures that can be considered in the event of undesired migration of CO₂ in the deep subsurface reservoirs. MiReCOL results support CO₂ storage project operators in assessing the value of specific corrective measures if the CO₂ in the storage reservoir does not behave as expected. MiReCOL focuses on corrective measures that can be taken while the CO₂ is in the deep subsurface. The general scenarios considered in MiReCOL are 1) loss of conformance in the reservoir (undesired migration of CO₂ within the reservoir), 2) natural barrier breach (CO₂ migration through faults or fractures), and 3) well barrier breach (CO₂ migration along the well bore).</p> <p>The MiReCOL project provides analysis of a wide range of possible mitigation and remediation measures for leakage from underground CO₂ storage reservoirs. This report concentrates on the assessing water injection as a remediation measure for unwanted migration of CO₂ within an underground storage reservoir. Four different investigations of water injection remediation have been performed by different partners, mostly by numerical simulation:- i) SINTEF have modelled migration in a portion of the Johansen formation model, three key reservoir to represent 20 sensitivities to the base case; ii) Using a generic model, Imperial College have studied reduction of CO₂ leakage through a sub-seismic fault by means of water injection; iii) GfZ have modelled and analysed a water injection experiment on the Ketzin CO₂ storage field to gain a better understanding of the drainage and imbibition processes, and iv) TNO have modelled 10 alternative scenarios of water injection and CO₂ back-production also using the Johansen model.</p>

TABLE OF CONTENTS

		Page
1	INTRODUCTION	3
2	MITIGATION BY WATER INJECTION IN JOHANSEN (SINTEF).....	5
	2.1 The model used.....	5
	2.2 The leakage site	7
	2.3 Requirements for data.....	10
	2.4 Results generated	11
	2.4.1 Output required	11
	2.4.2 Standard injection and remediation procedure	11
	2.4.3 Results.....	12
	2.5 Discussion.....	15
	2.5.1 Migration pattern	15
	2.5.2 Total leakage reduction.....	17
	2.5.3 Longevity of remediation.....	19
	2.5.4 Spatial extent of remediation	22
	2.5.5 Effect of reservoir depth on free gas.....	24
	2.6 Conclusions.....	25
3	BRINE INJECTION AS A FLOW DIVERSION OPTION (IMPERIAL COLLEGE)	27
	3.1 Reservoir model description	27
	3.1.1 Structural and geological model	27
	3.1.2 Dynamic properties of the reservoir model	29
	3.1.3 Modelling of CO ₂ flow diversion with brine injection	30
	3.2 CO ₂ Injection and leakage detection.....	31
	3.2.1 Scenario 1: Fault at 1km away from the CO ₂ injection well.....	31
	3.2.2 Scenario 2: Fault at 2km from the CO ₂ injection well	32
	3.2.3 Scenario 3: Fault at 3km from the CO ₂ injection well	33
	3.3 CO ₂ leakage remediation using brine injection	34
	3.3.1 Scenario 1: Fault at 1km from the CO ₂ injection well	34
	3.3.2 Scenario 2: Fault at 2km from the CO ₂ injection well	37
	3.3.3 Scenario 3: Fault at 3km from CO ₂ Injection well.....	40
	3.4 Discussion and conclusions	45
4	BRINE/WATER INJECTION AS A FLOW DIVERSION OPTION IN A CO ₂ STORAGE OPERATION (GFZ).....	49

4.1	Technical setup	50
4.2	Assessment of remediation impact	52
4.3	Multiphase flow simulation	53
4.4	Geoelectrical Monitoring.....	56
4.5	Conclusions	58
5	MITIGATION BY WATER INJECTION AND CO ₂ WITHDRAWAL (TNO)	59
5.1	Introduction	59
5.1.1	Description of the Johansen formation	59
5.2	Method.....	60
5.2.1	Simulator used Schlumberger’s Eclipse 100 black-oil simulator.....	60
5.2.2	Pressure, Volume, Temperature (PVT) data.....	61
5.2.3	Saturation functions and pressure dependent rock properties	62
5.2.4	Initial conditions	63
5.2.5	Well Locations.....	63
5.2.6	Critical scenarios	64
5.3	Results	66
5.3.1	Critical scenario 1	66
5.4	Conclusions	70
5.5	Appendix	70
5.5.1	Remediation scenario 1.....	71
5.5.2	Remediation scenario 2.....	74
5.5.3	Remediation scenario 3.....	77
5.5.4	Remediation scenario 4.....	80
5.5.5	Remediation scenario 5.....	83
5.5.6	Remediation scenario 6.....	86
5.5.7	Remediation scenario 7.....	89
5.5.8	Remediation scenario 8.....	93
5.5.9	Remediation scenario 9.....	97
5.5.10	Remediation scenario 10.....	101
6	SUMMARY AND CONCLUSIONS.....	105
7	REFERENCES	107

1 INTRODUCTION

Carbon capture and storage (CCS) technology involves capturing climate change inducing carbon dioxide emissions from industrial sources (e.g. cement, steel, ammonia production) and fossil fuel based power generation. The separated CO₂ stream is typically transported via a network of pipelines, injected in the subsurface and trapped within the pores of rocks located kilometres underground. The IPCC report on CCS, published in 2005, suggests that CCS could store up to 10 Gt of CO₂ per year when applied globally by 2050.

Many of the sites which are selected for CO₂ storage have held hydrocarbons for millions of years. This suggests that, because of the proven integrity of oil/gas storage, when CO₂ is injected into these formations it will also remain secure for geological timescales. Saline aquifers are also considered as potential CO₂ storage formations. These are not considered as proven storage sites and are likely to be less understood as relevant data may not have been collected. As a result, the possibility that CO₂ could migrate out of these formations needs to be studied carefully and potential leakage mitigation and remediation is an important element of a storage site licensing process according to the EU CCS Directive (2009).

The MiReCOL project provides analysis of a wide range of possible mitigation and remediation measures for leakage from underground CO₂ storage reservoirs. Both existing and new remediation and mitigation techniques are investigated, by means of numerical analysis, laboratory experiments and a field test.

One of the leakage categories considered in MiReCOL is the possibility of unwanted migration of CO₂ within the storage reservoir, i.e. within the storage formation, but escaping due to unforeseen circumstances such as:- a) a local high permeability channel or fractured region, b) an unseen feature in the structural geology, such as an unexpectedly high spill-point, c) an inclined CO₂-water interface due to lateral water flow through the reservoir.

Several remedial measures were identified for this type of migration including:- i) adjustment of the injection strategy, ii) gel or foam injection, iii) water injection and iv) injection of chemicals that react with CO₂ and precipitate it as a solid. This report concentrates on the assessing water injection as a remediation measure.

Four different examples of water injection remediation have been examined by different partners as follows.

- SINTEF have used a portion of the Johansen formation as the basic model with water injection in front of the CO₂ migration plume. The model was then modified to represent the key characteristics of 20 other possible CO₂ storage aquifers.
- Using a generic model, Imperial College have studied reduction of CO₂ leakage through a sub-seismic fault by means of water injection via the well previously used for CO₂ injection.
- GfZ have analysed and modelled a water injection experiment on the Ketzin CO₂ storage field to gain a better understanding of the drainage and imbibition processes.

- TNO also used the Johansen model to simulate 10 alternative scenarios of water injection and CO₂ back-production as remediation measures

The results of the MiReCOL project will be published both as handbook and as an interactive web-based tool, directed at storage project operators and competent authorities, to provide initial advice on the options available for remediation and mitigation.

2 MITIGATION BY WATER INJECTION IN JOHANSEN (SINTEF)

2.1 The model used

The reservoir selected for this study was a segment of the Johansen formation in the Norwegian North Sea, in the vicinity of the Troll field. This is part of a large aquifer which has been used several times as the subject for studies on CO₂ Geological Storage. The model was kindly made available to the project by Gassnova.

The Johansen formation is in the Jurassic Dunlin Group and consists of east to west dipping sandstone layers, from approximately 1600m to 2400m. The formation is bounded to the north and west by bounding faults and the sandstone layers pinch out to the eastern side, leaving the southern boundary potentially open. There are also several large vertical faults running north – south within the formation, which are considered to be sealing.

Only the extreme north-western corner of the formation is used for this study, with the open boundary conditions only to the south (see Figure 1). The overall dimensions of the model are 68km west-east, 250km north-south with thickness varying between approximately 100 to 500m. The formation is modelled by 7 layers of alternating sandstone and shale, the latter being sealing, but the shale layers pinches out towards the eastern and northern end of the reservoir. Grid blocks were used of approximate dimensions $\Delta x=500\text{m}$, $\Delta y= 500\text{m}$, $\Delta z=12\text{m}$ in the sandstone layers.

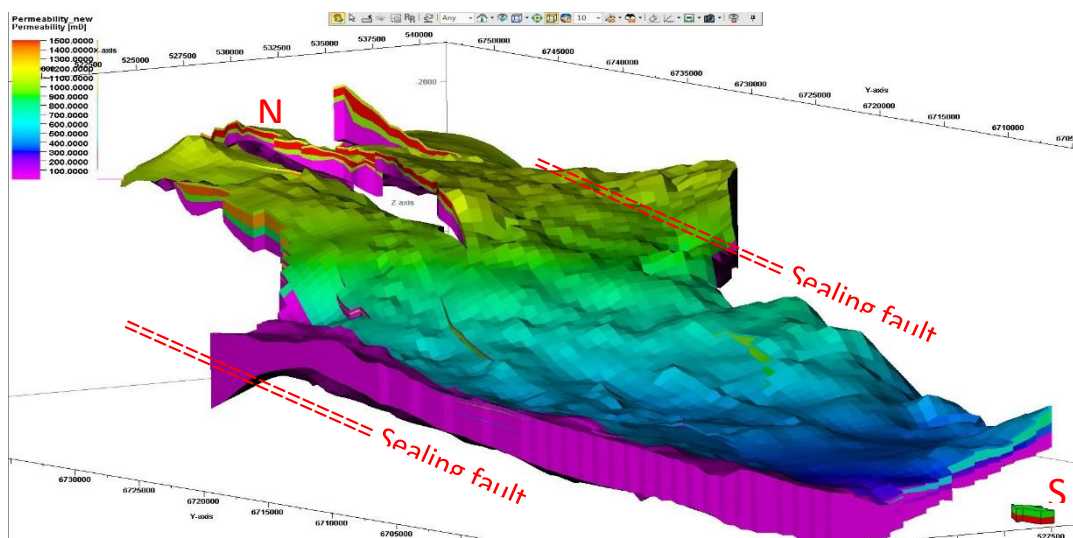


Figure 1. The part of the Johansen aquifer modelled..

The porosity and permeability distributions for the top of the formation are shown in Figure 2 and Figure 3. In the area used for leakage testing the average porosity is 0.24, permeability is 1125 mD and the depth varied from 2100 to 2200 m.

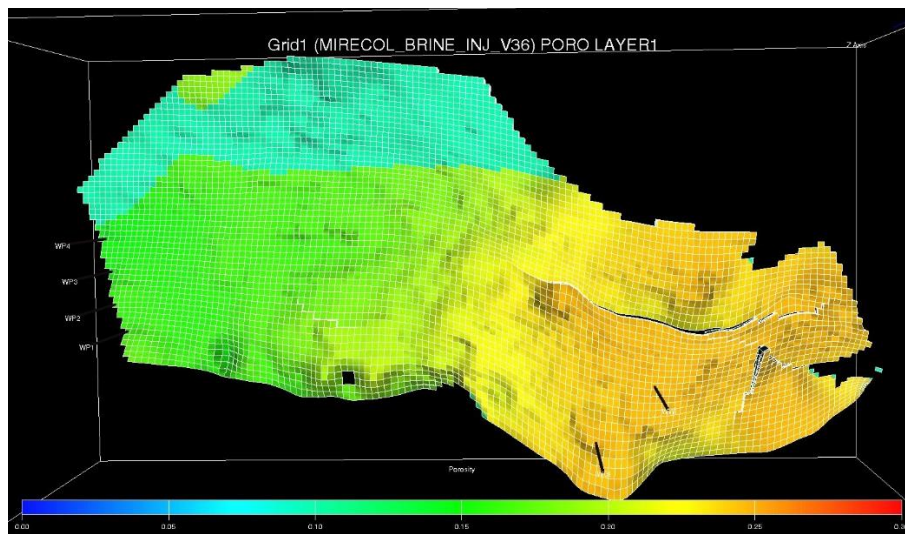


Figure 2. Porosity distribution in top layer of model.

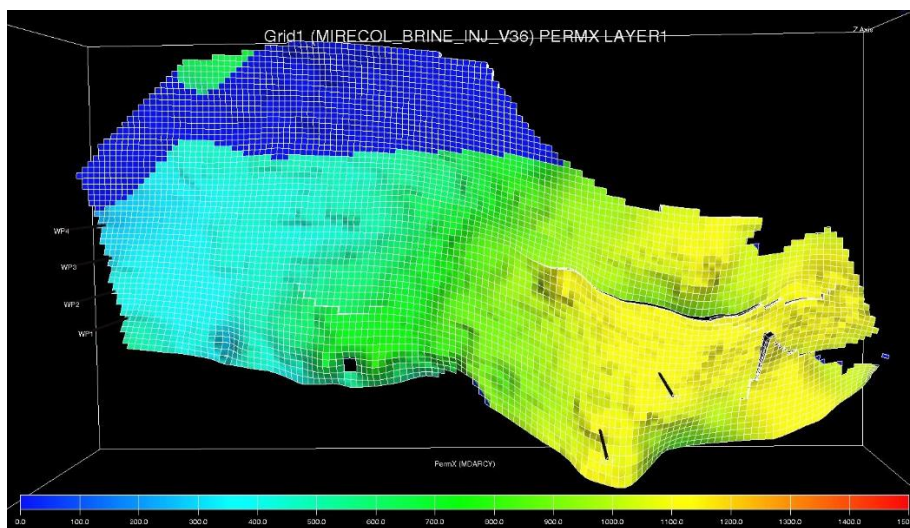


Figure 3. Permeability distribution in the top layer of the model.

A dynamic model was developed in Eclipse 100, using oil and gas fluid representations for pure water and CO₂ respectively. This provides a simple method to represent the dissolution of the CO₂ in water.

The dynamic properties were largely drawn from those previously developed for the MatMoRA project Ref <http://www.sintef.no/projectweb/matmora/downloads/johansen>

The open boundary at the south of the model was represented by 4 water production wells, which were operated only during periods of injection, at a total equivalent rate to the injection rate (at reservoir conditions).

A bottom-hole pressure upper limit was imposed on all injectors, representative of the fracture safety limit. This was set at 75% of the lithostatic pressure, which was never reached.

All layers in the model were used initially for injection and production, but it was evident that all the injected CO₂ floated up to the top layer very quickly inside a small radius. Therefore the procedure was adjusted to inject into and produce from only the top layer to improve speed and ease of monitoring.

2.2 The leakage site

First the model was explored to find a good site to simulate leakage. Rather than looking for a possibly non-existent spill-point, effort was concentrated on finding a location offering good controlled migration. An imaginary CO₂ injection well would mimic the instigation of leakage and thereafter the leaking CO₂ would migrate by gravity along a shallow ridge structure trending upwards in a known direction. The mitigating effect of water injection could be studied by introducing an injection well at a suitable place along the leakage path.

CO₂ was injected into several different locations in the reservoir to look for the most suitable site, as illustrated in Figure 4 to Figure 8. Location (c) in Figure 6 was chosen as the best, offering a reasonably concentrated migration path, a good upward trend to encourage migration and a "collection area" limited by faults.

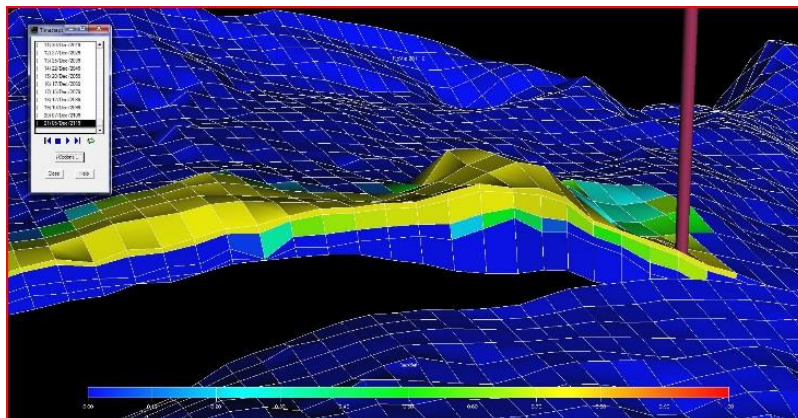


Figure 4. Location (a) looking eastward.

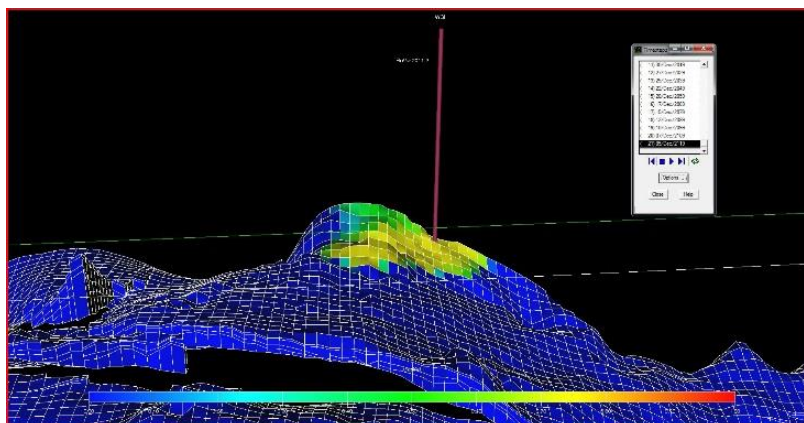


Figure 5. Location (b) looking eastward.

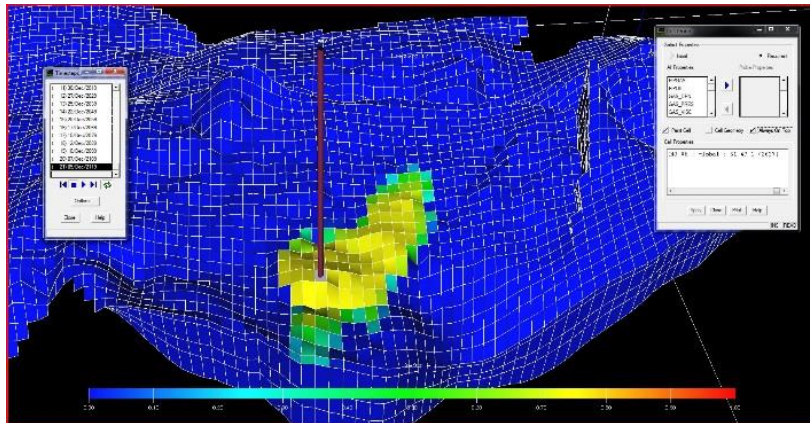


Figure 6. Location (c) looking westward.

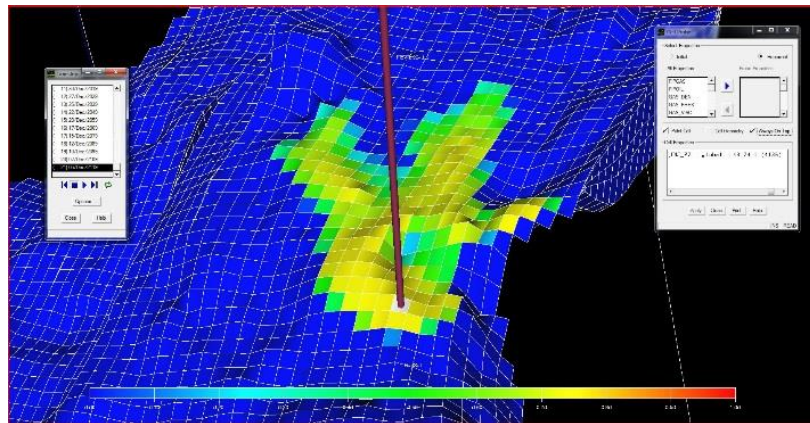


Figure 7. Location (d) looking northward.

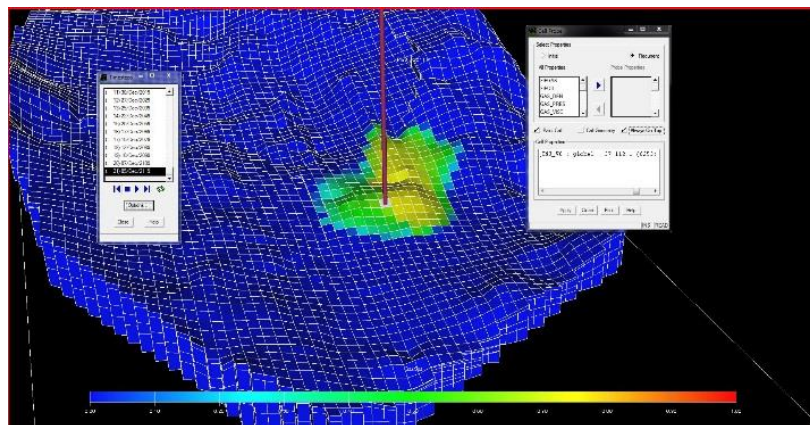


Figure 8. Location (e) looking northward.

A low-level view upwards along the path of leakage is shown in Figure 9.

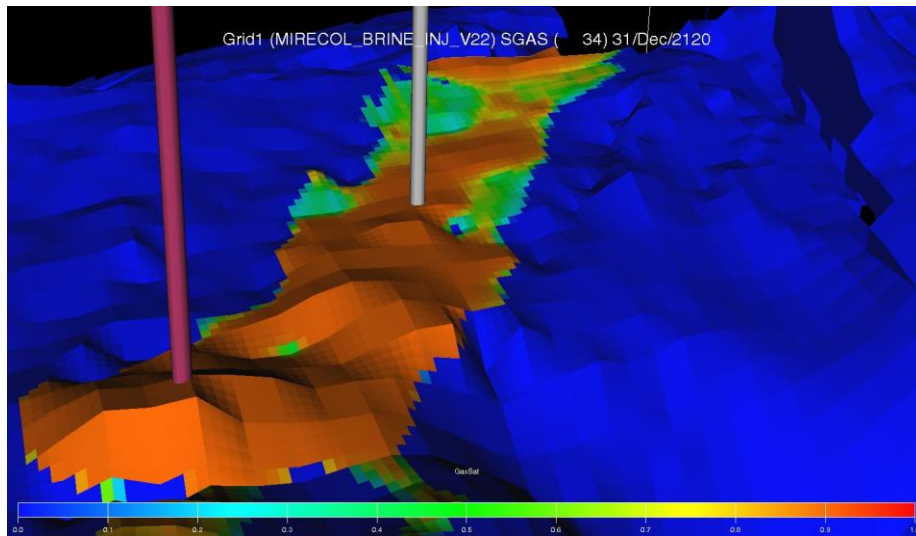


Figure 9. Leakage path along selected location.

In order to measure the leakage occurring, a "fluids in place numerical region" or FIPNUM was defined in the Eclipse model downstream of the water injection well, from a boundary perpendicular to the direction of migration and passing through the injection well. This is illustrated in Figure 10 . It was possible to obtain the total volume of CO₂ both free and dissolved, within this numerical region, thus quantifying the total leakage.

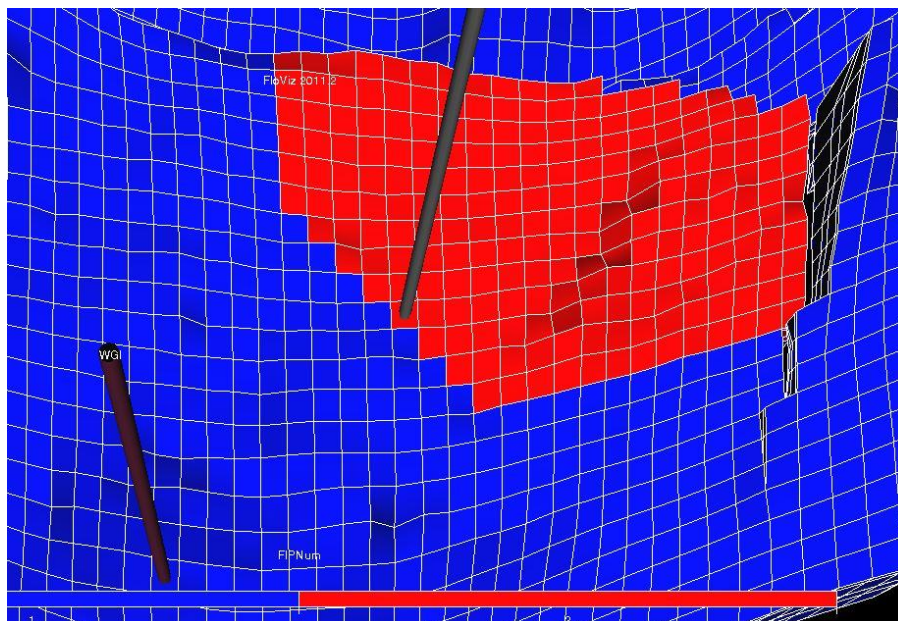


Figure 10. Location of FIPNUM (in red).

2.3 Requirements for data

The summary deliverable from the MiReCOL Project will be a web-tool to allow comparison of different remediation methods for a user's specific underground CO₂ leakage problem. The researchers working on each remediation method will generate data for this tool and will select the most relevant parameters against which they will generate performance data. For brine injection, Sintef considered the following parameters to be the most important:

- 1) CO₂ injection rate. Actually the CO₂ leakage rate is the most interesting parameter, but this is difficult to estimate in the case of real leakage, so injection rate is taken as the next-best approximation.
- 2) Average permeability, which controls the migration of CO₂ and water. This is also considered to be related to porosity.
- 3) Reservoir depth (reflecting reservoir pressure, but more obtainable), which affects the fluid properties.

In order to generate a representative range for these parameters the NPD's "CO₂ Storage Atlas of the Norwegian Continental Shelf" was used as a source (Norwegian Petroleum Directorate, 2014). In this the main aquifers with potential for CO₂ storage on the NCS are identified, together with their basic data. These data were grouped to provide a smaller number of cases for the present work (Table 1).

Table 1. List of reservoir cases considered.

CO ₂ Inj rate (t/yr)	K (mD)	Depth (m)	Case
5.0E+05	200	1800	v52
		2200	v49
	500	1700	v46
		2400	v43
	1000	1050	v40
		1650	v37
1.0E+06	1125	2200	v35
		200	1800
	2200		v50
		500	1700
	2400		v44
		1000	1050
1650	v38		
	1125	2200	v34
3.0E+06		200	1800
	2200		v51
		500	1700
	2400		v45
		1000	1050
	1650		v39
1125		2200	v36

2.4 Results generated

2.4.1 Output required

The outputs required for the web-tool for each leakage case are listed below:

- a) Likelihood of success – such a probability could not be estimated from the numerical simulations performed, but instead data was generated on the total reduction of leakage achieved by the water injection.
- b) Economic cost of implementing the remediation process. Typically this would include the total cost of planning, designing, drilling and completing a water injection well, including the water injection system and a rig or vessel to support these operations. Since SINTEF has no access to such cost data, typical costs will have to be suggested by the partner Operating Companies within the project.
- c) Response time – this is the time needed to implement a new water injection well once leakage has been detected. Lacking any practical data, this assumed to be one year in all cases.
- d) Longevity – how long the injected water restrains or significantly reduces the migration of the CO₂ plume.
- e) Spatial extent – this was taken to be the width of the cross-section of the CO₂ plume which is blocked by the injected water.

2.4.2 Standard injection and remediation procedure

It proved to be impossible to define a standard procedure for the leakage and remediation scenario which would satisfy all requirements, so the best compromise had to be used. The main alternatives identified were as follows:-

- a) To inject CO₂ at a fixed location for a constant 50 years, then to start injecting water one year later, for one year at a second fixed location along the migration path. This has the major disadvantage that the CO₂ plume extends to varying degrees depending on the parameters used and therefore is in a different position relative to the fixed water injector for each case.
- b) As (a), but the water injection well would be placed just ahead of the CO₂ plume at a fixed date. The disadvantages here were that the volume of the FIPNUM would vary, the topography around the water injector would vary and not least considerable effort would be required to redefine the FIPNUM for each case.
- c) As (a), but the duration of CO₂ injection would be varied to stop one year before the CO₂ plume reaches the water injection well. In this case the total amount of CO₂ injected would vary between cases, but since it was intended to use percentage total leakage reduction as the measure of effectiveness of remediation, this was considered to be best alternative.

Therefore the standard procedure used for generating all results was as follows:-

- i. Inject CO₂ for up to 250 years without any water injection, in order to determine when the CO₂ plume reaches the location of the water injection well, i.e. at x years.

- ii. Repeat the no-water injection simulation with initial CO₂ injection for x-1 years, i.e. allowing 1 year implementation time before starting water injection.
- iii. Water injection for 1 year, which is then stopped permanently. A standard water injection rate of 5000 sm³/d is used. A water injection period of only 1 year was adopted since it was clear that this remediation method has only a very short-term effect on migration of the CO₂.
- iv. The injected CO₂ is allowed to migrate further for the remainder of 510 years.

2.4.3 Results

For each of the 21 cases (Table 2) two main simulations were run for each case of reservoir properties, the first without any water injection, the second with water injection according to the standard procedure in Section 2.4.2.

The final volume of CO₂ in the FIPNUM was used as a measure of the leakage. The difference in these leakage values for the "no water injection" and the "water injection" sub-cases quantifies the effect of water injection in reducing CO₂ leakage. The resulting values obtained for all cases are given in Table 2, as absolute figures and as a percentage of the no water injection result.

In addition the estimated delay in leakage breakthrough obtained by water injection and the estimated lateral extent of the blockage to CO₂ flow are given for each case.

In order to assist analysis, the simulation results in Table 2 were summarised and re-ordered in three ways, according to each of the main parameters, as shown in Table 3, Table 4 and Table 5.

For each main parameter, the cases are ordered into a number of scenarios for comparison.

Table 2 Total CO₂ leakage, delay and extent values obtained from simulations.

Simulation	CO ₂ inj rate (te/yr)	K (mD)	Depth (m)	Water inj. Rate (sm ³ /d)	Total leakage (sm ³)	Final leakage reduction (sm ³)	Final Reductn (%)	Delay in leakage breakthrough (yrs)	Cross section extent (m)
v35e2	5.00E+05	1125	2200	0	8,871,106,610				
v35d2	5.00E+05	1125	2200	5000	8,850,286,082	-20,820,528	-0.23 %	1.8	700
v34d2	1.00E+06	1125	2200	0	12,265,447,757				
v34e2	1.00E+06	1125	2200	5000	12,219,293,672	-46,154,085	-0.38 %	1.4	1400
v36f2	3.00E+06	1125	2200	0	20,475,826,347				
v36g2	3.00E+06	1125	2200	5000	20,413,727,195	-62,099,152	-0.30 %	1.7	1400
v37e3	5.00E+05	1000	1650	0	7,559,248,729				
v37f3	5.00E+05	1000	1650	5000	7,531,059,577	-28,189,152	-0.37 %	1.6	1400
v38c2	1.00E+06	1000	1650	0	10,331,227,696				
v38d2	1.00E+06	1000	1650	5000	10,296,207,585	-35,020,111	-0.34 %	1.7	1400
v39c2	3.00E+06	1000	1650	0	18,353,103,572				
v39d2	3.00E+06	1000	1650	5000	18,289,216,449	-63,887,123	-0.35 %	1.6	1400
v40e2	5.00E+05	1000	1050	0	5,402,622,347				
v40f2	5.00E+05	1000	1050	5000	5,376,643,715	-25,978,632	-0.48 %	1.5	1400
v41c2	1.00E+06	1000	1050	0	7,555,634,286				
v41d2	1.00E+06	1000	1050	5000	7,522,112,842	-33,521,444	-0.44 %	1.6	1400
v42c2	3.00E+06	1000	1050	0	15,339,159,925				
v42d2	3.00E+06	1000	1050	5000	15,270,430,672	-68,729,253	-0.45 %	1.7	1400
v43c	5.00E+05	500	2400	0	11,562,423,630				
v43d	5.00E+05	500	2400	5000	11,482,916,024	-79,507,606	-0.69 %	2.7	1400
v44c2	1.00E+06	500	2400	0	16,226,764,770				
v44d2	1.00E+06	500	2400	5000	16,145,694,808	-81,069,962	-0.50 %	3.0	1400
v45c	3.00E+06	500	2400	0	30,685,062,619				
v45d	3.00E+06	500	2400	5000	30,565,233,760	-119,828,859	-0.39 %	3.5	1400
v46c2	5.00E+05	500	1700	0	9,892,909,045				
v46d2	5.00E+05	500	1700	5000	9,840,545,383	-52,363,662	-0.53 %	3	1400
v47c2	1.00E+06	500	1700	0	13,716,805,787				
v47d2	1.00E+06	500	1700	5000	13,646,235,482	-70,570,305	-0.51 %	2.3	1400
v48c2	3.00E+06	500	1700	0	28,461,666,370				
v48d2	3.00E+06	500	1700	5000	28,356,464,388	-105,201,982	-0.37 %	2.4	1400
v49c	5.00E+05	200	2200	0	7,463,343,829				
v49d	5.00E+05	200	2200	5000	7,336,503,515	-126,840,314	-1.70 %	6	1400
v50c	1.00E+06	200	2200	0	9,857,764,315				
v50d	1.00E+06	200	2200	5000	9,759,059,295	-98,705,020	-1.00 %	6	1400
v51c	3.00E+06	200	2200	0	11,366,574,297				
v51d	3.00E+06	200	2200	5000	11,388,303,241	21,728,944	0.19 %	5	1400
v52c2	5.00E+05	200	1800	0	8,556,323,198				
v52d2	5.00E+05	200	1800	5000	8,435,416,211	-120,906,987	-1.41 %	6	1400
v53c	1.00E+06	200	1800	0	10,912,528,220				
v53d	1.00E+06	200	1800	5000	10,781,550,516	-130,977,704	-1.20 %	7	1400
v54c	3.00E+06	200	1800	0	12,049,920,874				
v54d	3.00E+06	200	1800	5000	12,072,781,480	22,860,606	0.19 %	5	1400

Table 3 Results arranged according to CO₂ injection rate.

CO ₂ Inj rate (t/yr)	K (mD)	Depth (m)	Case	Final leakage reductn (%)	Delay in leakage break-through (yrs)	Scen-arios
5.0E+05	200	1800	v52	-1.41%	6.0	1
5.0E+05	200	2200	v49	-1.70%	6.0	2
5.0E+05	500	1700	v46	-0.53%	3.0	3
5.0E+05	500	2400	v43	-0.69%	2.7	4
5.0E+05	1000	1050	v40	-0.48%	1.5	5
5.0E+05	1000	1650	v37	-0.37%	1.6	6
5.0E+05	1125	2200	v35	-0.23%	1.8	7
1.0E+06	200	1800	v53	-1.20%	7.0	1
1.0E+06	200	2200	v50	-1.00%	6.0	2
1.0E+06	500	1700	v47	-0.51%	2.3	3
1.0E+06	500	2400	v44	-0.50%	3.0	4
1.0E+06	1000	1050	v41	-0.44%	1.6	5
1.0E+06	1000	1650	v38	-0.34%	1.7	6
1.0E+06	1125	2200	v34	-0.38%	1.4	7
3.0E+06	200	1800	v54	0.19%	5.0	1
3.0E+06	200	2200	v51	0.19%	5.0	2
3.0E+06	500	1700	v48	-0.37%	2.4	3
3.0E+06	500	2400	v45	-0.39%	3.5	4
3.0E+06	1000	1050	v42	-0.45%	1.7	5
3.0E+06	1000	1650	v39	-0.35%	1.6	6
3.0E+06	1125	2200	v36	-0.30%	1.7	7

Table 4 Results arranged according to permeability.

CO ₂ Inj rate (t/yr)	K (mD)	Depth (m)	Case	Final leakage reductn (%)	Delay in leakage break-through (yrs)	Scen-arios
5.0E+05	200	1800	v52	-1.41%	6.0	1
5.0E+05	200	2200	v49	-1.70%	6.0	2
1.0E+06	200	1800	v53	-1.20%	7.0	3
1.0E+06	200	2200	v50	-1.00%	6.0	4
3.0E+06	200	1800	v54	0.19%	5.0	5
3.0E+06	200	2200	v51	0.19%	5.0	6
5.0E+05	500	1700	v46	-0.53%	3.0	1
5.0E+05	500	2400	v43	-0.69%	2.7	2
1.0E+06	500	1700	v47	-0.51%	2.3	3
1.0E+06	500	2400	v44	-0.50%	3.0	4
3.0E+06	500	1700	v48	-0.37%	2.4	5
3.0E+06	500	2400	v45	-0.39%	3.5	6
5.0E+05	1000	1050	v40	-0.48%	1.5	
5.0E+05	1000	1650	v37	-0.37%	1.6	1
1.0E+06	1000	1050	v41	-0.44%	1.6	
1.0E+06	1000	1650	v38	-0.34%	1.7	3
3.0E+06	1000	1050	v42	-0.45%	1.7	
3.0E+06	1000	1650	v39	-0.35%	1.6	5
5.0E+05	1125	2200	v35	-0.23%	1.8	2
1.0E+06	1125	2200	v34	-0.38%	1.4	4
3.0E+06	1125	2200	v36	-0.30%	1.7	6

Table 5 Results arranged according to reservoir depth.

CO ₂ Inj rate (t/yr)	K (mD)	Depth (m)	Case	Final leakage reductn (%)	Delay in leakage break-through (yrs)	Scen-arios
5.0E+05	1000	1050	v40	-0.48%	1.5	1
1.0E+06	1000	1050	v41	-0.44%	1.6	2
3.0E+06	1000	1050	v42	-0.45%	1.7	3
5.0E+05	200	1800	v52	-1.41%	6.0	4
5.0E+05	500	1700	v46	-0.53%	3.0	5
5.0E+05	1000	1650	v37	-0.37%	1.6	1
1.0E+06	200	1800	v53	-1.20%	7.0	6
1.0E+06	500	1700	v47	-0.51%	2.3	7
1.0E+06	1000	1650	v38	-0.34%	1.7	2
3.0E+06	200	1800	v54	0.19%	5.0	8
3.0E+06	500	1700	v48	-0.37%	2.4	9
3.0E+06	1000	1650	v39	-0.35%	1.6	3
5.0E+05	200	2200	v49	-1.70%	6.0	4
5.0E+05	1125	2200	v35	-0.23%	1.8	1
1.0E+06	200	2200	v50	-1.00%	6.0	6
1.0E+06	1125	2200	v34	-0.38%	1.4	2
3.0E+06	200	2200	v51	0.19%	5.0	8
3.0E+06	1125	2200	v36	-0.30%	1.7	3
5.0E+05	500	2400	v43	-0.69%	2.7	5
1.0E+06	500	2400	v44	-0.50%	3.0	7
3.0E+06	500	2400	v45	-0.39%	3.5	9

2.5 Discussion

2.5.1 Migration pattern

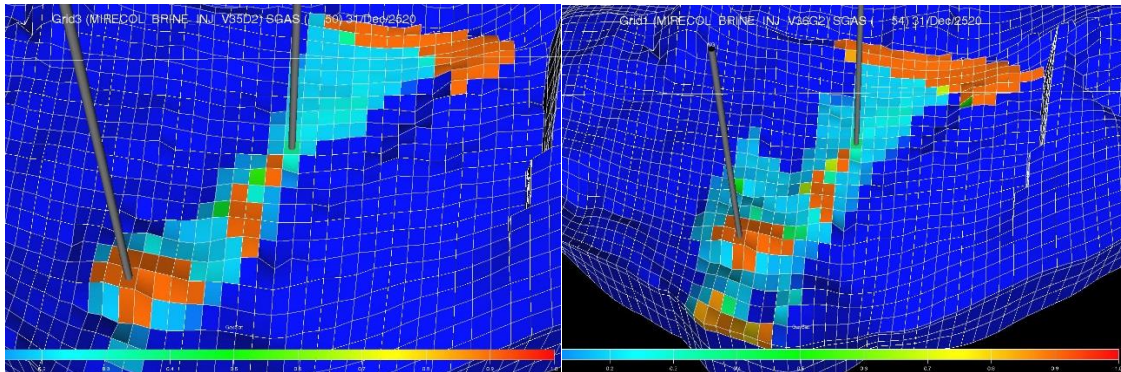
As an initial insight it is interesting to consider the variation in the overall migration pattern in terms of the reservoir parameters studied. The final CO₂ distributions for several cases are shown in Figure 11. It can be seen that:-

- At higher permeabilities (1125mD & 1000 mD) the injection rate has only a slight effect on the final saturation distribution after 510 years. At 3.0E6 t/y the narrowest part of the migration path is approximately twice as wide and there is a slight development of the secondary route to the west. Both of these features suggest that the capacity of the ridge structure is being exceeded at the highest injection rate.
- At 500mD permeability a wider migration path plus a secondary path are evident from 1.0E6 t/ r injection upwards. At 3.0E6 t/y injection the width of the migration path is nearly double that for 1125mD permeability.
- At 200mD the broadening of the migration path is even more pronounced for all CO₂ injection rates, with much more development of the secondary migration path.
- Variations in the reservoir depth were not found to give large changes in the migration pattern. Shallower reservoirs showed slightly more free gas, but this was less evident with higher permeability.

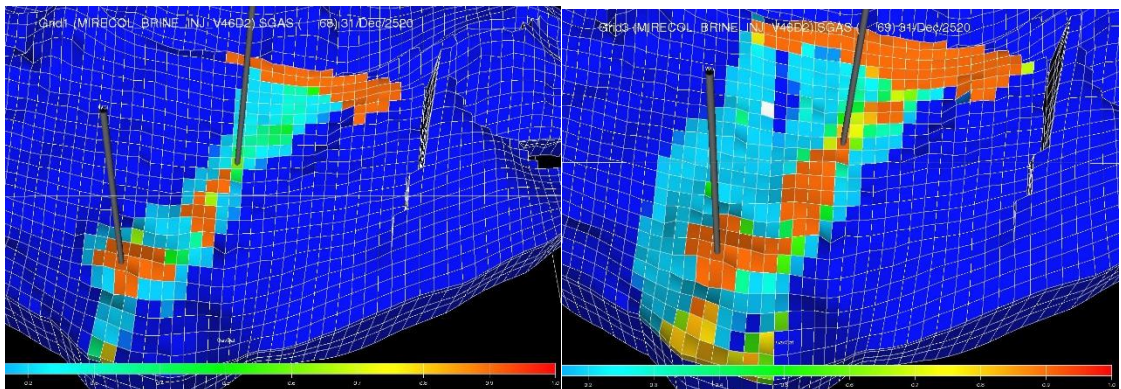
These observations are largely explained by the changing balance between the viscous and gravitational forces on the fluids. At high permeabilities it is easy for the CO₂ to

flow therefore the viscous forces are less and the relative effect of gravity (buoyancy) is more. Hence the effect of the topography is more pronounced and CO₂ tends to follow the top of the ridge structure. At low permeabilities and at higher injection rates it is much more difficult for the CO₂ to press forward, i.e. the viscous forces dominate and the CO₂ now spreads out over a greater area in a diffuse flow pattern.

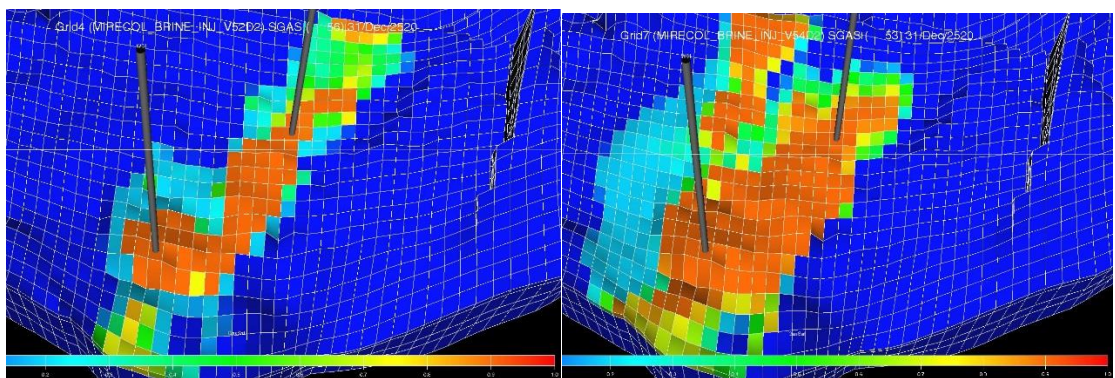
Note that the wider migration paths visible at the end of the simulation are developed long after the year of water injection and so do not refute the conclusions in Section 0 about the physical extent of remediation.



Final CO₂ saturations, 1125mD, 2200m deep, 0.5E6 t/y (left) & 3.0E6 t/y (right)



Final CO₂ saturations, 500mD, 1700m deep, 0.5E6 t/y (left) & 3.0E6 t/y (right)



Final CO₂ saturations, 200mD, 1800m deep, 0.5E6 t/y (left) & 3.0E6 t/y (right)

Figure 11. Examples of migration pattern at the end of the simulations (510 years).

2.5.2 Total leakage reduction

The results for leakage reduction as a percentage of the cases without water injection are given graphically in Figure 12, Figure 13 & Figure 14.

Firstly it should be re-iterated that the leakage reduction values obtained were very small (less than 0.2%), due to the fact that water injection was applied for only 1 year out of a total of 510 years of the simulation. However this is sufficient to see the relative effects in the different scenarios.

Figure 12 shows the effect of varying the CO₂ injection rate. Most of the scenarios show slightly less reduction in leakage with increasing injection rate, which might simply reflect the greater volume of CO₂ injected into the reservoir and the very brief effect of water injection. However the 200 mD scenarios exhibit a very strong decrease in the leakage reduction with increased CO₂ injection rate. This is attributed to the much broader migration occurring with low permeability, allowing much of the CO₂ to avoid the blockage caused by water injection.

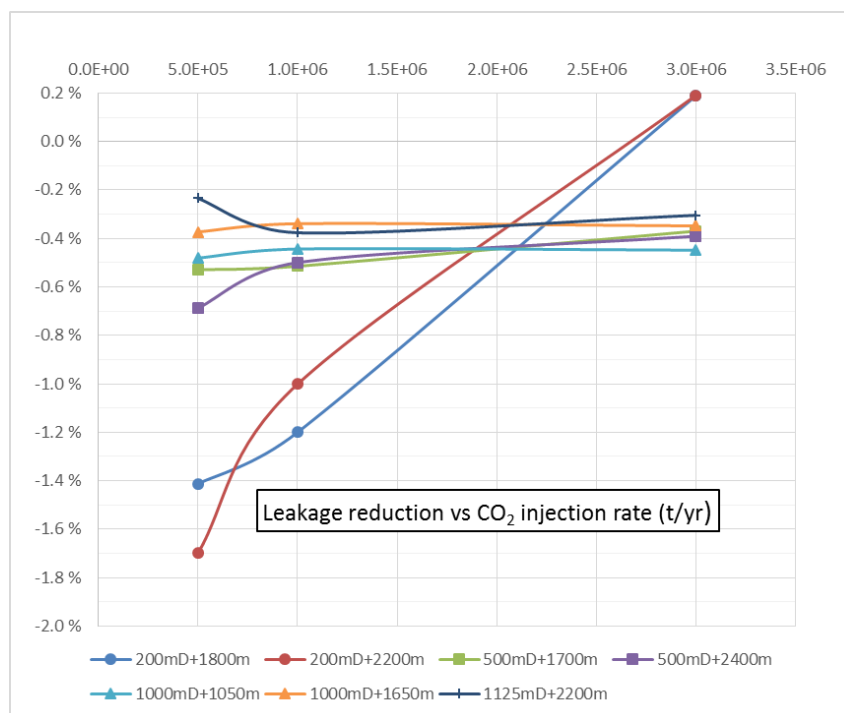


Figure 12. Leakage reduction vs CO₂ injection rate.

Figure 13 shows the effect of permeability on leakage reduction. For most scenarios increased permeability gives significantly less reduction in leakage, especially at the lower values of permeability. This might be explained by greater flowing capacity reducing the net effect of a short blockage by water injection.

The two scenarios with high CO₂ injection rates at very low permeability differ again from the rest, giving slightly increased leakage under water injection, as explained above for Figure 12.

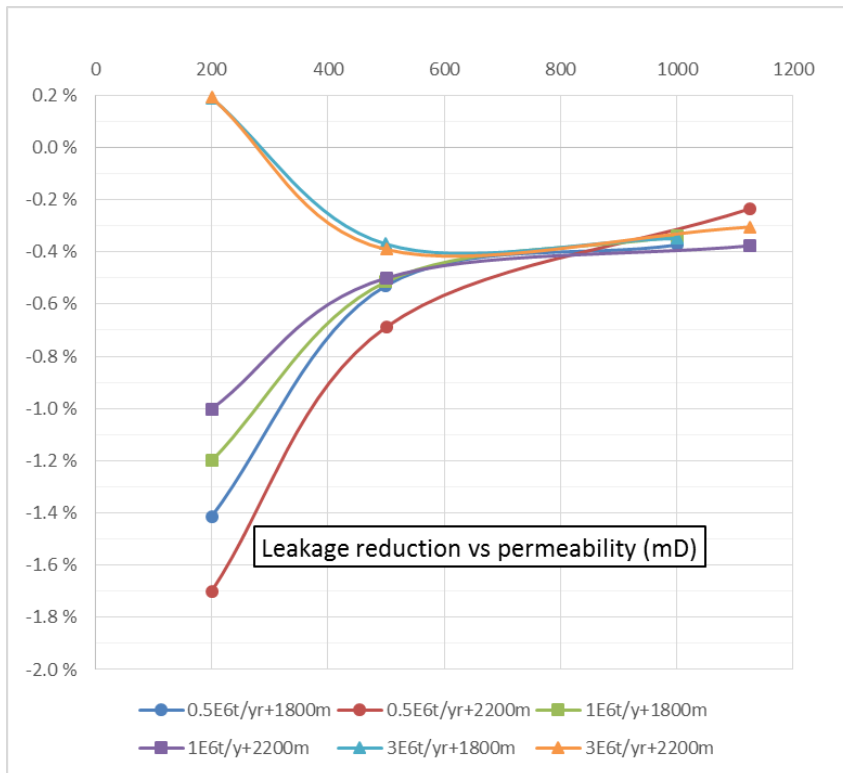


Figure 13. Leakage reduction versus permeability.

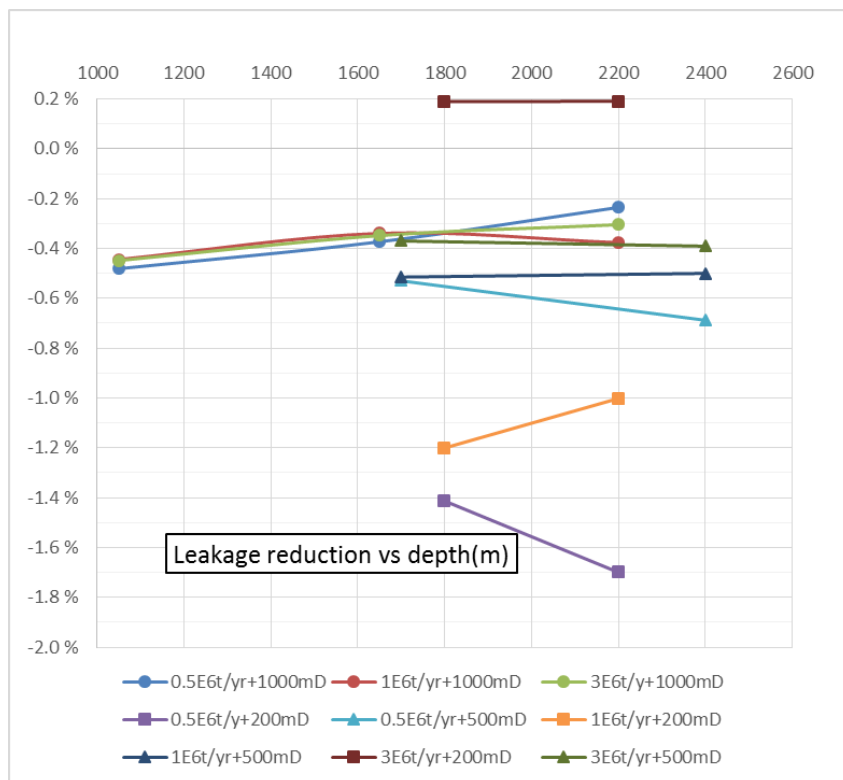


Figure 14. Leakage reduction vs reservoir depth.

Figure 14 shows the effect of reservoir depth on leakage reduction. In general no consistent trend can be seen, suggesting that this is not a significant parameter in the effectiveness of water injection as a migration mitigation measure.

2.5.3 Longevity of remediation

This characteristic was estimated by the delay to CO₂ leakage caused by water injection and it this was measured from the commencement of water injection. The average value for delay obtained from all the cases listed was 3.2 years.

Two means of measurement were tried: i) by comparing graphically the reported figures of the volume of gas in the FIPNUM for the water injection and no water injection cases, and ii) monitoring the onset of gas saturation in the grid block (43,38,1) containing the water injection well (on the boundary of the FIPNUM, in the centre of the main migration path) for both water injection and no water injection cases.

The first method is the most logical, being based on the definition of leakage in this study, and was tried first. Unfortunately it proved to be very difficult to extract a consistent delay period from the graphs of FIPNUM volume, due to the differing curvature of the two lines (see Figure 15 for an example).

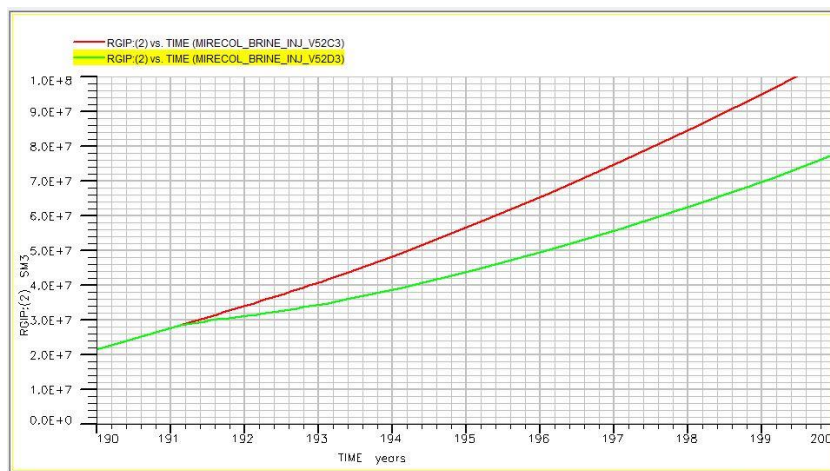


Figure 15. Gas leakage volume for 0.5E6 t/yr CO₂ injection, 200 mD permeability and 1800m reservoir depth, without and with water injection.

The second method offered a much more precise, albeit somewhat arbitrary measure, but gave easily measureable period for the delay in leakage, as shown in Figure 16. In a few cases a small preliminary leakage was observed, due to the start of water injection being slightly late, but this was judged to be insignificant.

It was noted that sometimes grid block (43,38,1) was found to be not the point of first leakage into the FIPNUM. The adjacent grid block to the southwest occasionally showed leakage before the reference grid block, but this was not important since a fixed

common location was the main requirement. This is a reason for slightly different gas break-through dates being obtained sometimes from the two methods.

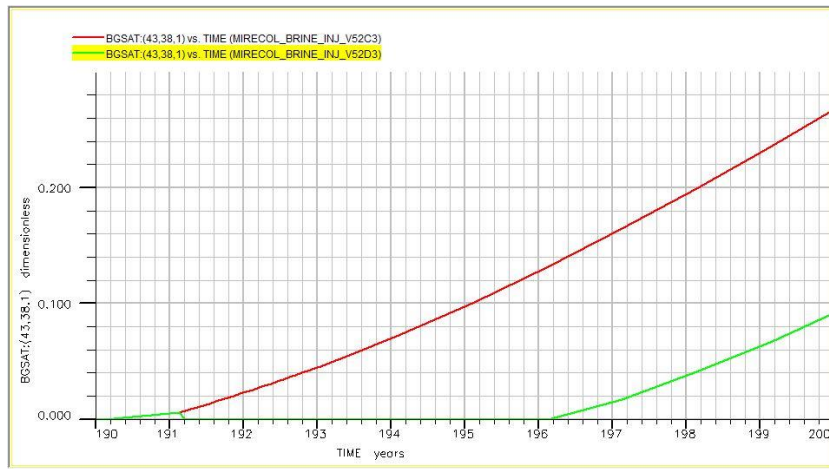


Figure 16. Onset of non-zero gas saturation in grid block (43, 38,1), for 0.5E5 t/yr CO₂ injection, 200 mD permeability and 1800 m reservoir depth, with and without water injection.

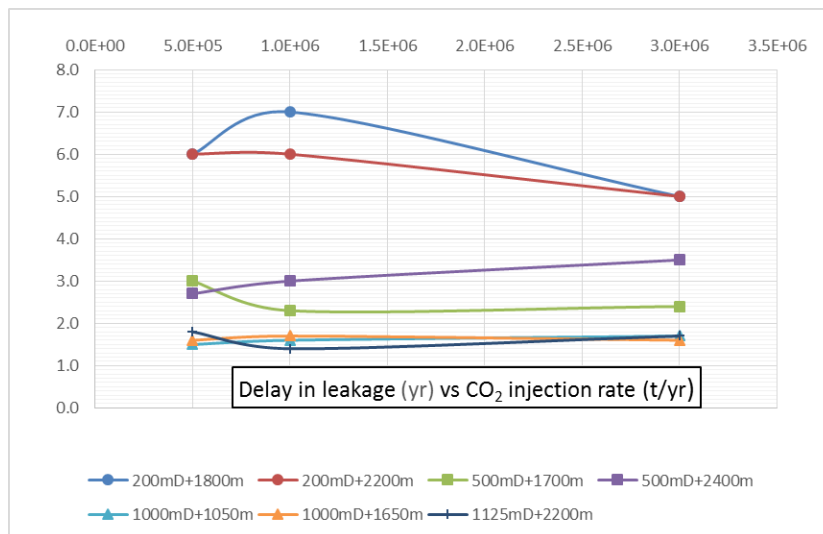


Figure 17. Delay in leakage vs CO₂ injection rate.

Figure 17 shows the effect of the different CO₂ injection rates on the delay in leakage, i.e. the longevity of the water injection remediation. It can be seen that in general the injection rate itself has relatively little effect on the delay. However significant differences can be seen between the scenarios, especially for the 200mD cases, which also exhibit a clear effect from varying CO₂ injection rate. These data show some similarity to Figure 12.

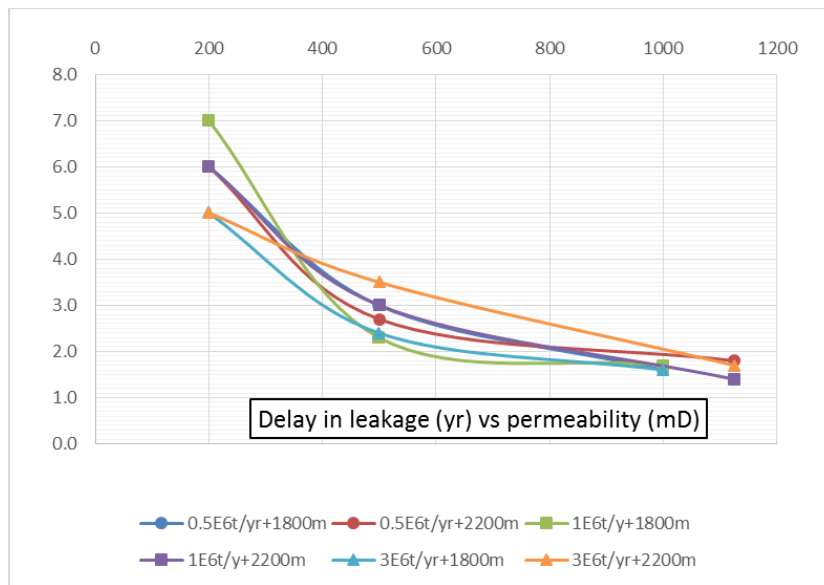


Figure 18. Delay in leakage vs permeability.

Figure 18 shows a clear reduction in leakage delay at higher permeability for all scenarios. This suggests that the higher local pressure and water concentration caused by water injection are more rapidly dissipated with higher permeability, hence shortening the migration effect. Note from Figure 16 that water injection appears to stop CO₂ migration very effectively for the delay period, at least near the injection well and within the simulation accuracy of the grid used.

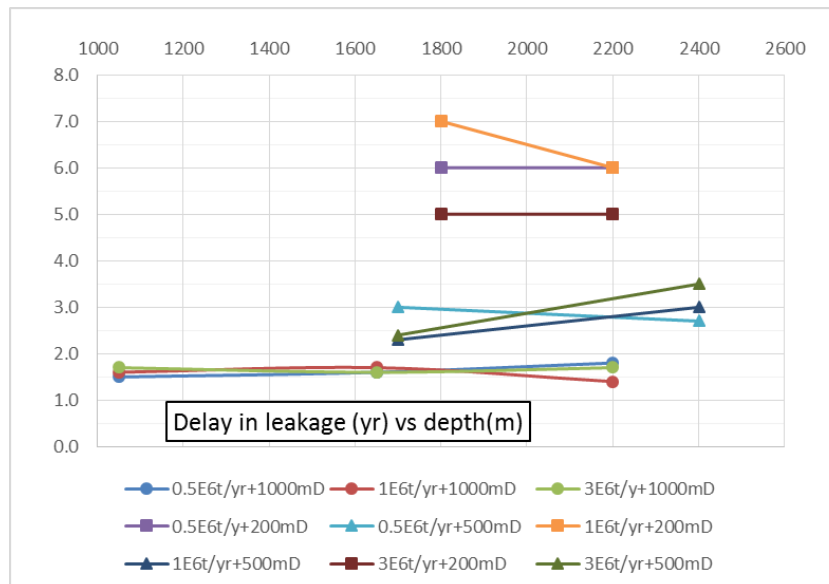


Figure 19. Delay in leakage vs reservoir depth.

Figure 19 shows very little overall effect of the reservoir depth on the delay in leakage derived from simulations.

In Figure 16 above the period of total blockage was 6 years, one of the longest measured. Looking at the total leakage curves for the same case with and without water injection in Figure 20 shows that there is no further effect on the leakage. This demonstrates that the mitigation effect of water injection is short-term if the water injection is not continued.

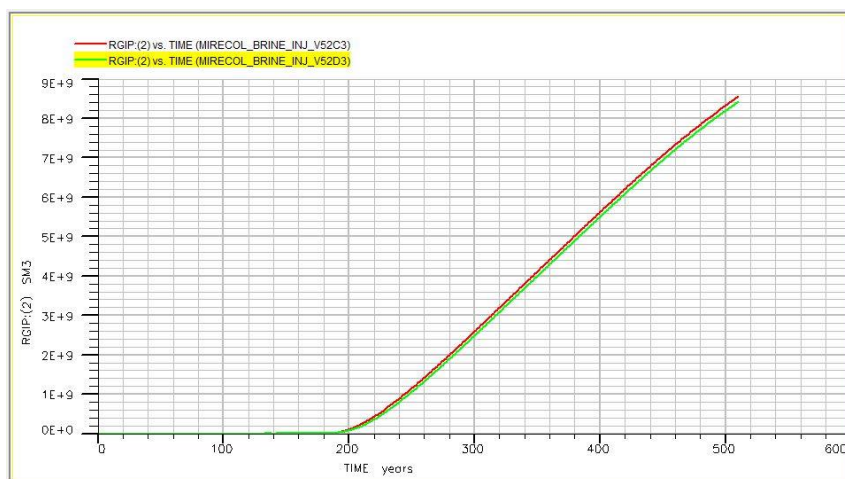


Figure 20. Complete leakage volume profiles over the entire simulation period for the 0.5E5 t/yr CO₂ injection, 200 mD permeability and 1800 m reservoir depth case, with and without water injection.

2.5.4 Spatial extent of remediation

Estimating the spatial extent of remediation proved to be a difficult objective. Initially the gridblock pressures along the entry boundary of the leakage numerical area were investigated, but lacking a clear criterion for the pressure increase required to block the migration of CO₂, this approach was of no use.

Instead the gas saturations were monitored in the cells surrounding the water injector (block 43, 38, 1) during and immediately following water injection. This was performed graphically using the FloViz utility. From the detected flow of gas it was possible to determine how many grid-blocks at the boundary experienced the break-through of CO₂, as illustrated in Figure 21. In this example it can be seen that the CO₂ reaches the leakage area diagonal boundary at two grid-blocks in year 73, is halted for two years (the CO₂ concentration builds up) and in year 75 it begins to migrate upwards from both grid-blocks. It was clear from spot-checks of saturation that the CO₂ did not enter the leakage region via any other grid-blocks.

Each grid-block measures 500 m in the x & y directions, so since the leakage boundary is diagonal across the grid-blocks at this location, the linear width of the CO₂ migration after water injection was 1410, say 1400m. This quantifies the spatial extent of remediation.

This method was applied to all cases and the results are shown in the last column of Table 2. From this table it can be seen that in all cases considered the observed spatial extent was the same, 1400m, except for the first case with 0.5 E6 t/yr CO₂ injection, 1125 mD permeability and 2200m depth, which showed a spatial extent of 700m. Thus the results from the model used show minimal variation between the cases considered.

The main reasons for so little difference in the spatial extent of mitigation are believed to be:-

- i) The CO₂ migration appears to be controlled primarily by the topography of the top layer of the model. The gas moves along the top of a ridge which is relatively narrow at the location of the water injection well.
- ii) There appears to be a relatively weak pressure gradient acting on the CO₂, which is then largely controlled by buoyancy.
- iii) Thus when the injected water blocks the migration of CO₂, there is little accumulated force to move the CO₂ further sideways than the two grid-blocks observed.
- iv) The use of smaller grid-blocks might have helped to differentiate between the cases, but because a local grid refinement could not be set-up in the same location as a FIPNUM, this could not be implemented so late in the study.

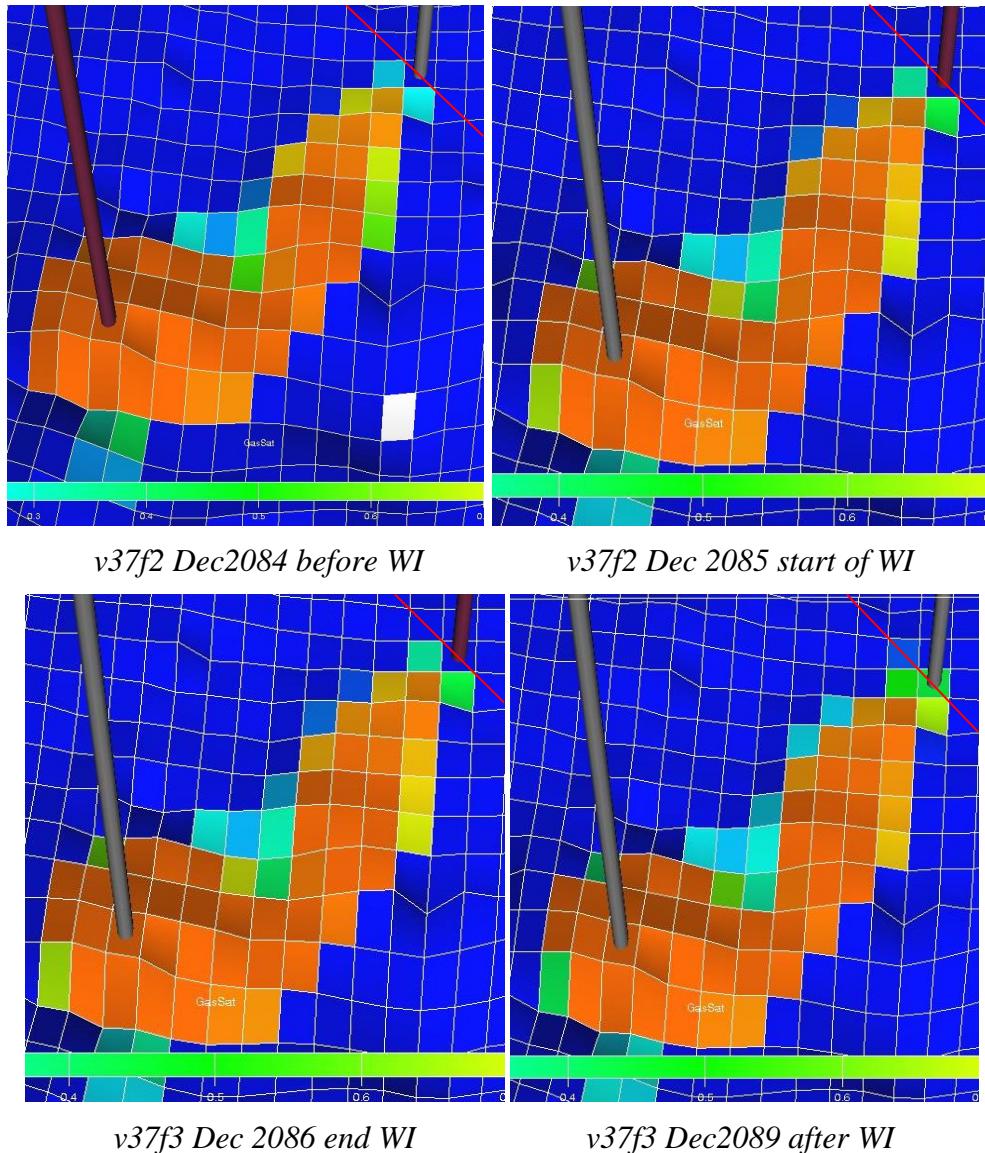


Figure 21. Examples of estimating mitigation extent by monitoring CO₂ saturation (the leakage boundary is shown as a red line).

2.5.5 Effect of reservoir depth on free gas

The main reason that reservoir depth was considered as a varied parameter in these simulations was that the lower ambient pressure in shallower reservoirs will give rise to more free CO₂ at lower density, which might affect the relative flow conditions for gaseous CO₂ versus water. The final amounts of both free CO₂ and dissolved CO₂ within the leakage reference area (FIPNUM) are given in the reports for each simulation and the fraction of free CO₂ in the total leakage volumes are summarised against reservoir depth for each case in Figure 22.

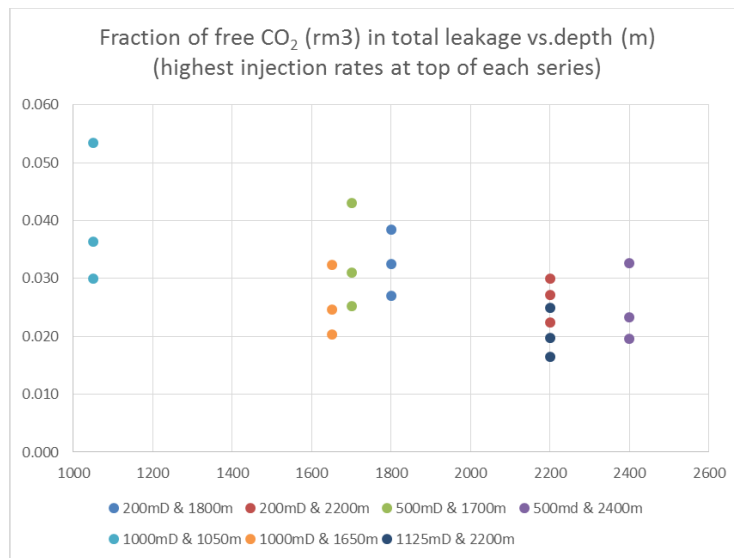


Figure 22. Fraction of free CO₂ in total leakage volume vs reservoir depth, for 0.5 E6, 1.0 E6 & 3.0 E6 t/yr injection rates.

Figure 22 confirms that at reduced reservoir depth, more free CO₂ occurs in the final leakage volume, presumably due to the lower ambient pressures releasing more free CO₂ and the resulting increased relative permeability of the gas. Higher injection rates also result in more free gas in the reservoir, offset somewhat by the higher pressure caused. The net result for higher injection rates also appears to be higher free CO₂ fractions in the final leakage volume.

2.6 Conclusions

- Simulations were performed of CO₂ migration along a ridge structure in the Johansen aquifer, in order to extract data on the effectiveness of water injection as a mitigation measure. Twenty-one combinations of CO₂ injection rate, permeability and reservoir depth, representing possible Norwegian CO₂ storage sites were simulated.
- The effect of one year of water injection, just ahead of the CO₂ plume, was studied. Data on the percentage reduction in leakage after 510 years migration were collected.
- In general it was seen that in high permeability reservoirs the CO₂ is able to migrate rapidly along a narrow path, since the viscous forces are low and buoyancy keeps the gas in the ridge structure. However at low permeabilities, especially with high CO₂ injection rates, high viscous forces cause the flow to become much more diffuse, thereby by-passing the water injector and potentially reducing its mitigating effect.
- In most cases CO₂ injection rate has little effect on the leakage reduction achieved by one year of water injection. However in very low permeability reservoirs the leakage reduction is reduced greatly by high CO₂ injection rates,

due to the very broad migration path largely avoiding area affected by water injection.

- For most reservoirs very low permeability results in large reductions in leakage, although at high CO₂ injection rates and low permeability the reductions are very small. These two extremes represent the difference between gravity and viscous forces controlling the flow pattern.
- No consistent trend in leakage reduction was observed due to variations in reservoir depth.
- The delay in CO₂ migration (i.e. the longevity of mitigation) resulting from water injection was generally found to be unaffected by variations in CO₂ injection rate or reservoir depth. However decreasing permeability has a strong increasing effect on the duration of mitigation, especially at lower permeabilities.
- The spatial effect of mitigation by water injection showed almost no variation between twenty of the cases studied. This is believed to be due to the topography of the location in the model used, namely that the ridge is relatively narrow. This, combined with the weak forces moving the CO₂, was enough to block the tip of the CO₂ plume in all cases.
- Shallower reservoir depth was found to create more CO₂ as free gas at lower density, due to the corresponding lower pressures. This effect and also higher CO₂ injection rates resulted in more free CO₂ in the leakage area.
- It is clear that water injection does not provide a long-lasting blockage to CO₂ migration, with its effect lasting only from 1.4 to 7 years from the beginning of water injection. Since migration of injected CO₂ will continue over many hundred years, water injection cannot be considered a long-term remediation measure. This suggests that it might well be better to drill a CO₂ producer instead of a water injector and concentrate on removing the CO₂ plume, possibly with a water injector or other remediation as a temporary measure.

3 BRINE INJECTION AS A FLOW DIVERSION OPTION (IMPERIAL COLLEGE)

In secondary oil recovery, brine or water injection has a long history either to support reservoir pressure or to displace oil towards producing wells. There is a range of techniques and theories (e.g. Buckley Leverett analysis) about how water injection can be used to increase oil recovery. Volumetric sweep management and realignment of production in contiguous layers are the nearest analogues in the oil industry to the use of water injection in order to stop the migration of CO₂ (Omorgie et al., 1995). Industry has studied several mechanisms by which water injection can be used to reduce CO₂ migration like creating a high pressure barrier in front of the migrating CO₂ plume (Kuuskraa and Gedec, 2007) or by chasing CO₂ with brine ensuring storage security (Qi et al., 2008) and injecting water directly into the advancing CO₂ plume (Esposito and Benson, 2010; Anchliya et al., 2012).

This section presents the results of the numerical modelling carried out by Imperial College, which investigated the application of brine injection for flow diversion of CO₂ plume within the storage reservoir. In the scenarios set up, it was assumed that a sub-seismic fault is present in the formation as a pre-defined undesired migration pathway. Three separate scenarios were considered by varying the fault location along the anticlinal structure if the model at distances of 1km, 2km and 3km from the CO₂ injection well, and the effectiveness of brine injection as a remediation technique assessed.

3.1 Reservoir model description

3.1.1 Structural and geological model

A numerical reservoir model was set up to study the flow diversion of CO₂ plume using brine water injection within a heterogeneous saline aquifer. The structural model used in this study represents a saline aquifer with a broad and considerably dipping anticlinal structure (Figure 23), where the containment of CO₂ is envisaged. The model grid spans an area of 36km×10km and includes five major sealing faults. The grid broadly comprises of three layers, namely: (1) a reservoir layer with an average thickness of 240m and resolution of 200m×200m×4m; (2) a caprock (seal) layer with an average thickness of 225m and resolution of 200m×200m×225m; and (3) a shallow aquifer layer with an average thickness of 175m and resolution of 200m×200m×175m. The depth of the model ranges between 1,087m and 3,471m.

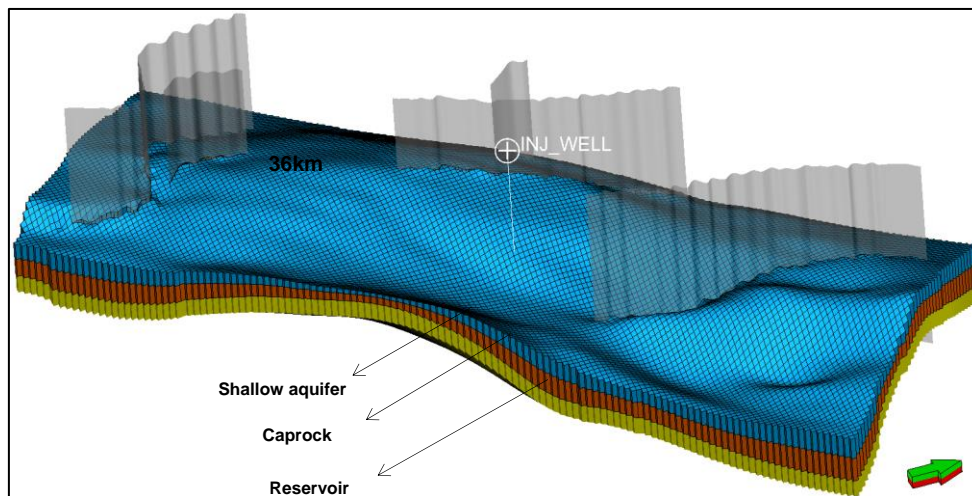


Figure 23. The structural model of the numerical saline aquifer (36km×10km) containing five major faults and three stratigraphic layers: reservoir layer, caprock (seal) layer and shallow aquifer layer.

The geological features of the reservoir layer represent a fluvial-channel system, typically containing braided sandstone channels and interbedded floodplain deposits (the inter-channel region) of mudstone or siltstone. These generally represent the fluviodeltaic progradation and floodplain deposition formations found in the Triassic of the Barents Sea. The channel layout parameters implemented in the model to represent the fluvial-channel system are given in Table 6. The range of the petrophysical properties used in the static geological model attribution (Table 7) are based on the Late Triassic Fruholmen Formation in the Hammerfest Basin (NPD, 2013), which is located at depths similar to those considered in this model. The petrophysical attributions of the geological model were generated using Sequential Gaussian Simulation (SGS) in order to represent the variability in the distribution of these values. Example realisations of the porosity and horizontal permeability distributions for the top reservoir layer are illustrated in Figure 2.

Table 6. Channel layout parameters used in the reservoir layer of the geological model.

	Min	Mean	Max
Amplitude [m]	400	500	600
Wavelength [m]	14,000	15,000	16,000
Width [m]	1,400	1,500	1,600
Thickness [m]	4	8	12

Table 7. Petrophysical properties used in the geological model.

Petrophysical properties		Channels	Inter-channel region	Caprock	Shallow aquifer
Porosity	Min, Mean, Max	0.1, 0.18, 0.25	0, 0.1, 0.25	0.01	0.05, 0.15, 0.25
	Standard deviation	0.05	0.05	0	0.05
Horizontal Permeability [mD] *	Min, Mean, Max	125, 3,000, 7,000	0.1, 10, 100	0.0001	100, 3,000, 5,000
	Standard deviation	2,000	40	0	1,000
NTG	Min, Mean, Max	0.6, 0.9, 1	0, 0.2, 0.5	0.01	0.6, 0.9, 1
	Standard deviation	0.05	0.05	0	0.05

*vertical permeability = 0.1 × horizontal permeability

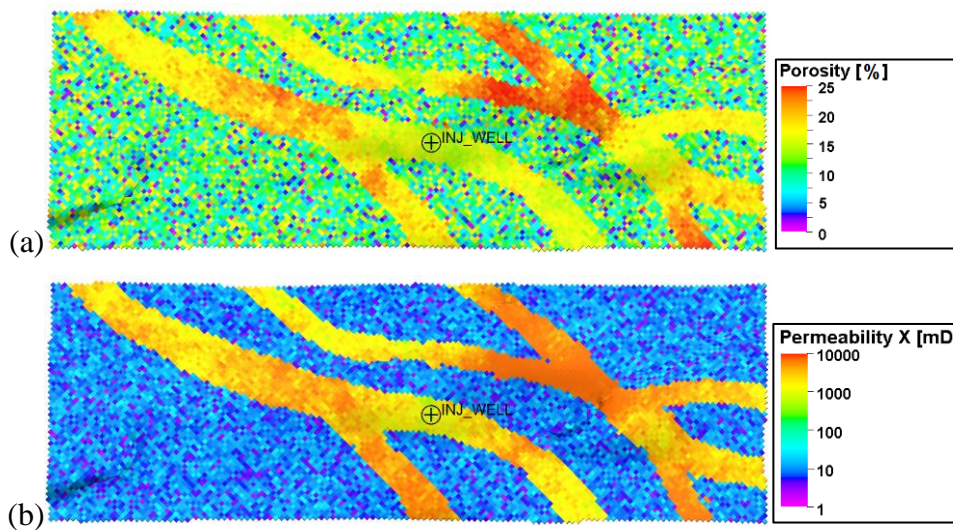


Figure 24. Example realisations of petrophysical properties distribution for the top layer of the reservoir: (a) Porosity; (b) Horizontal permeability covering the area of the reservoir model (36km×10km).

3.1.2 Dynamic properties of the reservoir model

Similar to the petrophysical properties of the geological model attribution, the dynamic properties of the reservoir model have been selected based on the values reported for the reservoir conditions found in the corresponding or neighbouring Barents Sea

formations. The salinity of the formation water was chosen to be 14% based on the values reported for the Tubåen formation of the Snøhvit field (Benson, 2006), which is also part of the Realgrunnen Subgroup overlying the Fruholmen. The reservoir temperature was set at 93°C and the initial pressure of the reservoir model was assumed to be at hydrostatic pressure.

3.1.3 Modelling of CO₂ flow diversion with brine injection

The dynamic model was set up in Schlumberger’s Eclipse 300 (E300) software using the static geological model and the dynamic reservoir parameters described in the previous sections. The compositional flow simulation of CO₂ storage in the saline aquifer model was carried out by implementing a quasi-isothermal, multi-phase, and multi-component algorithm, enabled by the CO2STORE option, wherein mutual solubilities of CO₂ and brine are considered. Simulations were carried out for 30 years, comprising of the CO₂ injection, leakage detection, remediation and observation phases.

For the purposes of this study, it was assumed that a sub-seismic fault is present in the formation as a pre-defined undesired migration pathway. This is represented by a local grid refinement introduced in the structural model by means of the CARFIN option in Eclipse. Three separate scenarios were considered by varying the fault locations along the anticlinal structure at distances of 1km, 2km and 3km with respect to the CO₂ injection well. The amount of leakage into the shallow aquifer and the time it takes to remediate the leakage were assessed.

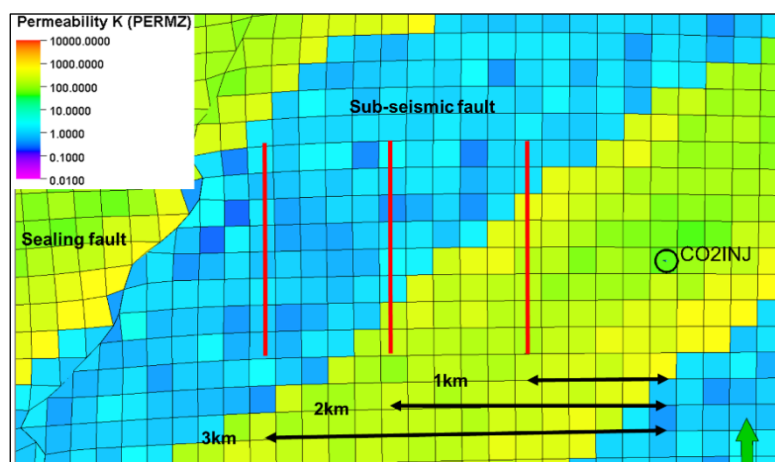


Figure 25. Permeability attribution and position of sub-seismic fault at 1km from the CO₂ injection well.

The fault has a lateral dimension of 800m×2m and is assumed to be non-sealing, with a uniform vertical permeability of 10,000mD and spanning the reservoir and the caprock thickness (approximately 450m), and without appreciable formation displacement between the two sides of the fault.

The simulation of CO₂ injection in the saline aquifer was carried out at a rate of 1Mt/year until leakage through the sub-seismic fault into the shallow aquifer is detected.

The leakage detection is based on a threshold which was assumed as 5,000 tonnes of mobile CO₂ (Benson, 2006). Once the leakage is detected, CO₂ injection was stopped and brine was injected for a maximum period of 12 months to investigate the effectiveness of flow diversion.

3.2 CO₂ Injection and leakage detection

3.2.1 Scenario 1: Fault at 1km away from the CO₂ injection well

When the sub-seismic fault was assumed at 1km away from the CO₂ injection well, leakage in the shallow aquifer was detected after 8 months from the start of injection. Figure 26 illustrates the simulation results indicating the free CO₂ plume distribution after: (a) 3 months of simulation; (b) when the leakage was detected and CO₂ injection was stopped (after 8 months); and (c) after 30 years of simulation (un-remediated).

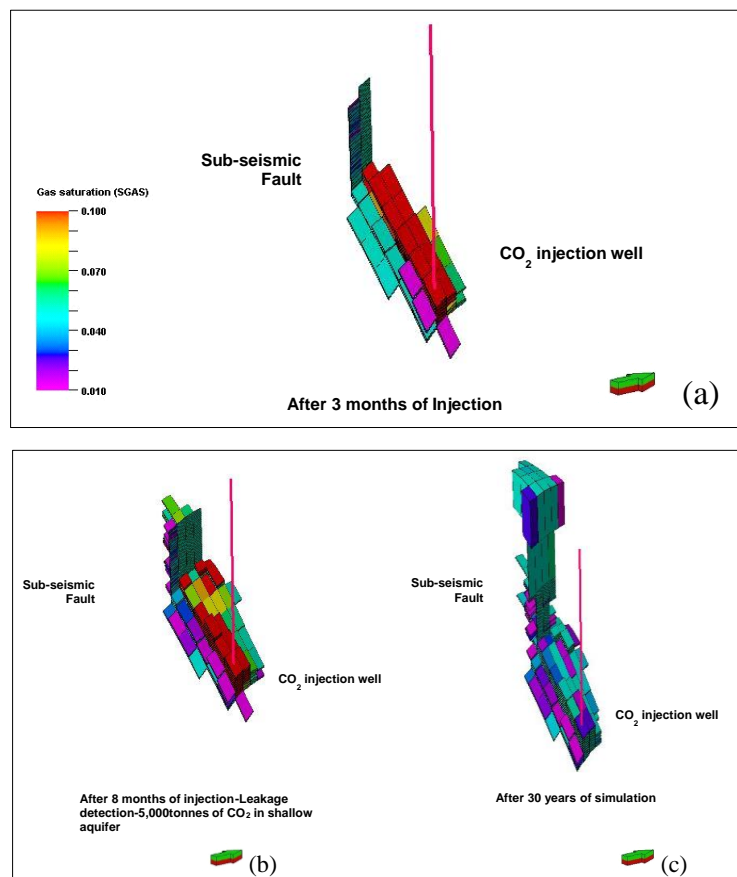


Figure 26. Plume distribution at different time steps in shallow aquifer for 1km fault scenario: (a) after 3 months; (b) after 8 months (when leakage is detected); (c) after 30 years of simulation (un-remediated).

The plume migration results for this case shows that, soon after the start of CO₂ injection the plume hits the sub-seismic leaky fault because of its proximity to the CO₂ injector well, and because it is in the high permeability channel. Due to the buoyancy effects, the CO₂ reaches the top of anticline and breaks into shallow the aquifer, and thus 5,000 tonnes of free CO₂ is detected just after 8 months of injection. After that, CO₂ injection was stopped and brine injection was started to stop further migration of the CO₂.

3.2.2 Scenario 2: Fault at 2km from the CO₂ injection well

When the sub-seismic fault was assumed at 2km away from the CO₂ injection well, leakage in shallow aquifer was detected after 12 months from the start of CO₂ injection. Figure 27 illustrates the simulation results indicating the free CO₂ plume distribution after: (a) 6 months of simulation; (b) when leakage was detected and CO₂ injection was stopped (after 12 months); and (c) after 30 years of simulation (un-remediated).

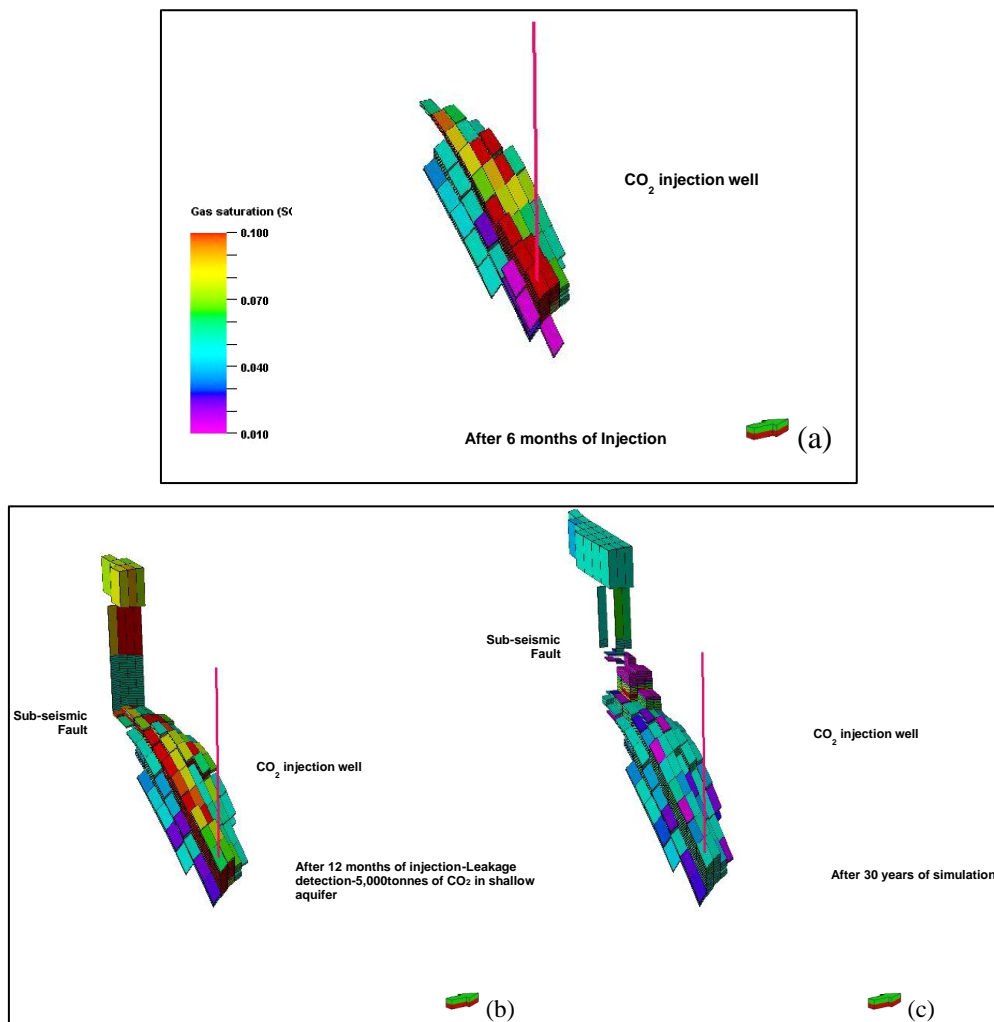


Figure 27. Plume distribution at different time steps in shallow aquifer for 2km fault scenario: (a) after 6 months; (b) after 12 months (when leakage is detected); (c) after 30 years of simulation (un-remediated).

The plume migration results for this case show that, the CO₂ plume does not hit the sub-seismic leaky fault immediately as compared to the fault at 1km. After 12 months of CO₂ injection, leakage in the sub-seismic leaky fault has been detected. After that CO₂ injection was stopped and brine injection was started to stop further migration of the CO₂.

3.2.3 Scenario 3: Fault at 3km from the CO₂ injection well

When the sub-seismic fault was assumed at 3km away from the CO₂ injection well, and relatively closer to the top of the anticlinal structure, leakage was detected in the shallow aquifer after 18 months from the start of CO₂ injection. Figure 28 illustrates the simulation results indicating the free CO₂ plume distribution after: (a) 6 months of simulation; (b) when leakage was detected and CO₂ injection was stopped (after 18 months); (c) after 30 years of simulation (un-remediated).

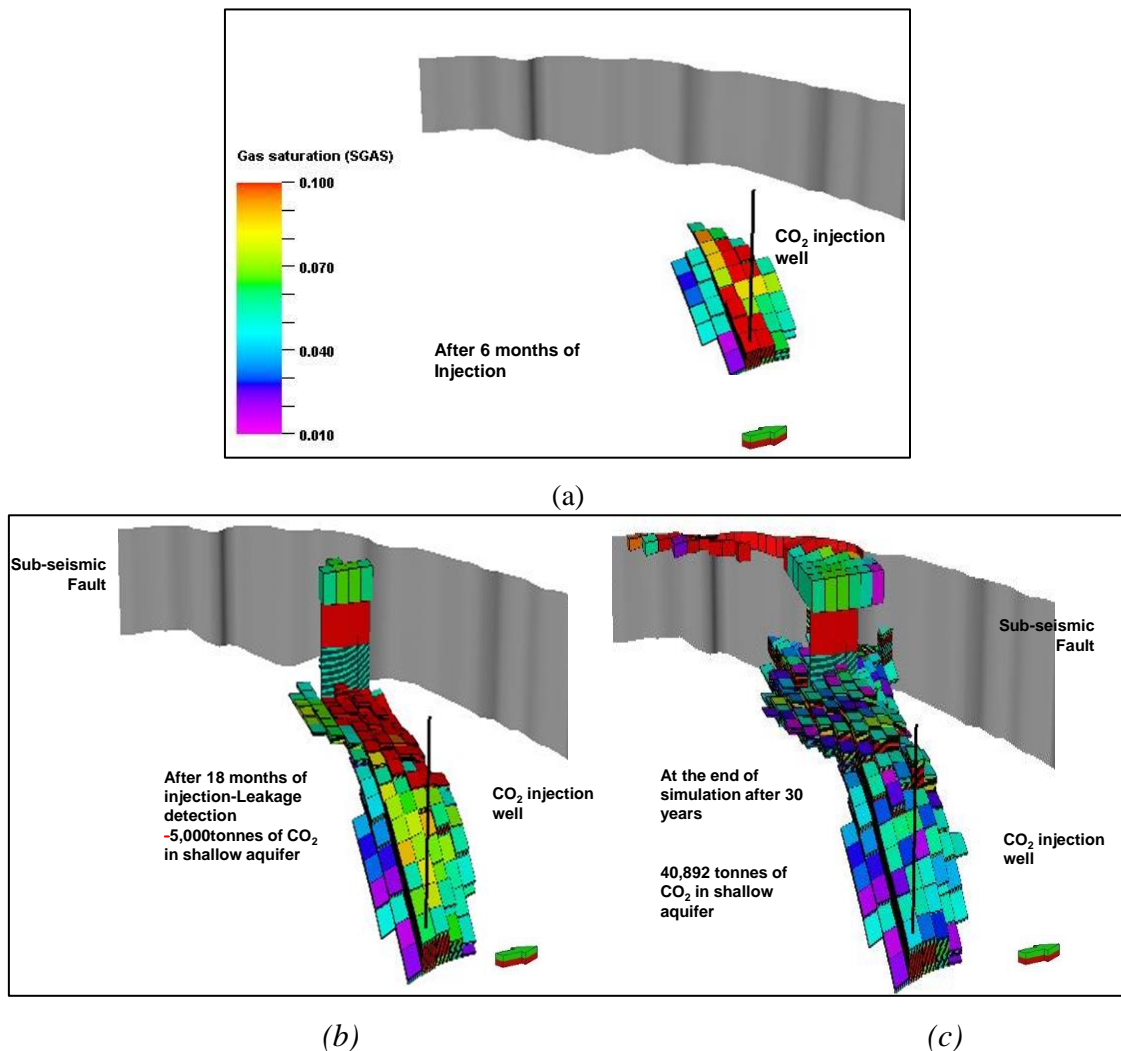


Figure 28. Plume distribution at different time steps in shallow aquifer for 3km fault scenario: (a) after 6 months; (b) after 18 months (when leakage is detected); (c) after 30 years of simulation (un-remediated).

The plume migration results for this case show that a significantly larger amount of CO₂ is injected before it reaches the sub-seismic leaky fault as compared to the scenarios when the fault was at 1km and 2km distance because 75% of the full extent of this fault is not in the high permeability channel (Figure 25).

3.3 CO₂ leakage remediation using brine injection

When injected in deep saline aquifers, CO₂ moves radially away from the injection well and progressively higher in the formation because of buoyancy forces. Once 5,000 tonnes of CO₂ has been detected in the shallow aquifer, CO₂ injection was stopped and the injection well was used for brine injection to investigate its effectiveness for flow diversion, thus remediate the leakage. Brine was injected at a rate of 1Mt/year and for a maximum period of 12 months. Secondary mode of control for brine injection was implemented in the model by setting an upper bottom hole pressure limit of 300 bars in order to maintain reservoir pressure below the fracture pressure limit.

3.3.1 Scenario 1: Fault at 1km from the CO₂ injection well

In the first scenario, wherein the sub-seismic fault is considered along the anticline at 1km from the CO₂ injector well, brine injection induces flow diversion because of the dissolution in the reservoir and consequently reduces the cumulative amount of CO₂ leakage into the shallow aquifer within 30 days of injection as compared to the non-remediated case where the leakage will continue up to 2 years (29 & 30).

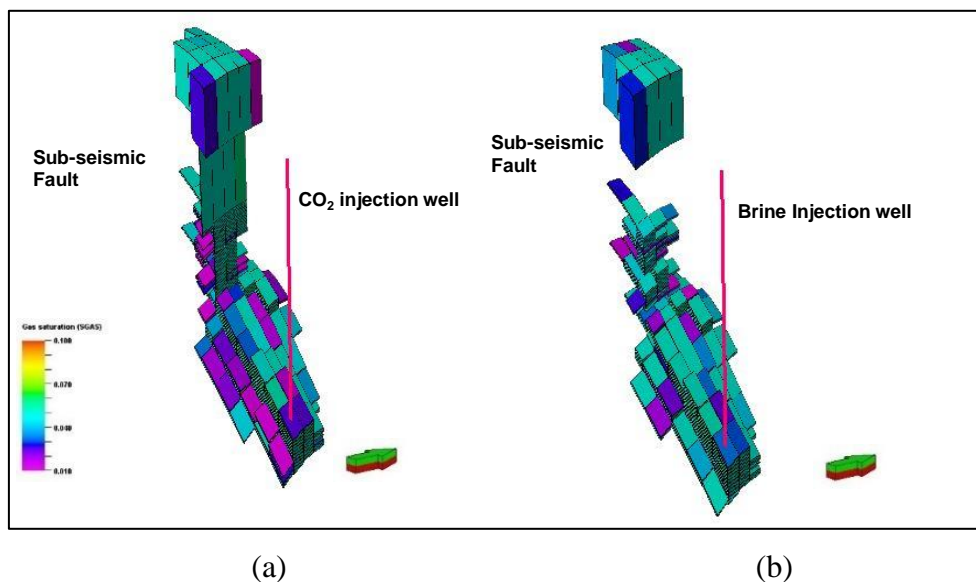


Figure 29. Plume distribution at the end of 30 years' simulation: (a) without remediation; (b) with brine injection.

The above plume migration results for with and without brine injection for 1km fault scenario clearly show that, with brine injection, the leakage of CO₂ from the sub-seismic fault has been stopped and no more leakage is taking place.

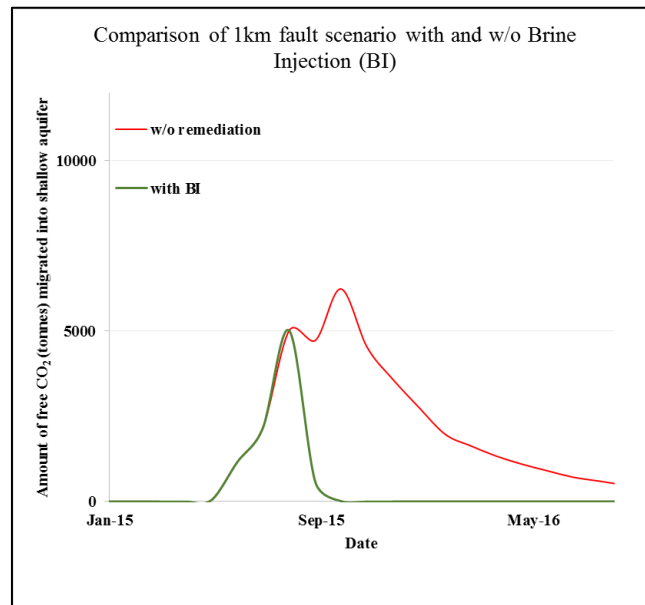


Figure 30. Estimated amount of free CO₂ that could leak in to the shallow aquifer for the 1km fault scenario.

The storage mechanism, which has the largest role in brine injection in reducing the amount of free CO₂ present in shallow aquifer is dissolution, as illustrated by the summary plots for the dissolved and free CO₂ in the reservoir (Figure 31). Dissolution increase with brine injection, which results in less amount of CO₂ in the mobile phase for leakage. Hence, the amount of CO₂ present in the mobile phase in the shallow aquifer is less as compared to un-remediated case.

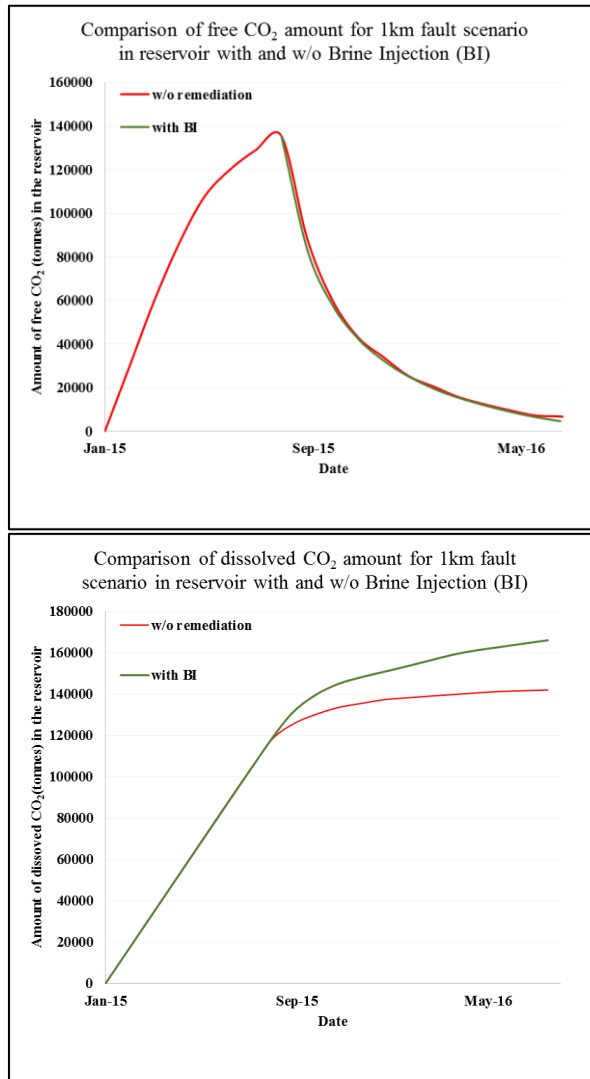


Figure 31. Estimated amount of free and dissolved CO₂ amount in reservoir with and without brine injection.

The top view of the reservoir for this scenario (Figure 32) clearly shows that less CO₂ has leaked when brine injection is implemented. This further strengthens the fact that, because of dissolution in the reservoir, less CO₂ free is available for leakage.

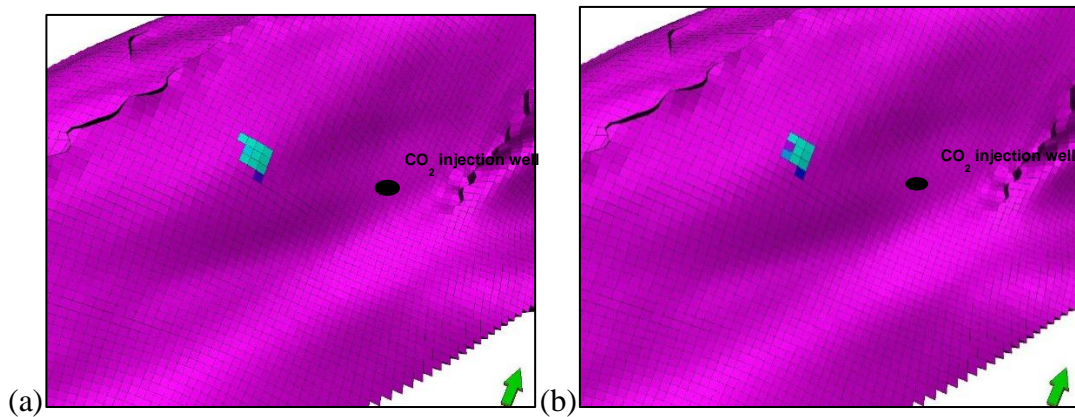


Figure 32. Top view of the reservoir for 1km scenario: (a) without remediation; (b) with brine injection.

3.3.2 Scenario 2: Fault at 2km from the CO₂ injection well

In the second scenario, wherein the sub-seismic fault is considered along the anticline at 2km from the CO₂ injector well, brine injection induces flow diversion because of dissolution in the reservoir and consequently reduces the cumulative amount of CO₂ leakage into the shallow aquifer within 2 months of brine injection as compared to the non-remediated case where the leakage will continue up to 2 years (Figure 33 & Figure 34).

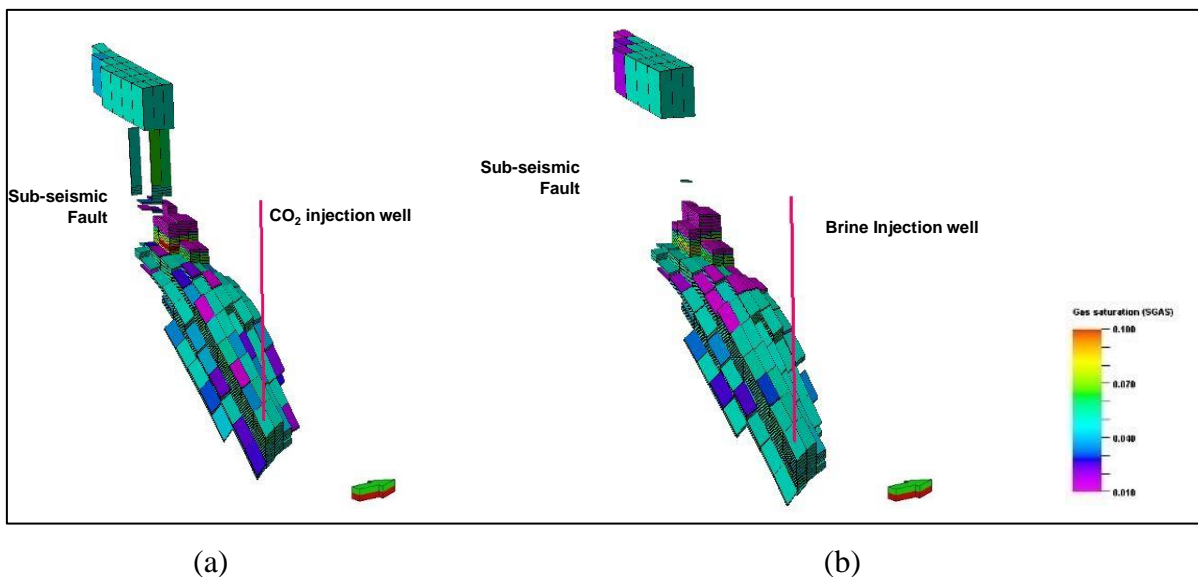


Figure 33. Plume distribution at the end of 30 years' simulation: (a) without remediation; (b) with brine injection.

The above plume migration results for with and without brine injection for the 2km fault scenario clearly show that, with brine injection, the leakage of CO₂ from the sub-seismic fault has been stopped and no more leakage is taking place.

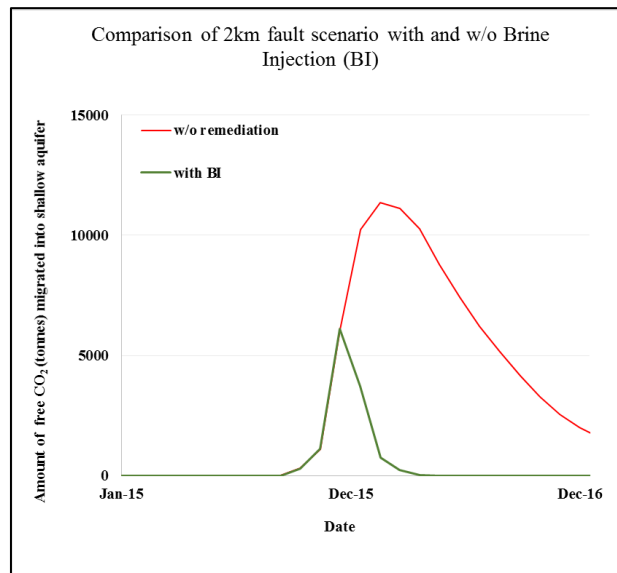


Figure 34. Estimated amount of free CO₂ that could leak into the shallow aquifer for the 2km fault scenario.

The storage mechanism, which has the largest role in reducing the amount of free CO₂ present in the shallow aquifer is dissolution, as illustrated by the summary plots for the dissolved and free CO₂ in the reservoir (**Error! Reference source not found.**). Dissolution increases with brine injection, which results in less amount of CO₂ in the mobile phase for leakage. Hence, the amount of CO₂ present in the mobile phase in the shallow aquifer is less as compared to the unremediated case.

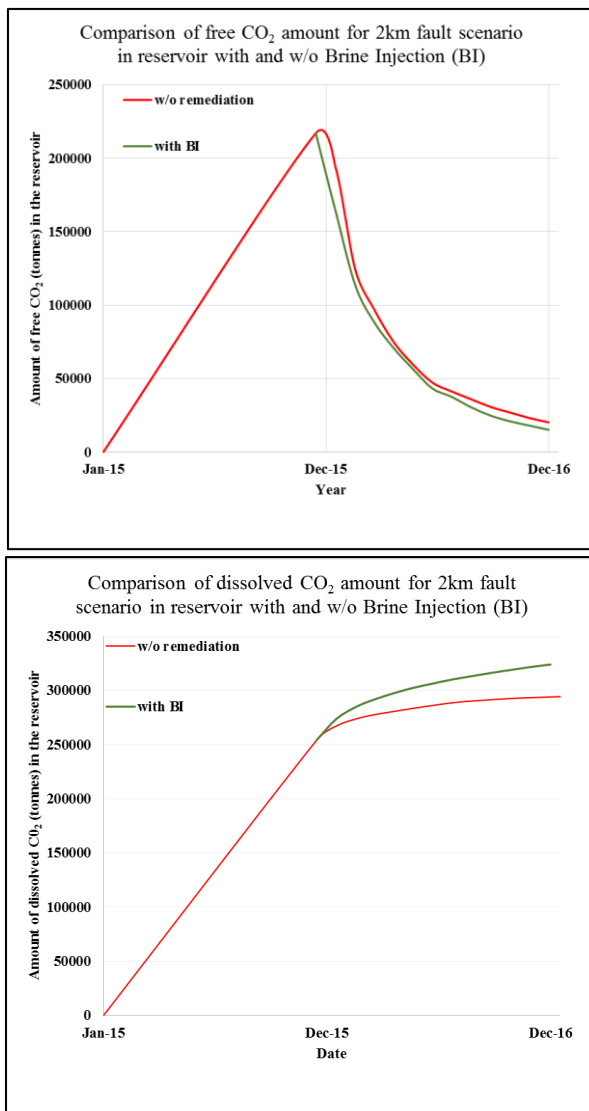


Figure 35. Estimated amount of free and dissolved CO₂ in the reservoir with and without brine injection.

The top view of the reservoir for this scenario (Figure 35) clearly shows that less CO₂ has leaked when brine injection is implemented. This further strengthens the fact that, because of dissolution in the reservoir, less free CO₂ is available for leakage.

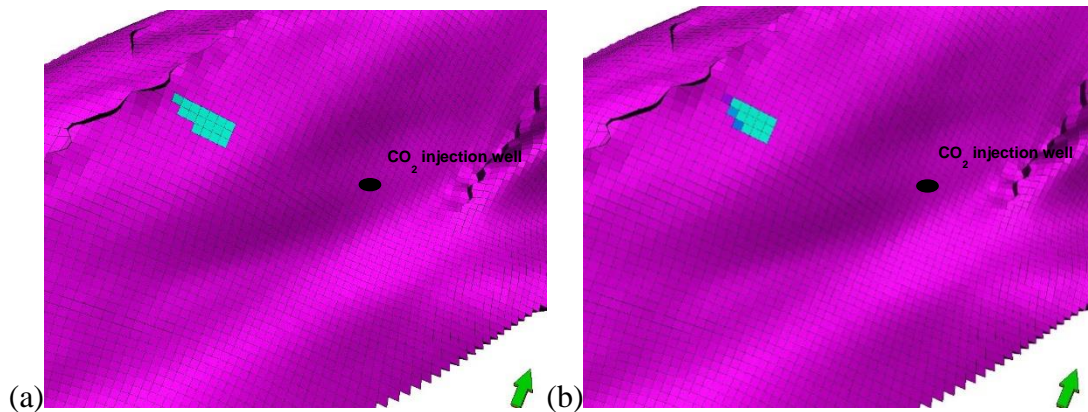


Figure 36. Top view of the reservoir for 2km scenario: (a) without remediation; (b) with brine injection.

3.3.3 Scenario 3: Fault at 3km from CO₂ Injection well

In the final scenario, wherein the sub-seismic fault is considered along the anticline at 3km from the CO₂ injector well, brine injection induces flow diversion and, it is estimated that the cumulative amount of CO₂ leakage into the shallow aquifer consequently reduces from 40,892 tonnes (for an un-remediated case) to 27,684 tonnes by the end of the thirty years simulation period (as shown in Figure 36 & Figure 37).

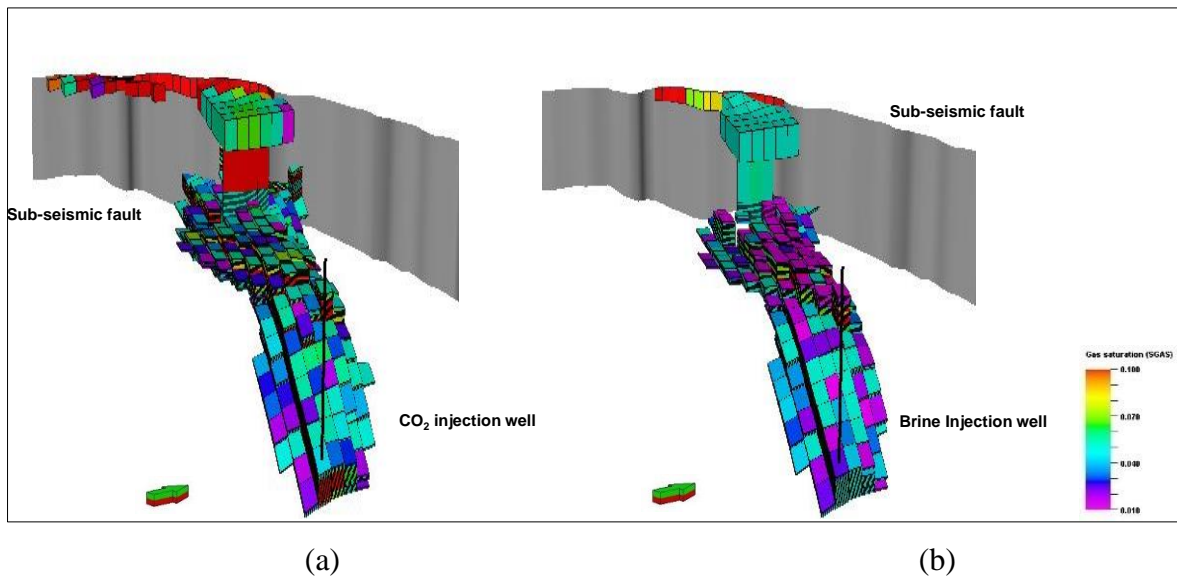


Figure 37. Plume distribution at the end of 30 years' simulation: (a) without remediation; (b) with brine injection.

The above plume migration results with brine injection clearly show that there is a reduction in the amount of leakage into shallow aquifer. In addition, the plume saturation results suggest that CO₂ dissolution enhancement owing to brine injection plays a significant role in leakage reduction.

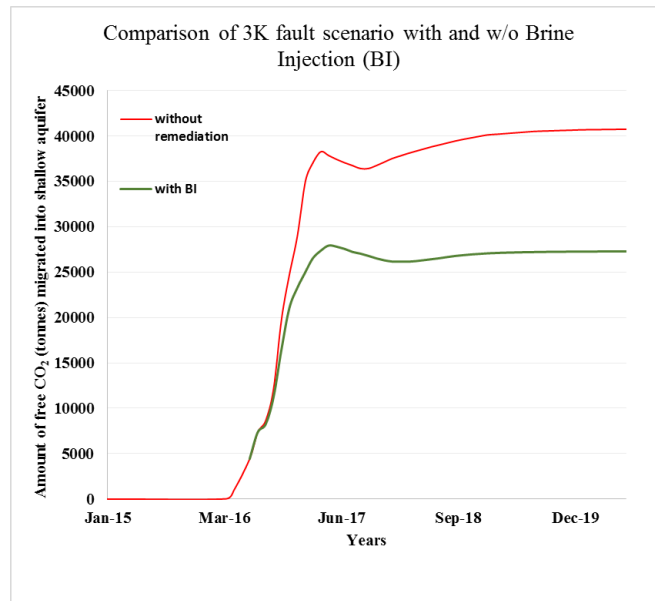


Figure 38. Estimated amount of free CO₂ that could leak for the 3km fault scenario.

The storage mechanism which has an impact in reducing the amount of free CO₂ present in shallow aquifer is CO₂ dissolution in the reservoir, as illustrated by the plots for the dissolved and mobile CO₂ in the reservoir (Figure 38). Dissolution increases with brine injection, which results in less amount of CO₂ in the mobile phase for leakage.

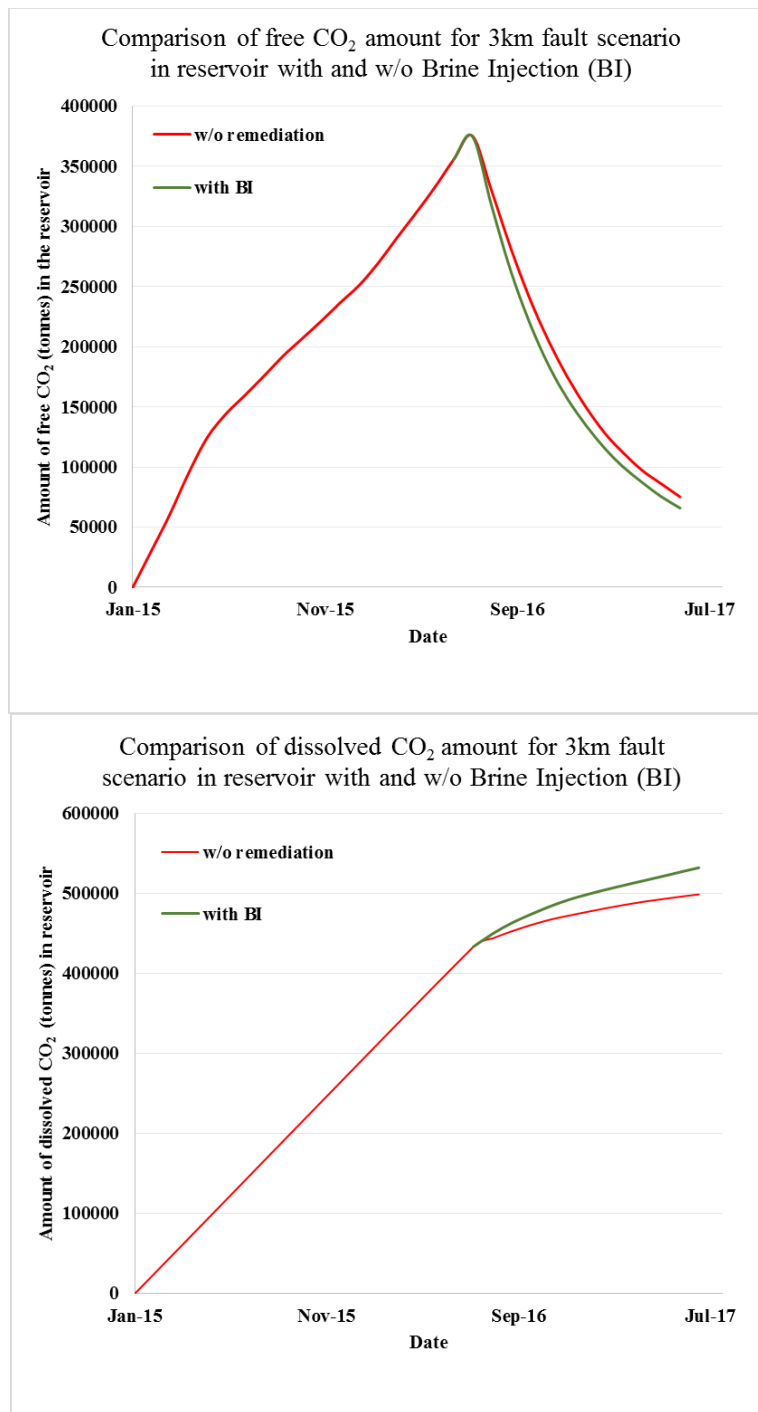


Figure 39. Estimated amount of dissolved and trapped CO₂ for the 3km fault scenario.

The top view of the reservoir for this scenario (Figure 39) clearly shows that less CO₂ has leaked when brine injection is implemented. This further strengthens the fact that, because of dissolution in the reservoir, less free CO₂ is available for leakage.

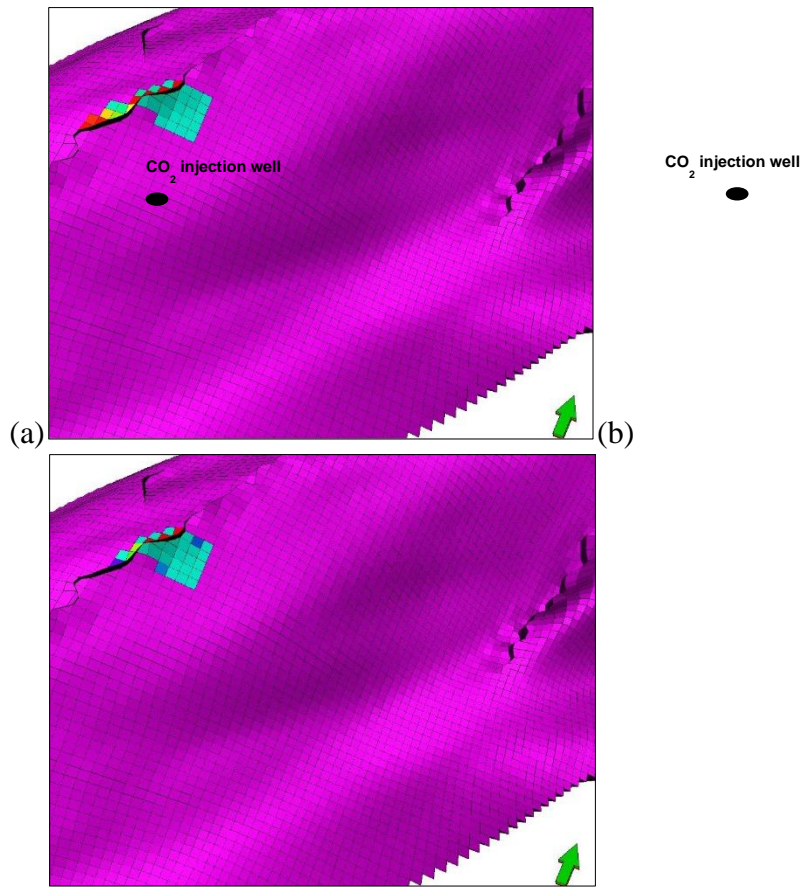


Figure 40. Top view of the reservoir for 1km scenario: (a) without remediation; (b) with brine injection.

In order to further investigate the flow diversion performance of brine injection for 3km scenario, brine injection rate as well as period of injection was varied. First brine injection rate was increased to 2Mt/year. The results show that there is a limit with which one can achieve remediation by using brine injection, as the difference in remediation achieved by using 1Mt/year and 2 Mt/year is not much. Table 8 illustrates the percentage of remediation achieved by using two different injection rates. Brine injection was continued up to 36 months and it was found that there is a very slight decrease in the amount of free CO₂ in shallow aquifer, which further illustrates this conclusion (Figure 40).

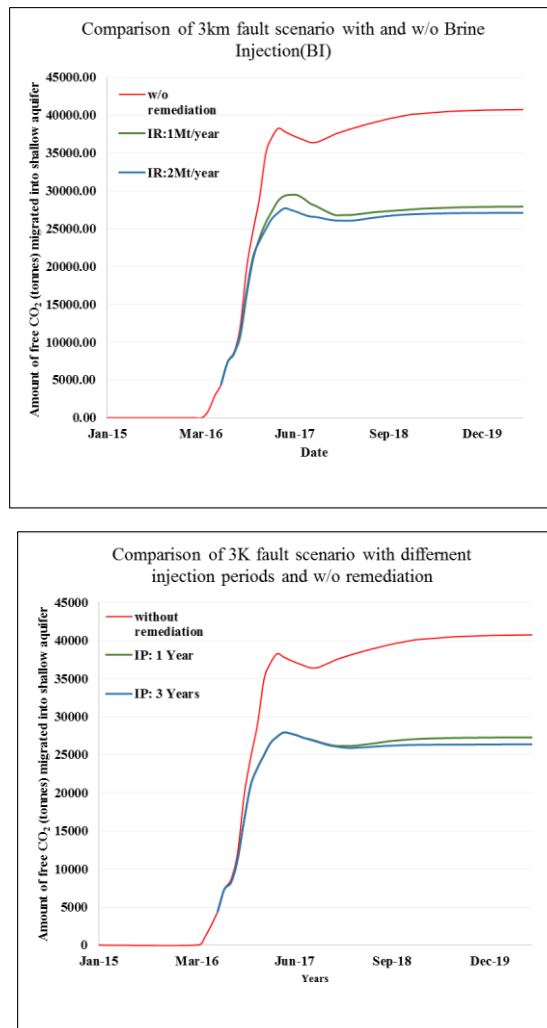


Figure 41. Estimated amount of free CO₂ that could leak for the 3km fault scenario with different injection rates and different injection periods.

The comparison between different injection rates and periods suggests that, by increasing the injection rate or injection period, the increase in the amount of remediation achieved is insignificant, which further confirms the fact that the amount of remediation achieved with brine injection will be limited beyond a certain threshold.

Table 8. Percentage remediation achieved for 3km fault scenarios at different injection rates.

Brine Injected for 12 months at a rate of	Remediation Achieved
1 Mt/year	27.9%
2 Mt/year	32.3%

Generally the storage mechanisms like capillary trapping and dissolution renders the CO₂ less mobile over a timescale of decades to hundreds of years. Overall, with brine injection, there is a decrease in the cumulative mass of CO₂ in the shallow aquifer (Figure 41).

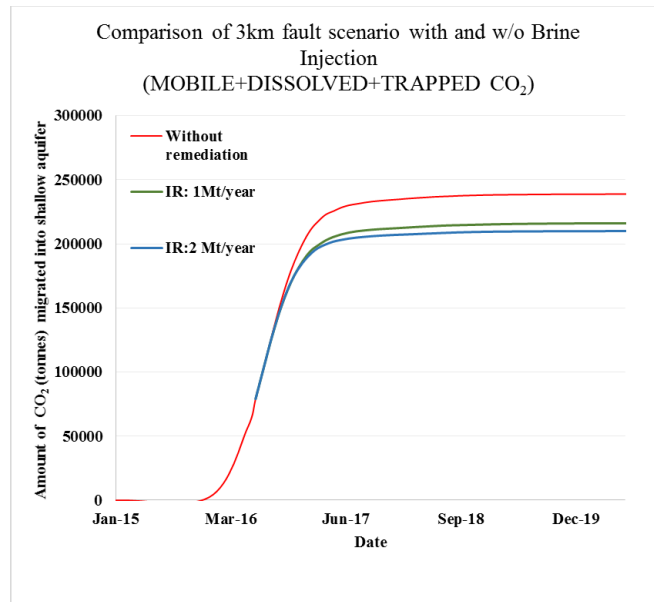


Figure 42. Estimated cumulative mass of CO₂ that could leak for the 3km fault scenario.

3.4 Discussion and conclusions

In this part of the project, the brine injection scenarios were defined based on the distance of the sub-seismic fault from the CO₂ injector along the anticlinal structure. Simulations were performed in order to assess the migration of the CO₂ plume and the effectiveness of brine injection as a mitigation measure. Brine was injected at a rate of 1Mt/year and for a maximum period of 12 months. Secondary mode of control for brine injection was implemented in the model by setting an upper bottom hole pressure limit of 300 bars in order to maintain reservoir pressure below the fracture pressure limit. Three scenarios were considered by changing the sub-seismic fault location as 1km, 2km and 3km away from the CO₂ injection well.

The comparison of fault scenarios without remediation (Figure 42) suggests that the fraction of the total amount of CO₂ that would migrate into the shallow aquifer depends on the injection period, and hence the cumulative amount of CO₂ injected until the time of leakage detection (Table 9). For a fault location along the anticline at distances greater than 2km from the CO₂ injector well, and particularly when it lies very close to the top of anticline, it is envisaged that CO₂ will continue to remain there because of buoyancy effects in the reservoir and shallow aquifer, and will not be dissolved or trapped significantly over a period of 30 years, which includes the post- CO₂ injection period.

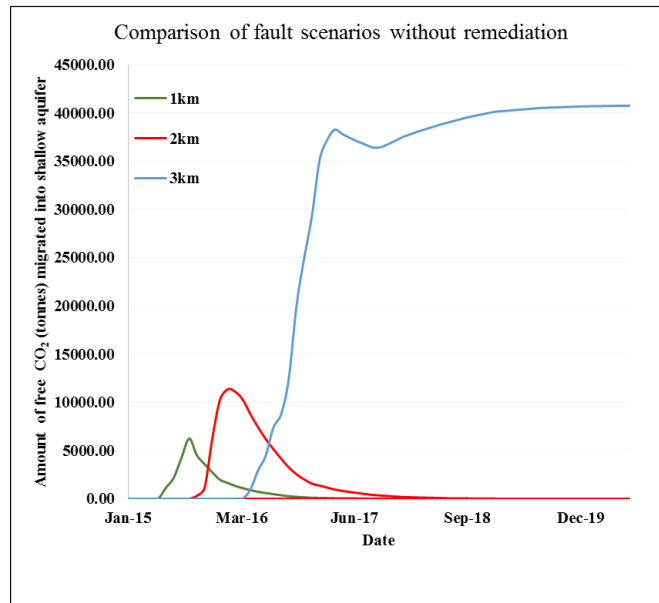


Figure 43. Estimated amount of free CO₂ that could leak for different fault scenarios without remediation.

Table 9. Percentage of CO₂ that has migrated into the shallow aquifer for different fault location scenarios.

Distance of Fault from CO ₂ Injection Well (km)	Time to detection (5,000 tonnes of CO ₂ leaked) after injection	Total amount of CO ₂ injected until leakage detection (Mt)	Percentage of CO ₂ Injected that has migrated into shallow aquifer (%)
1	8 months	0.66	9
2	12 months	1.00	11
3	18 months	1.50	26

The comparison between fault scenarios with brine injection (Figure 43) illustrates that, for a fault at 1km and 2km, brine injection very quickly stops the leakage and, in the long-term, the dissolution process in the reservoir/shallow aquifer plays an important role and the amount of mobile CO₂ decreases towards zero. Furthermore, the leakage is pressure driven and, where the fault is in the transient region of the reservoir, the timescale when mobile CO₂ is available for leakage is limited. However, for the 3km fault scenario, injecting brine at a rate of 2Mt/year for 12 months can reduce the amount of free CO₂ in the shallow aquifer to 67.7% of that which would otherwise be there after 30 years if not remediated. This is because the fault in this scenario is closer to the top of the anticline, hence the leakage is more buoyancy driven and more cumulative amount of CO₂ is available for leakage. These findings are summarised in Table 10.

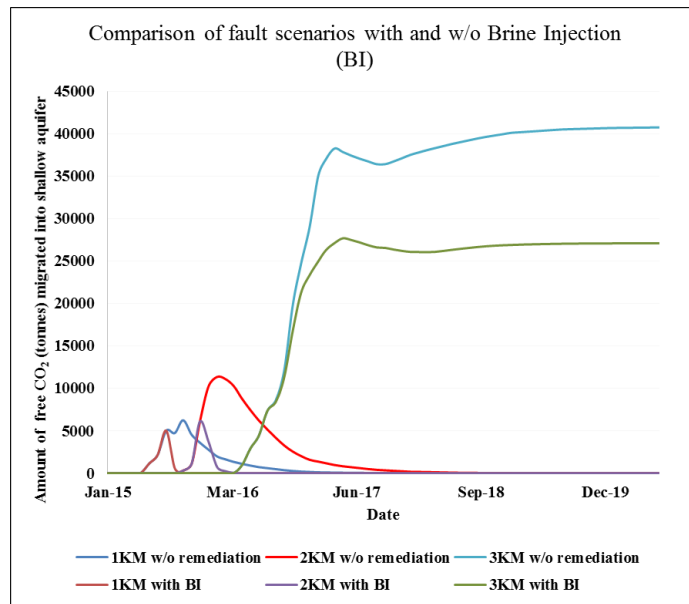


Figure 44. Estimated amount of free CO₂ that could leak for different fault scenario with brine injection.

Table 10. Percentage of Remediation achieved for different fault location scenarios.

Distance of Fault from CO ₂ Injection Well (km)	Time to leakage detection after start of injection	Total amount of CO ₂ injected until leakage detection (Mt)	Leakage into shallow aquifer without remediation (tonnes) (Leakage over total mass injected)	Leakage into shallow aquifer with remediation (tonnes) (Leakage over total mass injected)	Remediation achieved against leakage without remediation
1	8 months	0.66	6,240 (9.5%)	5,043 (7.6%)	19.2%
2	12 months	1.00	11,346 (11.3%)	6,096 (6.1%)	46.3%
3	18 months	1.50	40,892 (27.3%)	27,684 (18.5%)	32.3%

As planned, the performance of brine injection as a remediation measure for CO₂ leakage was evaluated by estimating the cost of implementing the scenarios considered here (USEPA, 2010; IEAGHG, 2011; Element Energy, 2012). Furthermore, the response time, spatial extent and length of remediation process were also assessed. These findings are presented in Table 11.

Table 11. Key Performance Indicators for brine injection (1Mt brine injection).

Location of sub-seismic fault with respect to the Injection well	Amount of brine injected (Mt)	Length of remediation (days)	Response time to remediation* (days)	Estimated cost (€)	Spatial extend of remediation# (km ²)
1km	1.0	360	30	640,000	2.80
2km	1.0	360	60		
3km	1.0	360	330		

*Response time: The time it takes for the leakage profile in the shallow aquifer to change through brine injection.

Spatial extent of remediation: The area covered by the injected fluid at the top layer of the reservoir at the end of 12 months injection period.

The results have shown that brine injection causes an increase in dissolution which consequently reduces the amount of mobile CO₂ available for leakage to the shallow aquifer. The comparison of CO₂ plume migration results between the un-remediated case (without brine injection) and remediated case (with brine injection) for 1km and 2km fault scenarios suggest that, with brine injection, the leakage of CO₂ from the sub-seismic fault has been effectively stopped. For the 3km fault scenario, however, CO₂ plume migration results suggest that, with brine injection, there is a reduction in the amount of CO₂ leakage to the shallow aquifer. Additionally, the gas saturation plots also show that without brine injection, more CO₂ migrates through the leaky fault and into the shallow aquifer. On the other hand, with brine injection, a higher gas saturation is retained in the reservoir. Naturally, reservoir topography and the heterogeneity introduced in the model also played a role on the results obtained from the three scenarios.

Further investigation on the flow diversion performance of brine injection for the 3km fault scenario was carried out by changing the injection rate as well as injection period. The results suggest that there is a limited benefit from flow diversion that can be achieved with longer term brine injection. The results were evaluated using four key performance indicators (KPI), namely: response time to remediation, length of remediation, spatial extent of remediation and remediation cost.

4 BRINE/WATER INJECTION AS A FLOW DIVERSION OPTION IN A CO₂ STORAGE OPERATION (GFZ)

The GFZ carried out a brine injection experiment at the pilot site for CO₂ storage at Ketzin. Between 12. Oct. 2015 and 6. Jan. 2016 a total amount of 2884 tons of brine were injected into the CO₂ reservoir (Möller et al., 2016). The experiment aimed to evaluate the use of brine injection as remediation technique. It could be carried out with existing equipment from oil and gas industry and requires less preparation compared to other remediation methods. Therefore it allows rapid action in case of leakage. Brine injection does not achieve a durable remediation effect, wherefore it must be followed by a permanently acting technique.

Ketzin is the first CO₂ storage site where a large amount of liquid was injected into a CO₂ reservoir. Therefore the experiment was operationally and scientifically challenging and addresses four main objectives:

1. Development of a technical setup
The field operation has not been carried out before. A technical setup for safe and reliable brine injection had to be developed. This should prevent reservoir damage and ensure monitoring of all relevant physical and chemical parameters.
2. Assessment of remediation impact
The oil and gas industry inactivate gas-filled wells in a so called kill operation by injection of heavy liquids. This injection typically aims at the well itself and therefore has a limited duration. The current experiment does not only aim at the well but also at the reservoir. The effective remediation time shall be determined to provide a timeframe in which to prepare further remediation measures.
3. Multiphase flow simulation
Prior to injection of CO₂ the reservoir was filled with brine. This brine is partly replaced by the injected CO₂, but residual brine remains in the rock matrix. This process is called drainage. The injection of brine into a reservoir that was previously drained by CO₂ replaces only a ratio of the CO₂ with the newly injected brine while a residual concentration of CO₂ phase remains in the pores. This process is called imbibition. On a lab scale these processes are well described (Bachu and Bennion, 2008). The residual CO₂ phase in the pores is commonly referred to as capillary-trapped CO₂. It is very important to consider the residual CO₂ also on the field scale.
4. Evaluate the potential of geoelectric monitoring
The injection well is equipped with a downhole geoelectrical array (Schmidt-Hattenberger et al., 2011). The injection brine changes the reservoir resistivity by replacing the low conductive CO₂ with highly conductive brine. The natural reservoir brine has a slightly lower conductivity than the injection brine and is also replaced during the imbibition process. It is investigated to which extent these processes can be monitored with geoelectric methods.

4.1 Technical setup

The brine injection was carried out between 12. Oct. 2015 and 6. Jan. 2016 with a total amount of 2884 tons of brine being injected. The equipment was provided and the technical operation was carried out by UGS Geotechnologiesysteme (Mittenwalde, Germany).

The brine was made oxygen free with sodium sulfite, delivered by trucks and pumped into the brine storage tanks on site (Figure 45). From these the brine was pumped by electric pumps through candle filters, electrical conductivity measurement and a coriolis flow meter to the wellhead of Ktzi 201 (Figure 46).

The maximum pressure was 81.15 bar at the reservoir reference level of 630 m, the maximum allowable reservoir pressure is 85 bar. During the test the following brine parameters were continuously recorded: mass flux, cumulated mass, density, temperature and electrical conductivity. Further, pressure was monitored at 550 m below ground level in the injection well. The average conductivity of the brine was 250 mS/cm, the mean density was 1.17 kg/dm³ with only minor temporal variations.



Figure 45. Installation of the storage tanks with 35 m³ capacity each. The left tank acts as backup.

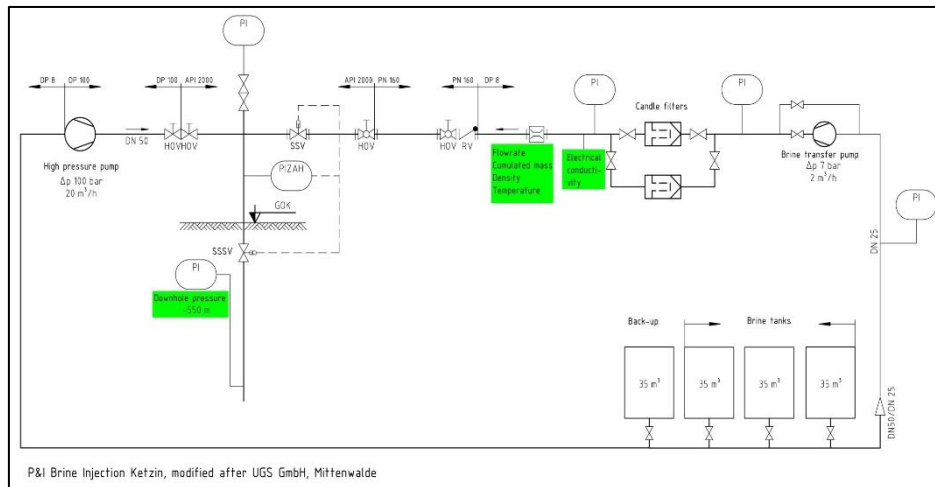


Figure 46. Flow chart of technical installations used for the brine injection. Green fields indicate gauges.

The most demanding point of the operation is the so-called well killing. The borehole is filled with CO₂ gas and the head pressure is about 50 bars. This pressure was to be exceeded with the amount of 4.7 tons of brine with a high injection rate, to fill the well with brine and entrain all gas bubbles with the brine into the reservoir. The operation was carried out with a high performance diesel-powered piston pump. After the successful operation the liquid column decreases below wellhead level and pumping was switched to the electrical centrifugal pump.

The target rate was 1400 kg/h until the 9th of November (Figure 47). From this time two pumps were cascaded to increase the injection rate. The rate shows higher variations due to interruptions for testing different pumps, pump failures and repairs. In the following period the rate was adjusted manually to maximize injection rate and simultaneously to ensure that the pressure does not exceed 81 bars at reservoir level.

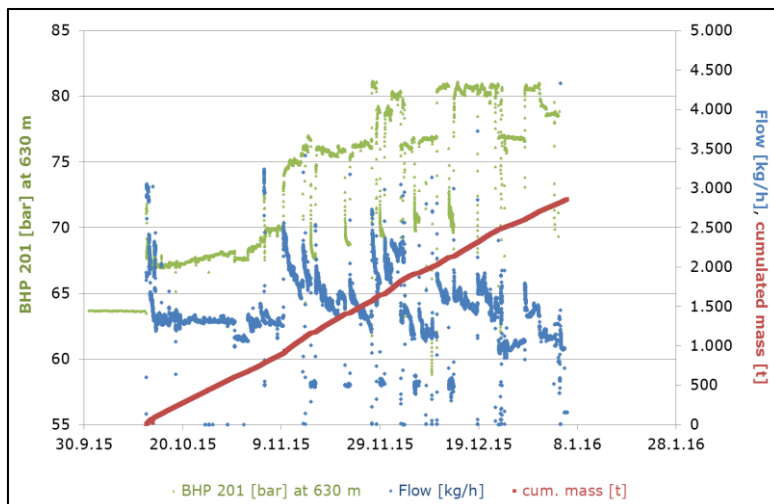


Figure 47. Overview on the operational parameters during the injection period.

4.2 Assessment of remediation impact

One of the key questions is the a priori estimation of the possible injection rate. As a first approximation the experiment is compared a pre-injection pumping (production) test (Wiese et al., 2010). This allows the application of characteristic numbers that provide a general overview to the operator. The injection test shows a larger differential pressure and longer duration compared with the pre-injection pumping test (Table 12). Nevertheless, the tests are comparable with respect to injectivity. The productivity index decreased from values slightly lower than 1 (m³/hr/bar) in the first minutes to a pseudostatic value of about 0.25 m³/hr/bar during the pumping test. Similarly, the values decreased from 0.77 in the first minutes to about 0.35 during the first week of brine injection (Figure 48). Within the next 5 weeks the productivity index decreases almost linearly to 0.1. Within the next 7 weeks the index decreases more slowly to 0.07. During a pumping test a productivity index is determined, during an injection test an injectivity index is determined. Both values are physically equivalent and therefore used synonymous in the following.

Table 12. Comparison of the key characteristics of the pre-injection pumping test in Ktzi 201 and the brine injection (injection test) 8 years later.

	Pumping Test	Injection Test
Date	Sep 2007	Oct 2015 - Jan 2016
Volume [m ³]	71	2414
Duration [d]	2.7	85
Max. differential pressure [bar]	-4.5	+17
Mean rate [m ³ /d]	26.3	28.4

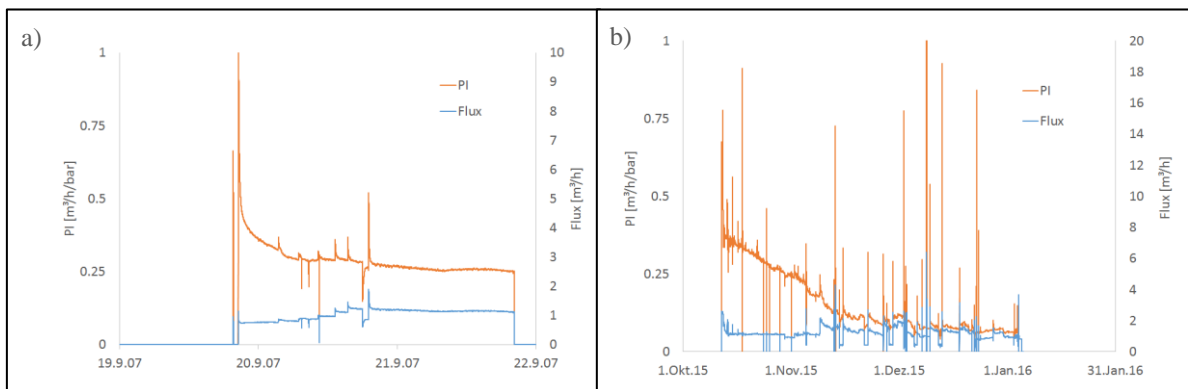


Figure 48. Productivity index PI (orange, left axis) and pumping rate (blue, right axis) for the pumping test (a) and the brine injection (b). Please note that the productivity index has the same y- scale on both figures, but can only be compared for the first days, since the brine injection had a much longer duration.

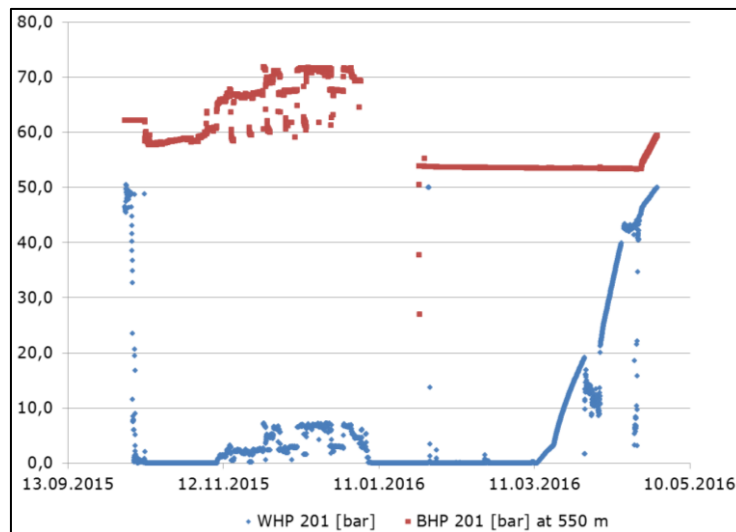


Figure 49. Wellhead (WHP) and bottomhole (BHP) pressure at the injection well Ktzi 201 between beginning of the brine injection and re-establishment of saturated CO₂ conditions.

During injection, the brine replaced the CO₂ in the injection well until the 11. March 2016, in total slightly more than two months (Figure 49). During this time there is no mobile CO₂ present in the reservoir at the location of the injection well. From this point CO₂ starts trickling back into the well and it takes one month to fill the volume of 2.5 m³ between the wellhead and 550 m depth. Re-drainage opens only small preferential flow paths, therefore it is a slow process. It has to be taken into account that the center of mass of the CO₂ plume migrated away from the well Ktzi 201 in a north-western direction and the reservoir pressure was already again close to the pre-injection values.

4.3 Multiphase flow simulation

A multiphase flow model of the Ketzin reservoir has been set up. The model comprises an area of 5x5 km. The model comprises four permeable layers of which the two upper layers are the main reservoir layers and two minor layers located below (Figure 50). It is based on the hydrogeophysical model presented by Wiese et al., (in short), and follows its spatial extent and discretisation. The intrinsic permeability of the sandstone facies is calibrated and spatially distributed. The relative permeability curvature parameters of a Brooks-Corey parameterization are also calibrated.

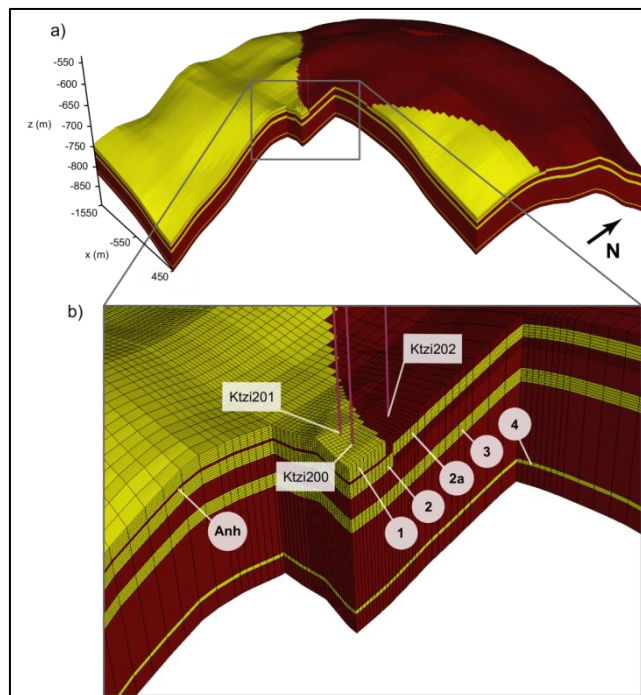


Figure 50. (a) Model domain of the Ketzin reservoir model. The yellow colour indicates sandstone facies with good reservoir quality, the brown colour indicates mudstone with poor reservoir quality. (b) The vertical distribution of reservoir facies in the vicinity of the wells.

Some modifications were introduced to the existing model in order to meet the requirements of the brine injection. The model of Wiese et al. (in short) comprises the first 270 days of Ketzin injection history until the arrival of CO₂ in all observation wells. To include the brine injection, it was necessary to include the entire reservoir injection history and the brine injection itself. The model represents the operation between June 2008 and October 2016.

The model is calibrated to the extended duration with the goal to match the pressure of three pre-injection cross-hole pumping tests (of which the injectivity of the injection well is calculated in the previous section, see Figure 48a) and reservoir pressure at the injection well Ktzi 201. The pressure match for the latter is shown in Figure 51. The pressure match shows a satisfying fit during the entire injection history. The trend of the pressure level is well matched for the entire injection history between 2008 until 2013. Also the short term pressure fluctuations that occur on variations of the injection rate have the same magnitude for observed and calibrated values.

The simulated pressure fluctuations during the brine injection test at the end of 2015/beginning of 2016, however, show a magnitude that is significantly smaller than observed fluctuations. The calibration model does not take into account the complex drainage and imbibition processes that are mathematically described with hysteresis. During brine injection residual CO₂ remains in the largest pores and therefore reduces the relative permeability compared with previous conditions. This effect is simulated with a further reservoir model. The resulting pressure curves are shown in Figure 52.

It can be seen that the hysteresis model shows a much stronger pressure response to the brine injection than the model without hysteresis. However, the response is still significantly too small to explain the high pressure dynamics in the reservoir.

The significant mismatch between a calibrated reservoir model including hysteresis and the pressure response of the brine injection is remarkable. A possible reason for the mismatch is the model discretisation of 10 m grid size in the vicinity of the injection well Ktzi 201. A finer resolution may be required to capture fine scale saturation changes and therefore impact the pressure indirectly by the relative permeability. Another reason may be the presence of cemented fractures, as hypothesized by Wiese et al., 2010. For saturated conditions they have a smaller permeability compared to the dominating sandstone facies. Under alternating saturations, these cemented areas may trap residual CO₂ more efficiently due to the smaller pore size and therefore are transformed to a practically impermeable matrix. Further simulations are required to test these hypotheses.

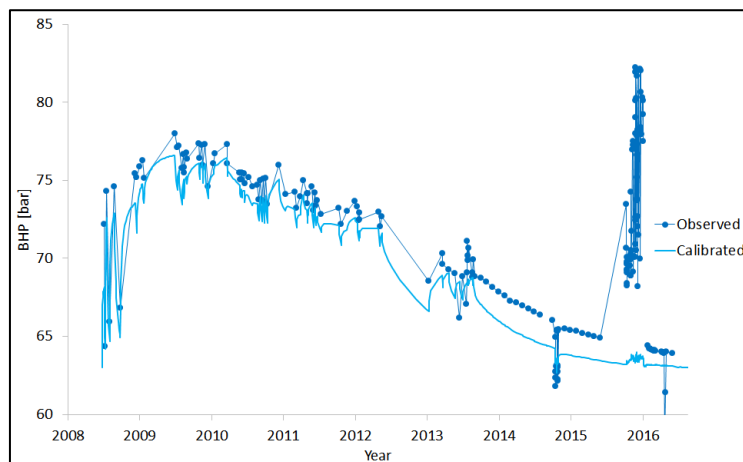


Figure 51. Observed and calibrated bottom-hole pressure of injection well Ktzi 201 for the entire injection history.

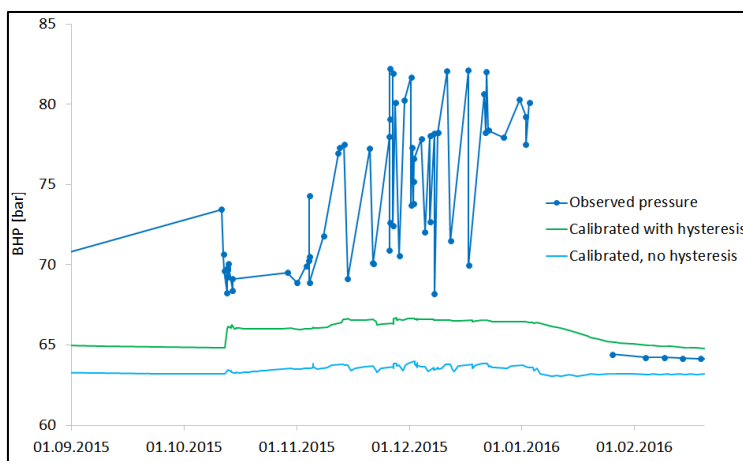


Figure 52. Observed and calibrated bottomhole pressure of injection well Ktzi 201 for the brine injection experiment. The calibration is carried out without and with hysteresis, the pressures are indicated by the light blue and green curve, respectively.

4.4 Geoelectrical Monitoring

The brine injection was monitored by geoelectric cross-hole measurements between wells Ktzi 200 and Ktzi 201 (Schmidt-Hattenberger et al., 2011). In addition to the 15 electrodes for each borehole, three newly installed permanent surface electrodes allows for surface-downhole measurements (Rippe et al., 2016).

A geoelectric baseline was measured directly before brine injection at the 5th Oct 2016. During the injection a combined dataset of cross-hole and surface-downhole measurements was obtained and allows a high temporal resolution. The measurement of such a combined dataset takes approximately 12 hours and passes all relevant AB-MN electrode configurations with a sufficient signal to noise ratio. This results in a dataset with daily resolution, which is inverted with respect to the baseline.

Furthermore, the contact resistances of each neighbored electrode pair are measured several times a day. This allows the coupling of the electrodes to the host rock and between each other to be quantified. Electrodes that are located in an open borehole annulus show a change of contact resistance on a change of the fluid. In the present situation a low contact resistance indicates that the electrodes are located in brine, and a high contact resistance indicates that the electrodes are located in CO₂. Electrodes that are located in concrete are not affected and show a constant contact resistance (Figure 53).

Electrodes in Ktzi 201 are located in an open annulus. The configurations #18-#19 and #19-#20 show a significant drop from 2000 to 50-60 ohm, which is reasonable since the injected brine replaces the CO₂. The uppermost electrode configuration #15-#16, however, shows a constant increase of the contact resistance from 100 to 300 ohm. This is caused by xanthan gum that resides in the borehole annulus due to operations during well drilling and combined accumulation of CO₂, since the borehole annulus is a dead end in the upwards direction. Changes in the contact resistance show a good correlation to the corresponding changes in the injection rate.

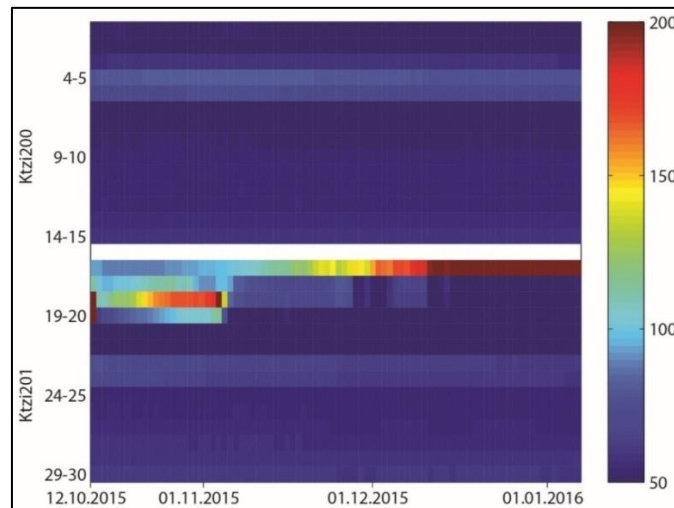


Figure 53. Contact resistances of well Ktzi 200 (upper graph) and Ktzi 201 (lower graph). Blue colour indicates low contact resistance, red colour indicates high contact resistance (Ohm). The largest changes occur for the upper four electrode configurations in well Ktzi 201.

The first tomographic time-lapse inversions of the cross-hole measurements carried out by Rippe et al., 2016, show decreasing resistivities in the reservoir compared to the baseline and therefore show the displacement (imbibition) of the reservoir CO₂ by the injected brine (Figure 54). Due to the open annulus the smallest resistivities are in the vicinity of the injection well, following the highest brine saturation there. However, the values for the baseline and the injection are comparable. Probably the lower borehole electrodes were filled with brine from the beginning. The inversion results show a lower resistivity between both wells at reservoir elevation. The temporal development is shown in the lower part of Figure 54. The decrease is not continuous but resembles a step function. These steps may be induced by rapid changes in the pumping rate that occurred during a pump failure. At changing pressure the steps may be induced by rapid mobilization of CO₂ due to formation of preferential flow paths.

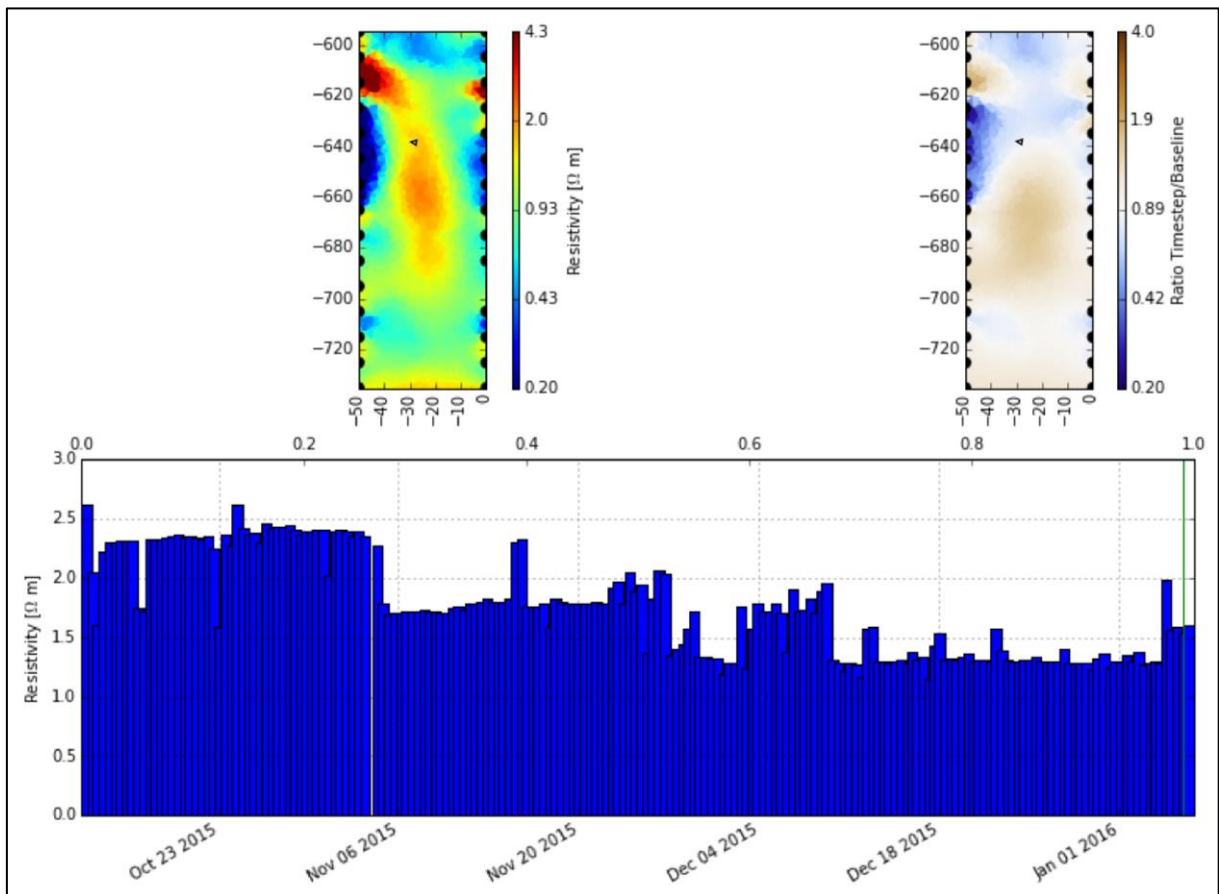


Figure 54. Tomographic time lapse inversion of the cross-hole measurements for the last day of brine injection (top left) compared to the baseline a few days before brine injection (top right). The lower bar chart shows the temporal resistivity development of a model cell between both wells. The cell is located in the reservoir, the position is indicated by a small black triangle in the cross sections.

4.5 Conclusions

The brine injection experiment was carried out successfully. The well was successfully killed with a high power diesel piston pump. The operational procedures were appropriate to inject 2884 t of brine between 12. Oct. 2015 and the 6. Jan. 2016. The well was maintained brine filled during the entire operation, also during short interruptions on the scale of several hours due to pump failures. The injectivity was similar to pre-injection values. This is somehow surprising, as pre-injection values have been determined with single phase a pumping test. The additional physical processes due to multiphase flow and hysteresis approximately cancel out each other.

First simulation attempts have been carried out. A reservoir model was calibrated to the CO₂ injection history. However, the model is not appropriate to reproduce the pressure response during the brine injection experiment. A slight improvement could be achieved by considering hysteresis. Geoelectrical monitoring can reproduce the general trend of higher electrical conductivity due to higher brine concentration and shows a close correlation to the injection dynamics. Temporally some discontinuities occur for which the underlying processes cannot be definitely identified. Further simulations aim to combining hydraulic and geoelectrical simulations to obtain a better constrained inverse problem and get an improved understanding of the drainage and imbibition processes.

5 MITIGATION BY WATER INJECTION AND CO₂ WITHDRAWAL (TNO)

5.1 Introduction

In Deliverable 3.2 “Adaptation of injection strategy as flow diversion option” two critical scenarios were created in which unwanted migration of CO₂ appeared. These scenarios serve as the base case for the mitigation simulations using brine/water injection and/or CO₂ withdrawal considered in this part of the report.

For completeness the setup and the description of the Johansen model described in Deliverable D3.2 is included in this report.

In the next section the reservoir simulator is described including the critical scenarios.

5.1.1 Description of the Johansen formation

The field under consideration for this study is the Johansen formation, located off the coast of Norway (*Figure 55*). The aquifer is located at a depth of 2100-2400 m with an average thickness of roughly 100m (Eigestad et al, 2009, Christiansen et al, 2009). The lateral extent is about 100 km in the North-South direction and 60 km in the east-west direction. The average porosity is approximately 20-25 percent and permeability ranging from 64 to 1660 mDarcy. A theoretical storage capacity of >1Gton is estimated by Eigestad et al. (2009).

The area of most interest is around the Troll field (red lines in *Figure 55*), which is located in the upper part of the aquifer. In this way the storage project can benefit from most of the existing infrastructure and is also close to the CO₂ source in Mongstad.

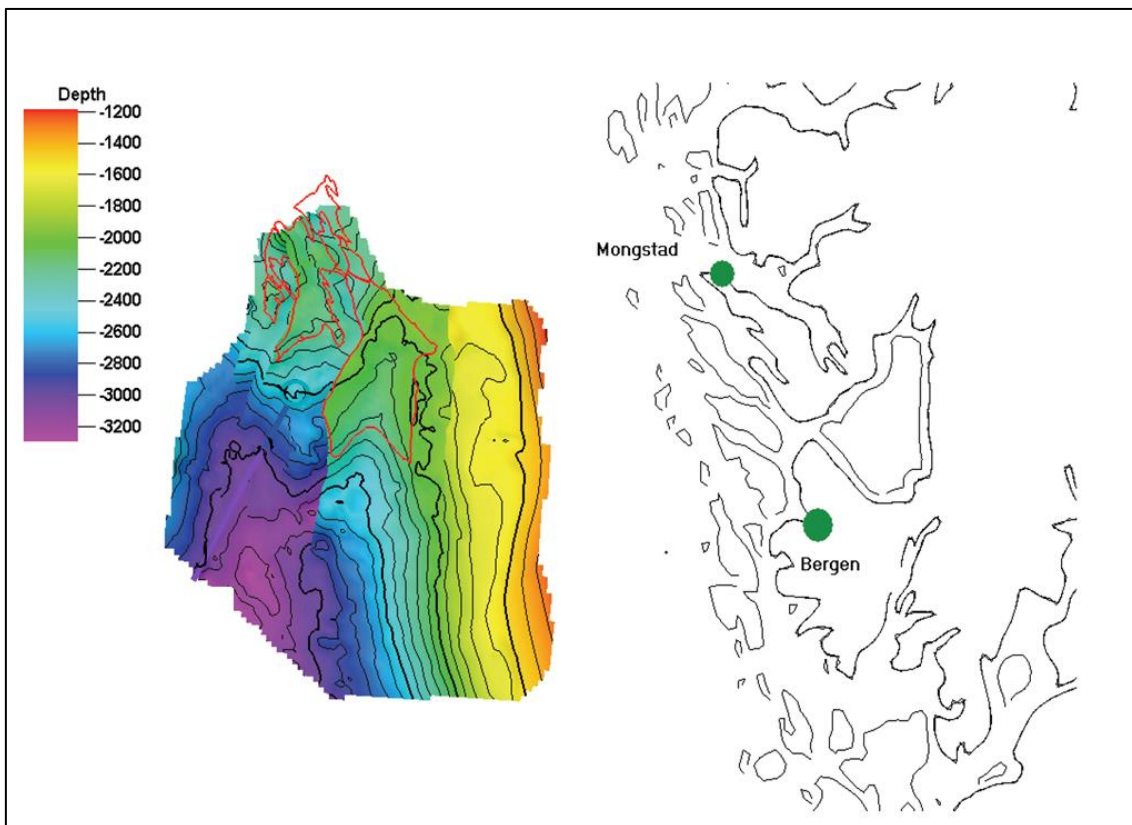


Figure 55. Depth map of the top of the Johansen formation and its location, with respect to the coast of Norway. (from Bergmo et al, 2009).

5.2 Method

In Deliverable 3.2 “Adaptation of injection strategy as flow diversion option” two critical scenarios were created in which unwanted migration of CO₂ appeared. These scenarios serve as a base case for the mitigation by brine/water injection as a flow diversion option.

5.2.1 Simulator used Schlumberger’s Eclipse 100 black-oil simulator

For the dynamic modeling of the Johansen field we have used Schlumberger’s Eclipse black-oil simulator (also known as Eclipse 100). The Eclipse black-oil reservoir simulation software is a fully implicit, three-phase, three-dimensional, general purpose black-oil simulator. The black-oil model assumes that the reservoir fluids consist of three phases namely oil, water, and gas, with gas dissolving in oil. In our model we only enabled the water and the gas phases, representing water and CO₂ respectively. Dissolution of CO₂ is not considered.

The geological grid used in this study is described by Bergmo et al (2008). In this report we focus on a smaller area of the Johansen field and a section was made inactive, which can be seen in the number of grid blocks used in the final dynamic model.

Table 13: Overview of grid dimensions in the simulation model.

	Number grid blocks x-direction NX	Number grid blocks y-direction NY	Number grid blocks z-direction NZ	Total number of grid blocks	Number of active grid blocks
Dynamic grid	55	281	83	995,170	526,272

5.2.2 Pressure, Volume, Temperature (PVT) data

5.2.2.1 Gas PVT

For the Gas PVT we applied NIST data to generate tables based on an aquifer temperature of 94 °C (Bergmo et al, 2008).

The gas viscosity and the formation volume factor as function of pressure of the pure CO₂ are shown in *Figure 56* and *Figure 57*, respectively.

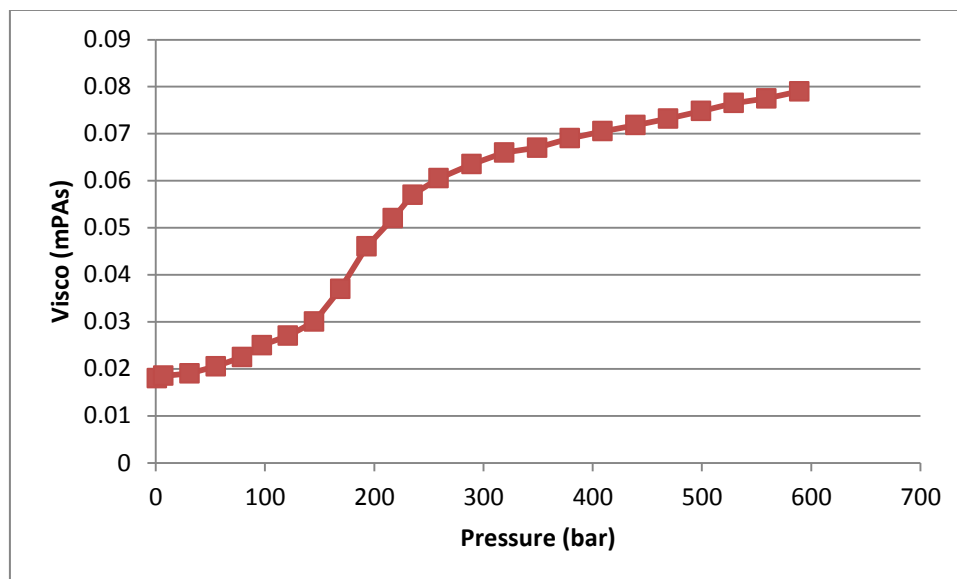


Figure 56. Viscosity of pure CO₂ as function of pressure, at a temperature of 94 °C.

5.2.2.2 Water PVT

The water formation volume factor is 1.0132 m³/m³ at reservoir conditions at a reference pressure of 215 bar. The water compressibility at reservoir conditions is 3.97954×10⁻⁵/bar. The water viscosity is 0.39851 (mPas) at a reference pressure of 215 bar.

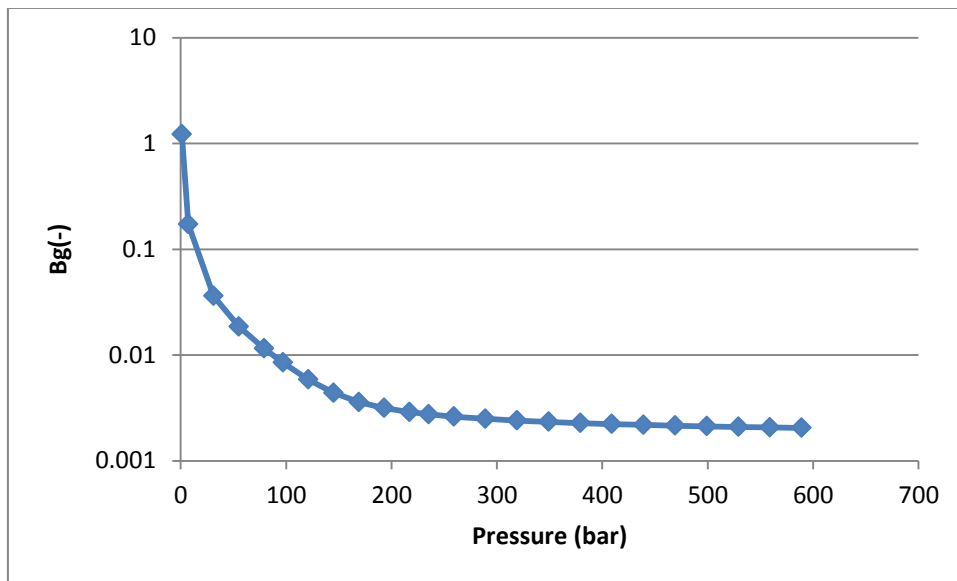


Figure 57. Reservoir volume factor (B_G) versus pressure, at a temperature of 94 °C.

5.2.3 Saturation functions and pressure dependent rock properties

5.2.3.1 Relative permeability

The relative permeability-saturation curves for the carbon dioxide were made hysteretic, by using the EHYSTER keyword in the Eclipse reservoir simulation software, with an entrapped non-wetting fluid saturation of 0.1 while those of the wetting fluid (brine) were left non-hysteretic (see Figure 58). This means that below a minimum CO₂ saturation (0.1 in this case), the gaseous phase is considered to be discontinuous and the relative permeability of the CO₂ phase goes to zero.

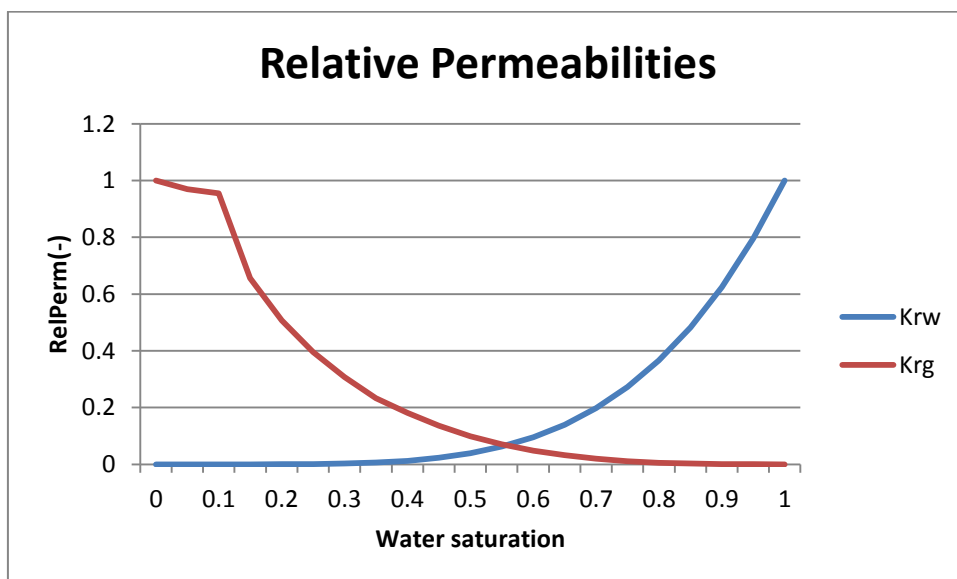


Figure 58. Original non-hysteretic relative permeability values, (based on a Dutch aquifer).

5.2.3.2 Capillary pressure

In our modelling we assumed the capillary pressure does not play an important role and was set to 0.

5.2.3.3 Rock Compressibility

The rock compressibility is set to standard value of 5.0e-5 1/bar at a reference pressure of 200 bar

5.2.4 Initial conditions

The starting point of the reservoir model was a static geological model of the Johansen aquifer, as supplied by Bergmo et al, 2008. From the complete model geological model only the western section was used with a total of 63x183x36 grid cells.

The reservoir is initially assumed to be in hydrodynamic equilibrium with a reservoir pressure of 220 bar at a depth of 2200 m and a reservoir temperature of 94 °C. We used an isothermal model, hence all temperature dependent fluid and rock properties are specified at reservoir temperature.

5.2.5 Well Locations

In all simulations 1.1 Mton CO₂ per year was injected for 113 years in layer 15-18 (which is the Johansen formation) of the model. Various injection locations were chosen and the resulting migration paths investigated for critical issues concerning the storage compartment integrity. To allow enough time for the migration the modelling was continued until the year 9000. The various injection locations are displayed in *Figure 59*.

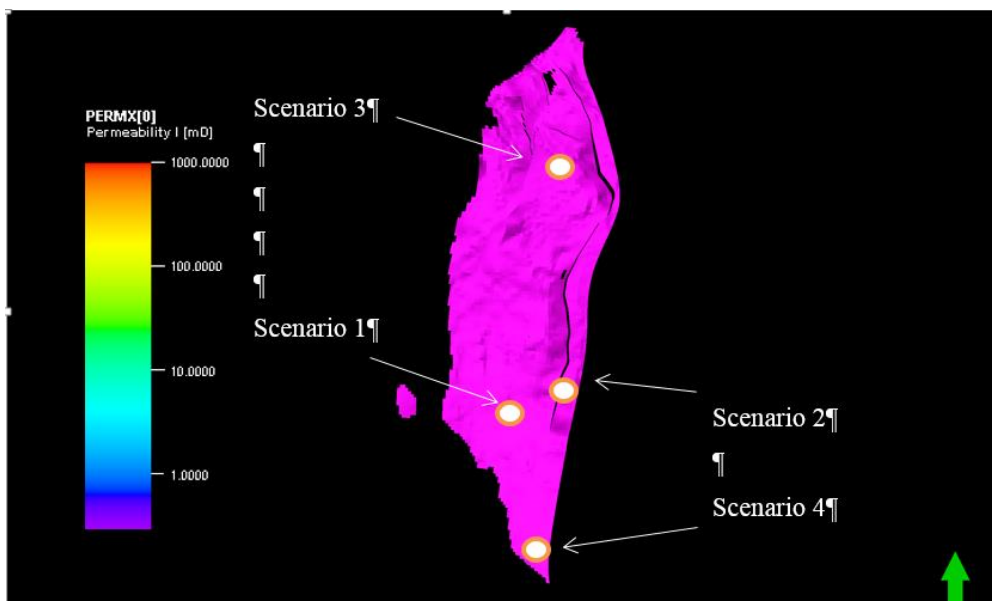


Figure 59. Plane view of layer 18 in the static model with the four hypothetical injector locations as used in this study.

5.2.6 Critical scenarios

5.2.6.1 Critical Scenario 1

In scenario 1 a well is placed down dip from a fault and the CO₂ starts migrating to the fault (*Figure 60*). We assume in this scenario the fault appears to be not sealing or safe and therefore corrective measures are needed.

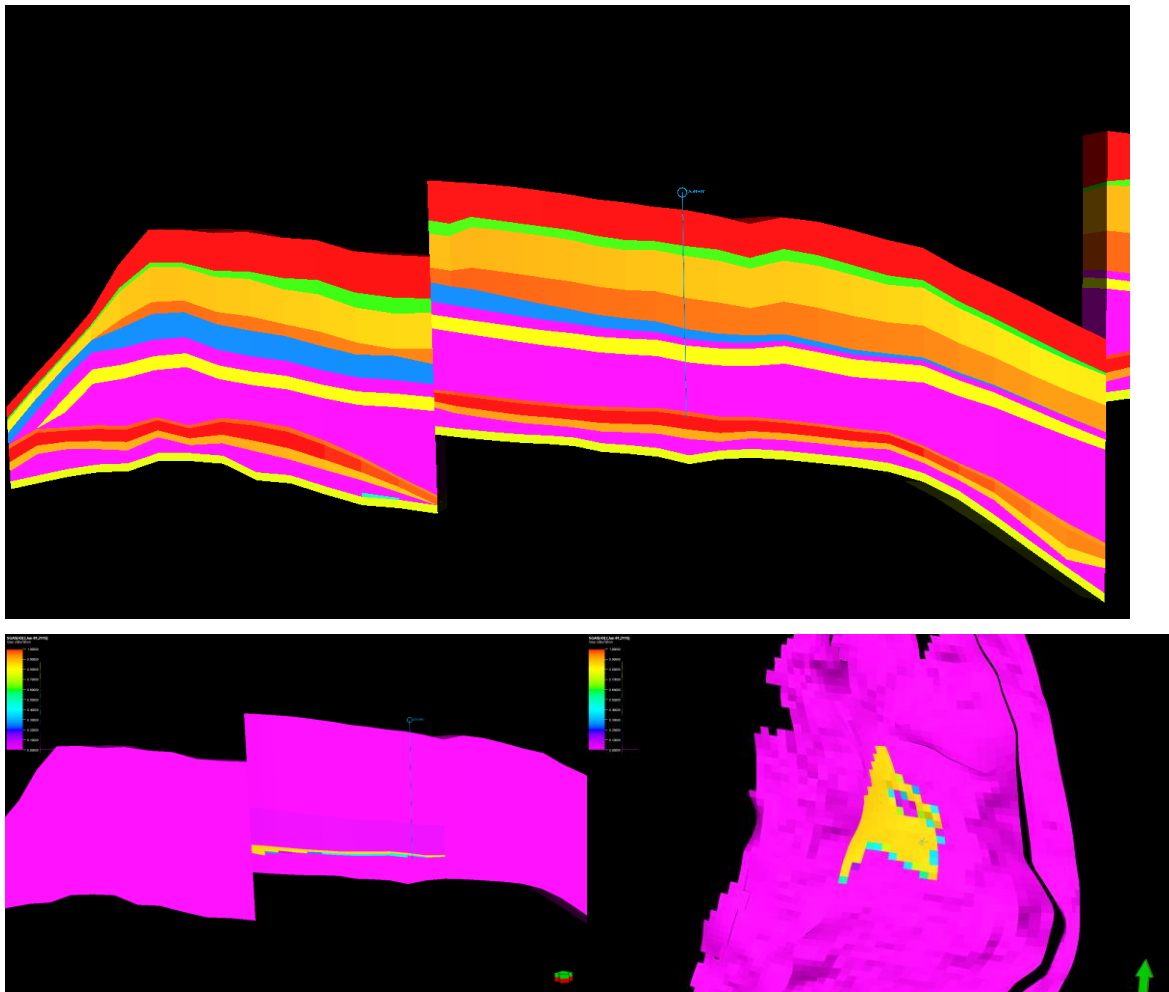


Figure 60. (top) Permeability (scale see Figure 61) (lower left) Sideview CO₂ migration after injection and (lower right) CO₂ migration top view after injection.

5.2.6.2 Critical Scenario 2

In the second critical scenario the injection well is placed in the eastern part of the model, close to a major fault. During injection the plume migrates from injector to the north along the fault with a large offset. These faults are usually sealing due to clay smearing. In our simulation we considered the migration along a fault not as a risk and no corrective measure is necessary. In *Figure 61* we observed that the Johansen formation varies in thickness laterally and becomes very thin just north of the injection well (*Figure 61*).

We identified this as a spill-point and the anticipated storage location is before the thin zone, where a pinch out almost occurs.

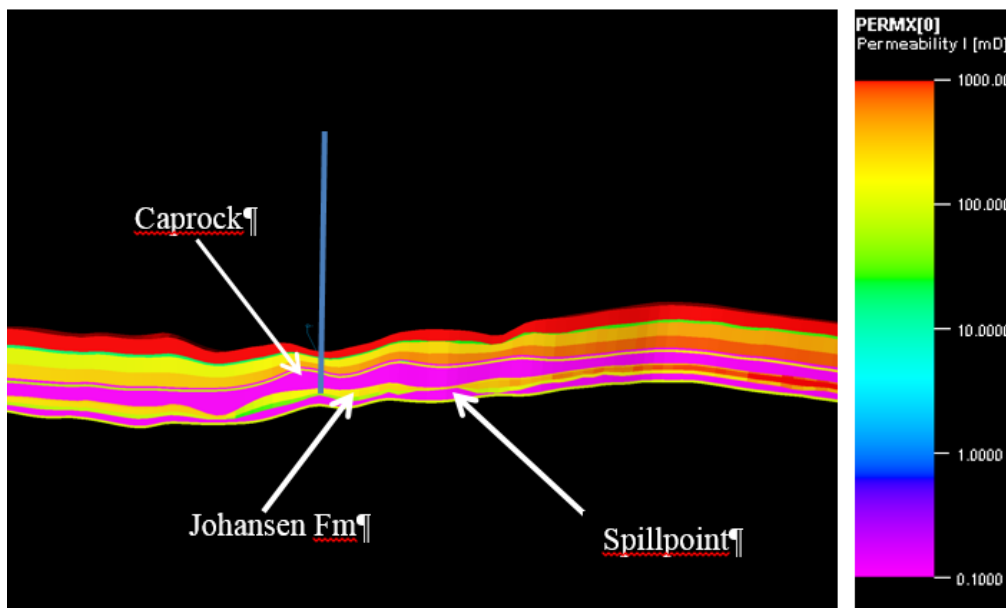


Figure 61. Permeability of scenario 2.

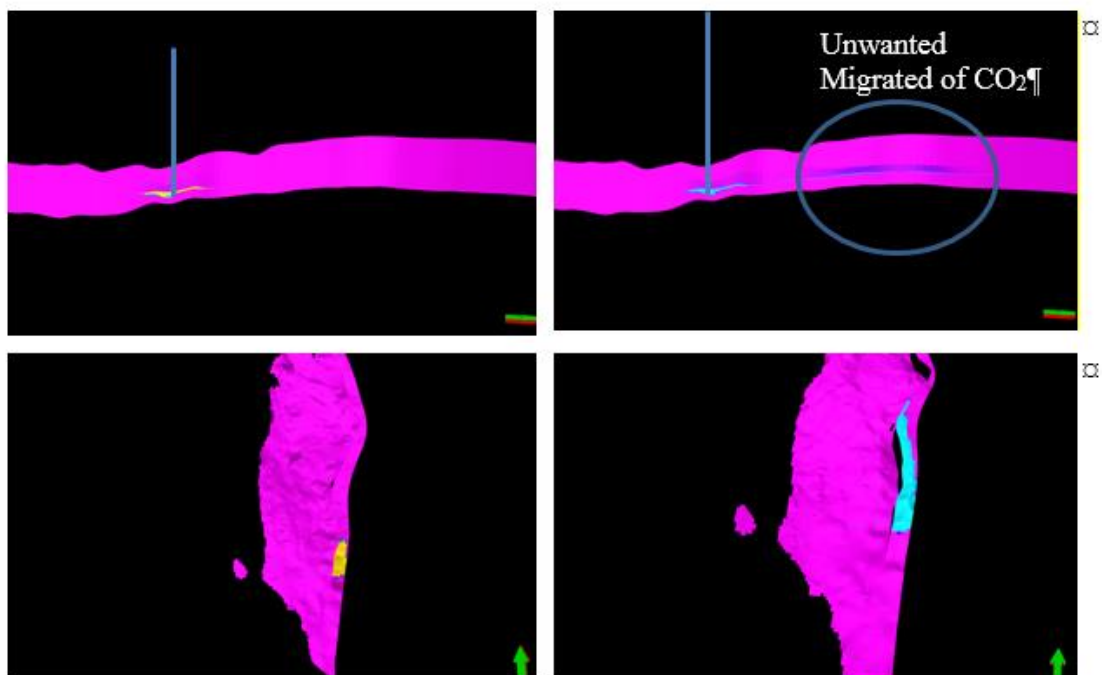


Figure 62. Gas saturation in scenario 2. Sideview directly after injection (top left) and after 9000 years (top right). Topview directly after injection (bottom left) and after 9000 years (bottom right).

Immediately after the injection period the CO₂ migrated within the intended storage zone (Figure 62). However after a longer period (now 9000 years is shown) the CO₂ migrated further to the north beyond the spill point. An unwanted migration and a corrective measure is needed here.

5.3 Results

5.3.1 Critical scenario 1

In critical scenario 1 the CO₂ is migrating into the direction of the fault, since the fault appears to be not sealing, a safety area around the fault is defined which we consider as unwanted migration, as shown in *Figure 63*.

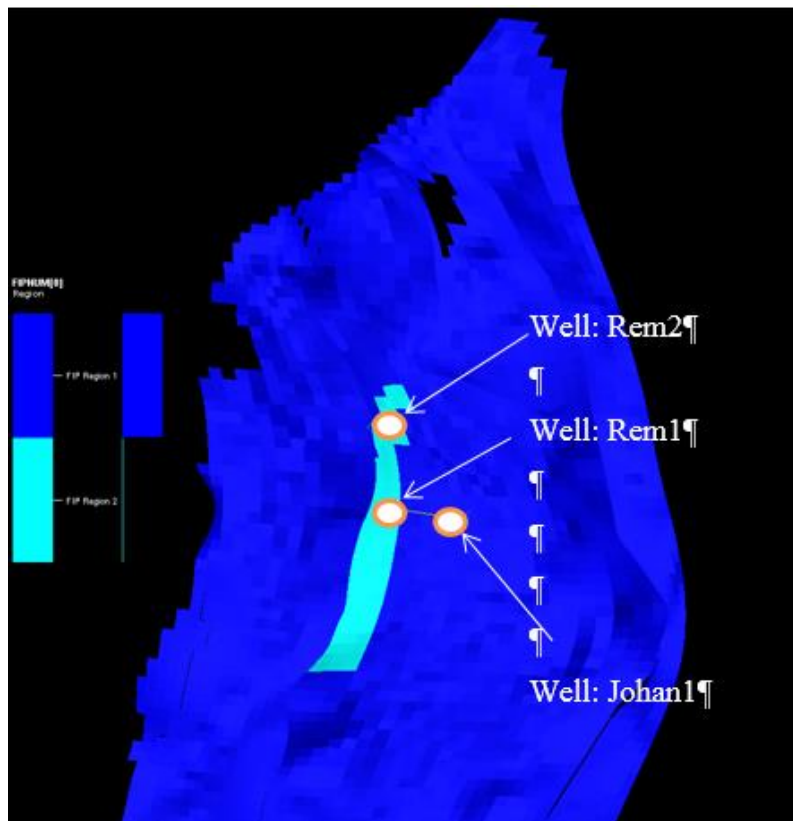


Figure 63. Safety area along the fault indicated in light blue and the CO₂ injection well Johan1 and the remediation wells Rem1, and Rem2.

An injection rate of 1Mton/yr was applied on the Johan1 well, after 17 years of injection unwanted migration was detected and the injection was stopped. The base case scenario is the “do nothing” scenario. No remediation is performed by water injection, but just monitoring of the CO₂ volumes migrating into the safety area defined in Figure 63. By comparing the mitigation scenarios to the base case scenario, it is possible to identify how efficient the mitigation strategy is. A short description of the mitigation scenarios is

given in *Table 14* and full results of the mitigation scenarios are given in Section 5.5 Appendix. The summary of the results is presented in the present section.

Table 14. Description of the mitigation scenarios.

Name scenario	Description	Injection control & production rate
Base Case	Injection of 1Mton/yr CO ₂ for 17 years and no water injection by the remediation wells, CO ₂ is monitored for the whole simulation period (91 years)	
Scenario 1	After detection of unwanted migration of CO ₂ , CO ₂ injection stopped and injection of water by one remediation well for 64 years	BHP constraint (10% above initial pressure, approximately 20.000 m ³ /day)
Scenario 2	After detection of unwanted migration of CO ₂ , CO ₂ injection stopped and injection of water by two remediation wells for 64 years	BHP constraint (10% above initial pressure, approximately 40.000 m ³ /day)
Scenario 3	After detection of unwanted migration of CO ₂ , CO ₂ injection stopped and injection of water by two remediation wells for 64 years and the second remediation well after 30 years.	BHP constraint (10% above initial pressure, approximately 20.000 m ³ /day)
Scenario 4	After detection of unwanted migration of CO ₂ , CO ₂ injection stopped and injection of water for 5 years by one remediation well	BHP constraint (10% above initial pressure, approximately 20.000 m ³ /day)
Scenario 5	After detection of unwanted migration of CO ₂ , CO ₂ injection stopped and injection of water for 10 years by one remediation well	BHP constraint (10% above initial pressure, approximately 20.000 m ³ /day)
Scenario 6	After detection of unwanted migration of CO ₂ , CO ₂ injection stopped and injection of water for 18 years by one remediation well	BHP constraint (10% above initial pressure, approximately 20.000 m ³ /day)
Scenario 7	After detection of unwanted migration of CO ₂ , CO ₂ injection stopped and back production started for a period of 50 years (gas rate constraint of 1 Mton/yr). Injection of water for 18 years by one well.	BHP constraint (10% above initial pressure, approximately 20.000 - 90.000 m ³ /day)
Scenario 8	After detection of unwanted migration of CO ₂ , CO ₂ injection stopped and back production started for a period of 50 years (gas rate constraint of 0.5Mt/yr). Injection of water for 18 years by one well.	BHP constraint (10% above initial pressure, approximately 20.000 - 90.000 m ³ /day)
Scenario 9	After detection of unwanted migration of CO ₂ , CO ₂ injection stopped and back production started for a period of 50 years (gas rate constraint of 1 Mton/yr). Injection of water for 10 years by one well.	BHP constraint (10% above initial pressure, approximately 20.000 - 90.000 m ³ /day)
Scenario 10	After detection of unwanted migration of CO ₂ , CO ₂ injection stopped and back production started for a period of 50 years (gas rate constraint of 1 Mton/yr). Injection of water for 10 years by one well.	5000 m ³ /day

The efficiency of the scenarios is defined as combination of the amount of water injected versus how much CO₂ has reached the safety zone around the fault (and is assumed to migrate to the fault). The safety zone is defined in Eclipse by the FIPNUM keyword and the CO₂ in this zone can be traced by the regional gas in place (RGIP) keyword. In Figure 63 the CO₂ volumes migrating into this safety zone is given for each individual scenario.

The base case scenario shows obviously the highest leakage rate. Scenarios 4,5 & 6 also show relatively high leakage rates (see *Figure 64*) compared to the other scenarios (scenario 1- 3 and 7-10). The reason for this is that these 3 scenarios have only 5, 10 and 18 years of water injection during the remediation period, which is relatively short compared to scenario 1-3. Obviously in scenario 7-10 back production of the CO₂ gives a lower migration to the fault.

The scenarios shows that injection of water for a short period is not a good remediation method for CO₂ leakage. It will only postpone the leakage and reduce the total amount of CO₂ migration for a few percent as can be seen in *Table 15*. The remediation method can be improved significantly by not only injecting water but also or back producing of the CO₂, which is performed in scenario 7-10.

The results of *Table 17* shows that the amount of CO₂ remediation by water injection is not an efficient option and the combination of back production and water injection is the most optimal approach.

Table 15. Results of the mitigation scenarios.

	% of the total amount of CO ₂ injected migrated to the safety zone	total CO ₂ leakage (Mton)	Cum CO ₂ back produced
Base_Case	15.42%	2.62	0.00%
Remediation_1	0.98%	0.17	0.00%
Remediation_2	0.28%	0.05	0.00%
Remediation_3	0.18%	0.03	0.00%
Remediation_4	12.06%	2.05	0.00%
Remediation_5	10.35%	1.76	0.00%
Remediation_6	8.00%	1.36	0.00%
Remediation_7	0.17%	0.03	66.79%
Remediation_8	0.17%	0.03	62.54%
Remediation_9	0.17%	0.03	68.34%
Remediation_10	0.40%	0.07	70.97%

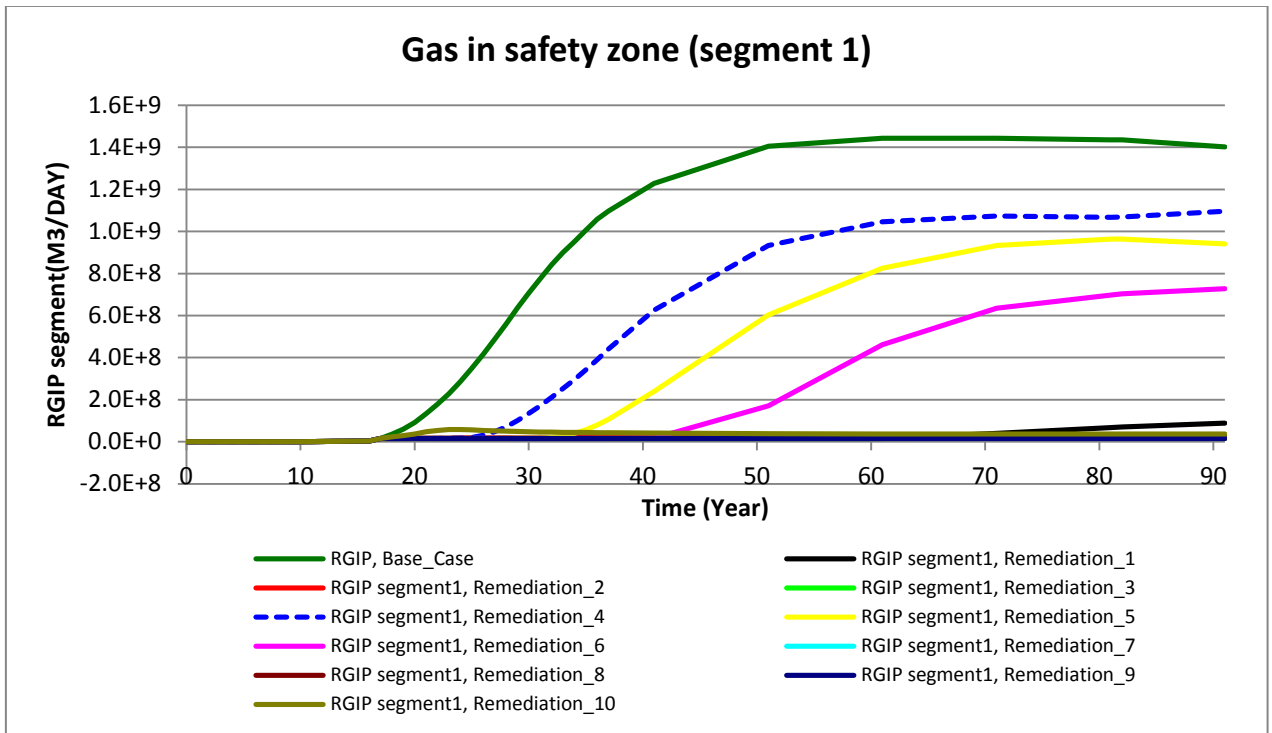


Figure 64. Gas in segment safety zone around the fault. Once the gas is in the safety area it is assumed to migrate to the fault.

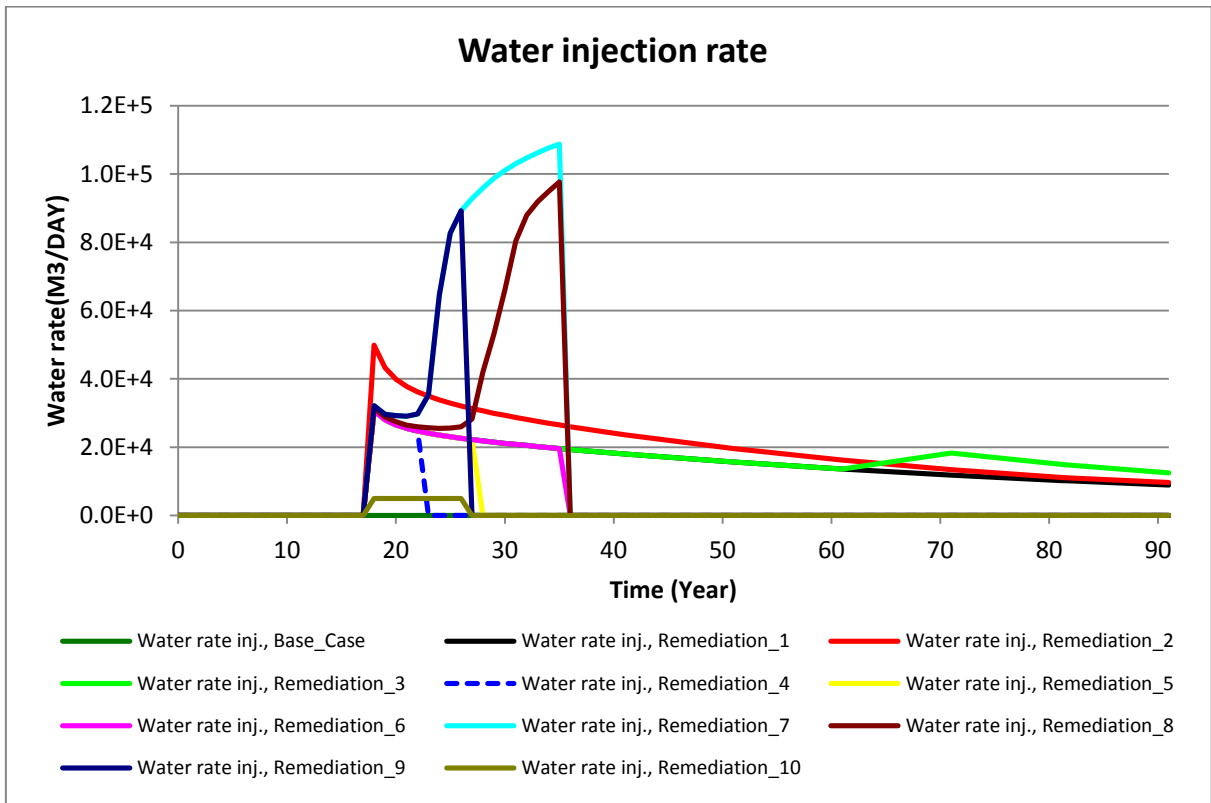


Figure 65. Water injection rate for the different mitigation scenarios.

5.4 Conclusions

After CO₂ leakage is observed the remediation technique by water injection only is not efficient and back production in combination with water injection is the most efficient option to avoid further migration of the CO₂ present in the aquifer near the spill point or fault.

5.5 Appendix

Table 16. Summary of the results of the mitigation scenarios.

	Total Water injected (SM3)	CO ₂ in segment 1 (SM3)	CO ₂ leaked to segment 2 (SM3)	total CO ₂ leakage reduction (SM3)	total CO ₂ in reservoir (SM3)	Cum water back produced (SM3)	Cum CO ₂ back produced (SM3)
Base_Case	0.00E+00	7.69E+09	1.40E+09	0.00E+00	9.09E+09	0.00E+00	0.00E+00
Remediation_1	4.30E+08	9.00E+09	8.93E+07	1.31E+09	9.09E+09	0.00E+00	0.00E+00
Remediation_2	5.57E+08	9.06E+09	2.59E+07	1.38E+09	9.09E+09	0.00E+00	0.00E+00
Remediation_3	4.95E+08	9.07E+09	1.68E+07	1.38E+09	9.09E+09	0.00E+00	0.00E+00
Remediation_4	5.15E+07	7.99E+09	1.10E+09	3.05E+08	9.09E+09	0.00E+00	0.00E+00
Remediation_5	9.40E+07	8.15E+09	9.41E+08	4.60E+08	9.09E+09	0.00E+00	0.00E+00
Remediation_6	1.55E+08	8.36E+09	7.27E+08	6.74E+08	9.09E+09	0.00E+00	0.00E+00
Remediation_7	4.83E+08	3.00E+09	1.54E+07	1.39E+09	3.02E+09	1.74E+09	6.07E+09
Remediation_8	3.18E+08	3.39E+09	1.56E+07	1.39E+09	3.40E+09	1.46E+09	5.68E+09
Remediation_9	1.48E+08	2.86E+09	1.51E+07	1.39E+09	2.87E+09	1.60E+09	6.21E+09
Remediation_10	1.64E+07	2.60E+09	3.65E+07	1.37E+09	2.64E+09	1.53E+09	6.45E+09

5.5.1 Remediation scenario 1

Table 17. Scenario description.

Scenario	Remediation 1
Description	After detection of unwanted migration of CO ₂ , CO ₂ injection stopped and injection of water by remediation well for 64 years (whole simulation period)

Table 18. Simulation settings.

General		Remarks
Begin simulation	0	(year)
End simulation	91	(year)
CO₂ Injection well	JOHAN1	
Constraints	Rate constraint: 1 Mton/yr BHP constraint 360*BAR	
Location	Vertical well in gridblock (x,y)→(45, 47)	
Perforation	Z-coordinates of gridblock (15-17)	
On stream	From 0 to 17 years	
Remediation well	REM 1	
Constraints	BHP constraint 234*BAR (10% above P initial)	
Location	Vertical well in gridblock (x,y)→(38, 47)	
Perforation	Z-coordinates of gridblock (15-17)	
On stream	From 18 to 91 years	

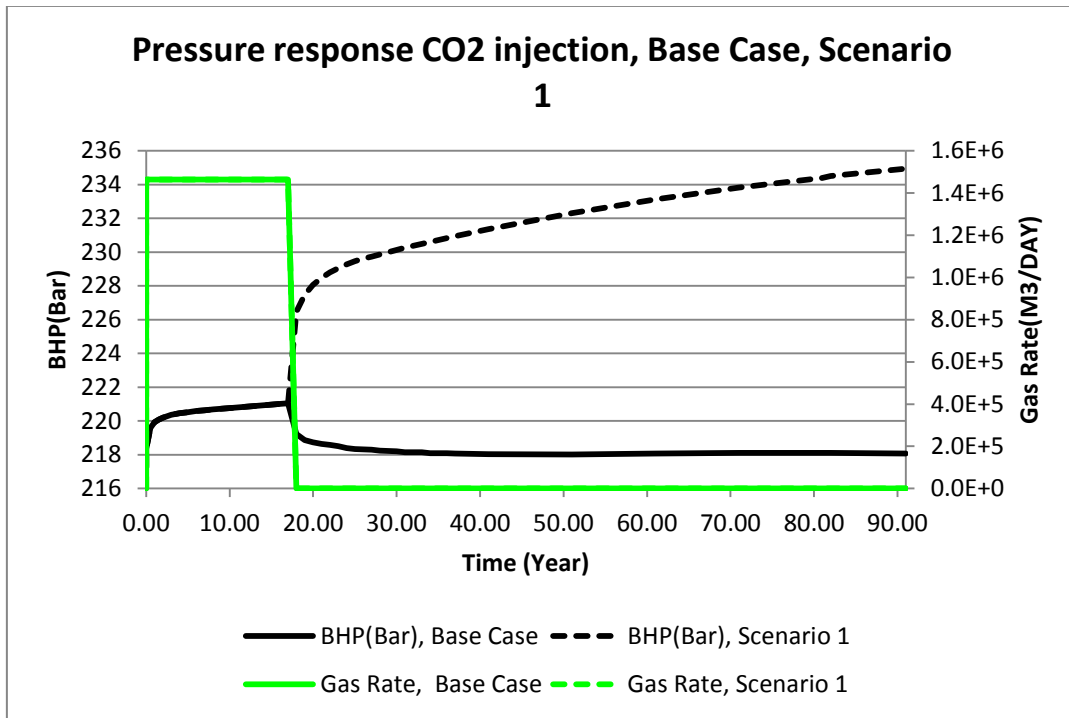


Figure 66. Gas injection rate and pressure response, compared to the base case (no remediation).

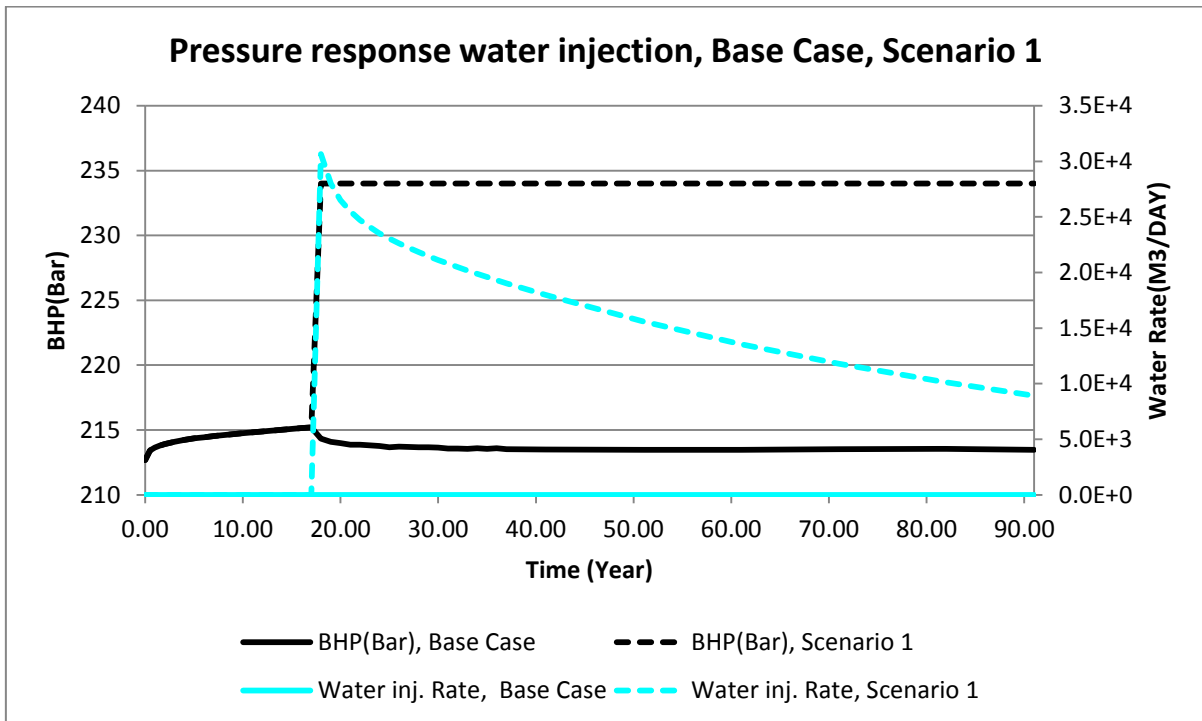


Figure 67. Water injection rates and cumulatives of well REM1, compared to the base case (no remediation) scenario.

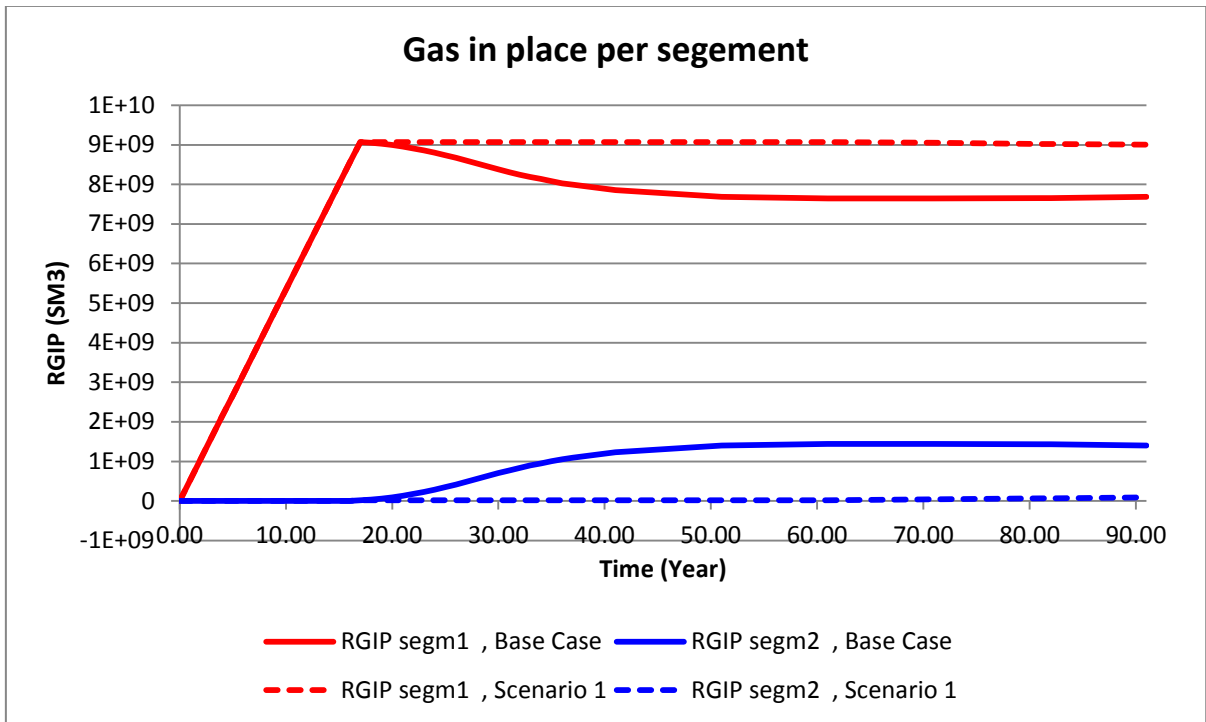


Figure 68. Unwanted migration to segment 2 compared to the base case (no remediation) scenario.

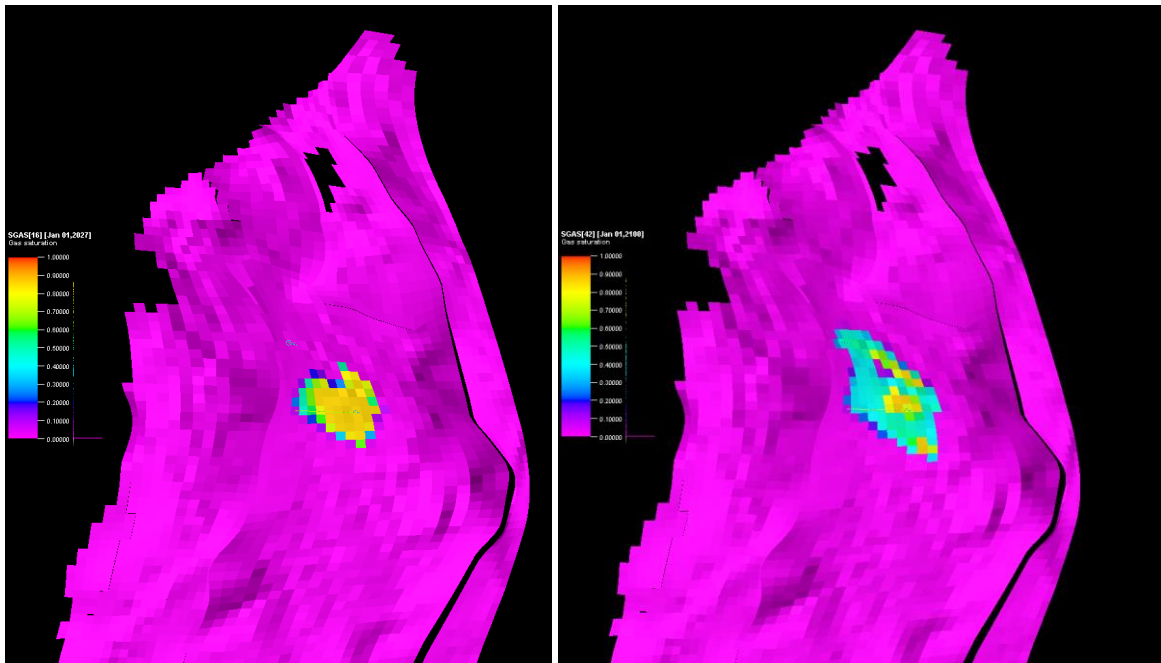


Figure 69. CO₂ plume after first detection of unwanted migration (right) CO₂ plume after 93 years

5.5.2 Remediation scenario 2

Table 19: Scenario description.

Scenario	Remediation 2
Description	After detection of unwanted migration of CO ₂ , CO ₂ injection stopped and injection of water by two remediation wells for 64 years (whole simulation period)

Table 20. Simulation settings.

General		Remarks
Begin simulation	0	(year)
End simulation	91	(year)
CO₂ Injection well		
JOHAN1		
Constraints	Rate constraint: 1 Mton/yr BHP constraint 360*BAR	
Location	Vertical well in gridblock (x,y)→(45, 47)	
Perforation	Z-coordinates of gridblock (15-17)	
On stream	From 0 to 17 years	
Remediation well		
REM 1		
Constraints	BHP constraint 234*BAR (10% above P initial)	
Location	Vertical well in gridblock (x,y)→(38, 47)	
Perforation	Z-coordinates of gridblock (15-17)	
On stream	From 18 to 91 years	
Remediation well		
REM 2		
Constraints	BHP constraint 234*BAR (10% above P initial)	
Location	Vertical well in gridblock (x,y)→(40, 40)	
Perforation	Z-coordinates of gridblock (15-17)	
On stream	From 18 to 91 years	

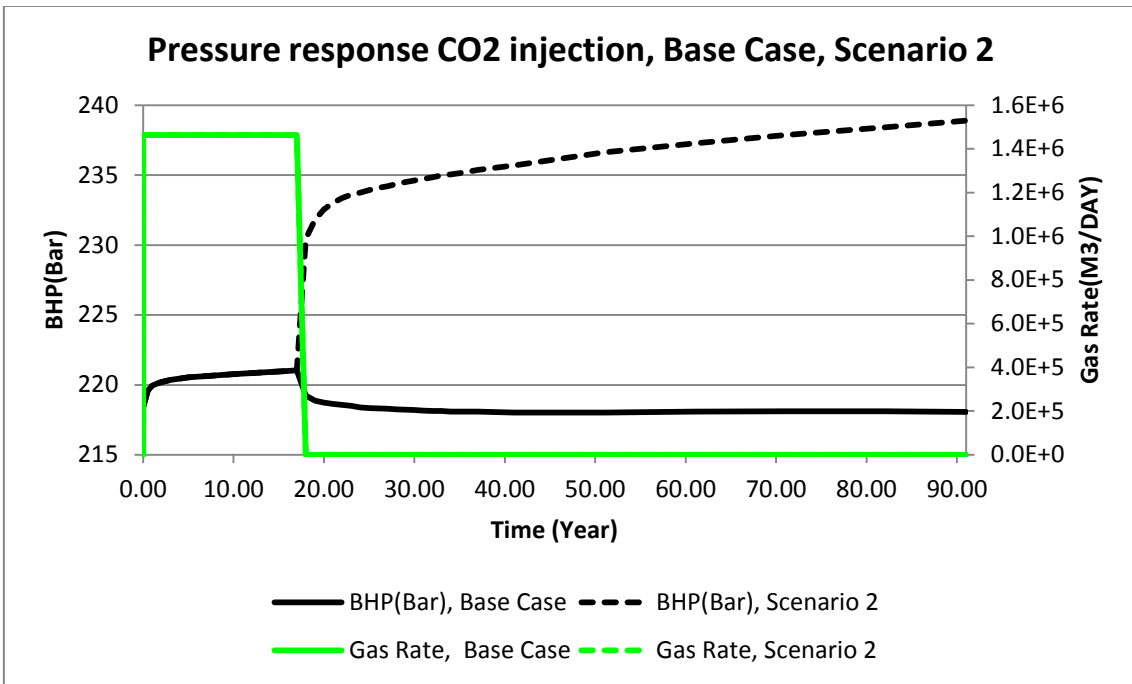


Figure 70. Gas injection rate and pressure response, compared to the base case (no remediation).

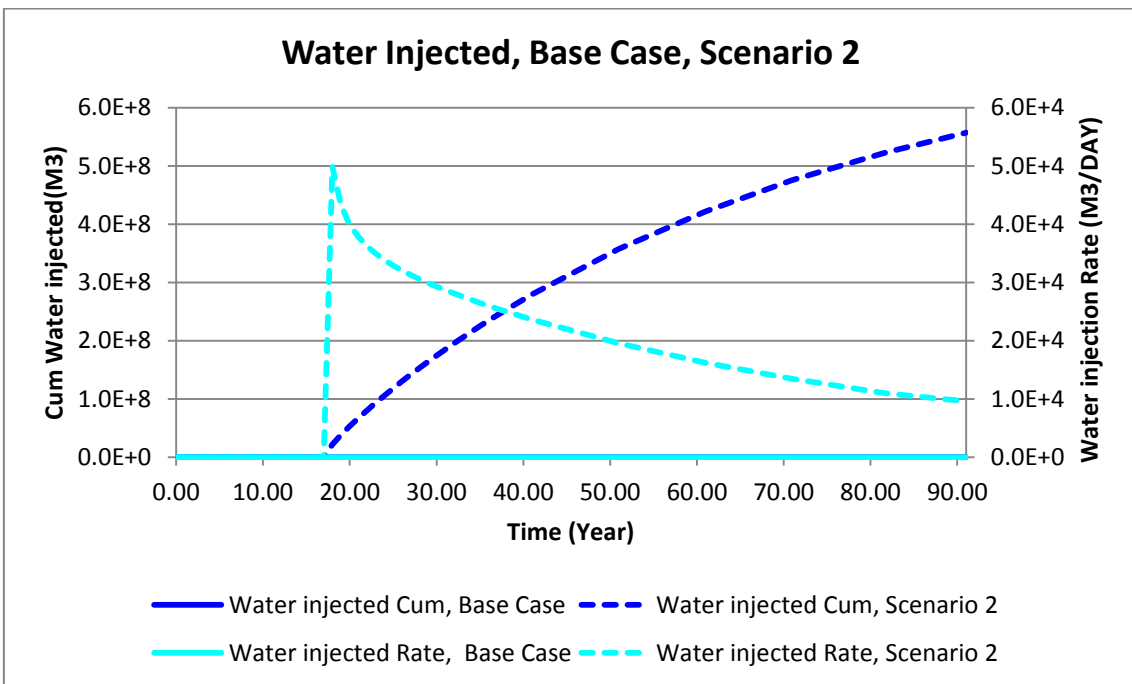


Figure 71. Water injection rates and cumulatives of well REM1, compared to the base case (no remediation) scenario.

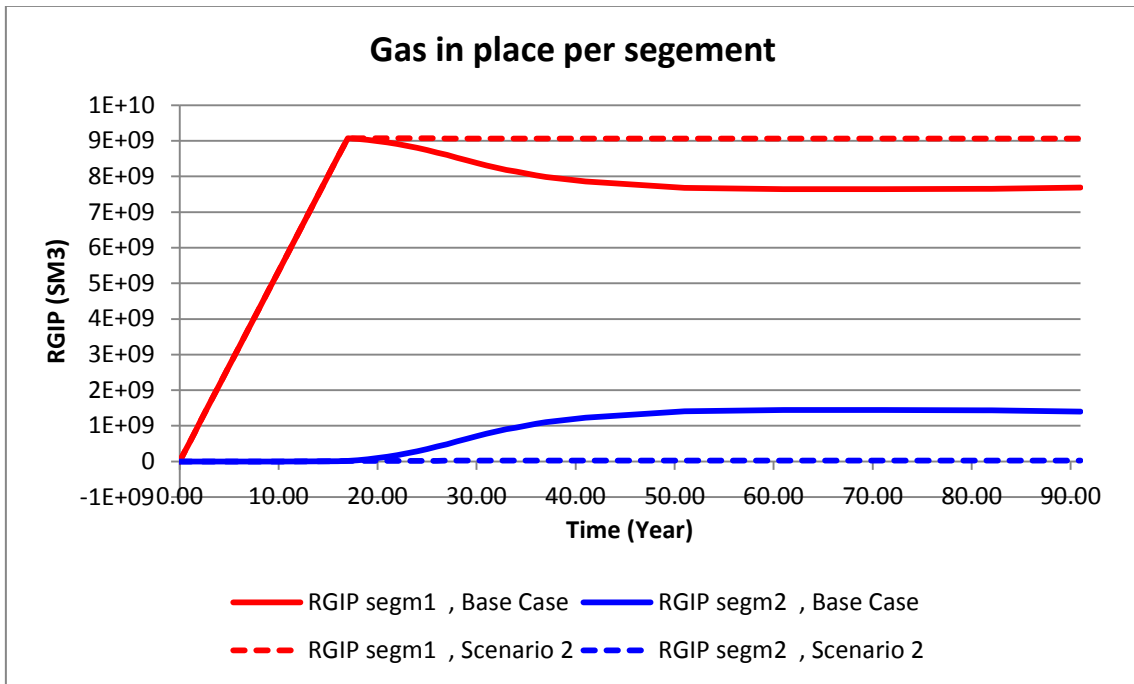


Figure 72. Unwanted migration to segment 2 compared to the base case (no remediation) scenario.

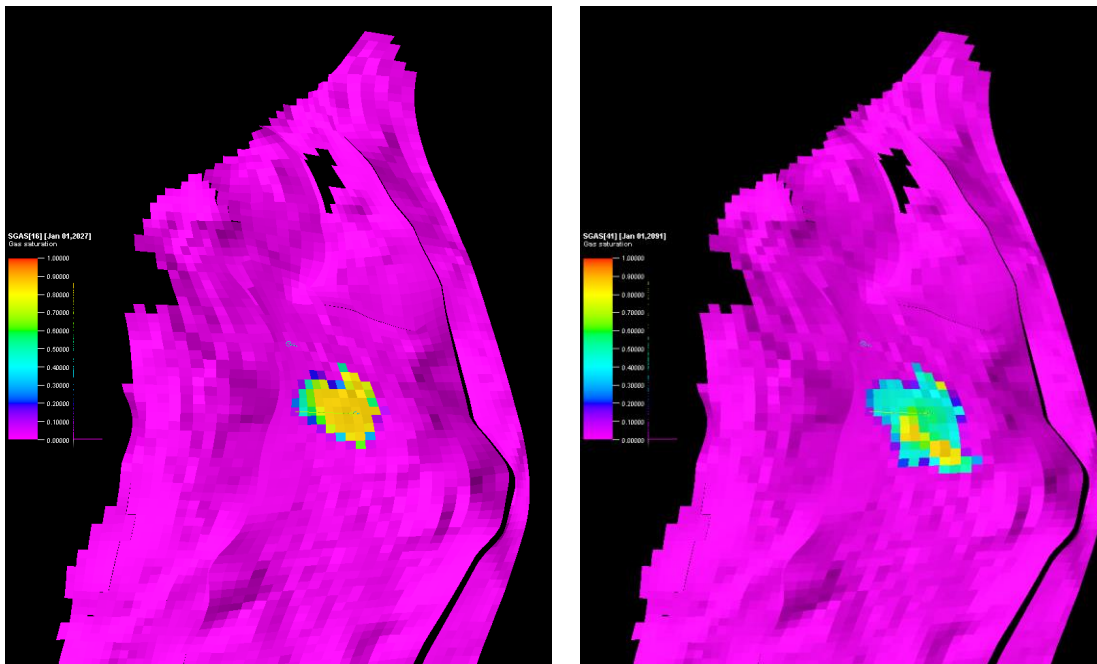


Figure 73. CO₂ plume after first detection of unwanted migration (left) and CO₂ plume after remediation at the end of simulation period of 93 years (right).

5.5.3 Remediation scenario 3

Table 21. Scenario description.

Scenario	Remediation 3
Description	After detection of unwanted migration of CO ₂ , CO ₂ injection stopped and injection for 64 years (whole simulation period)

Table 22. Simulation settings.

General		Remarks
Begin simulation	0	(year)
End simulation	91	(year)
CO₂ Injection well	JOHAN1	
Constraints	Rate constraint: 1 Mton/yr BHP constraint 360*BAR	
Location	Vertical well in gridblock (x,y)→(45, 47)	
Perforation	Z-coordinates of gridblock (15-17)	
On stream	From 0 to 17 years	
Remediation well	REM 1	
Constraints	BHP constraint 234*BAR (10% above P initial)	
Location	Vertical well in gridblock (x,y)→(38, 47)	
Perforation	Z-coordinates of gridblock (15-17)	
On stream	From 18 to 91 years	
Remediation well	REM 2	
Constraints	BHP constraint 234*BAR (10% above P initial)	
Location	Vertical well in gridblock (x,y)→(40, 40)	
Perforation	Z-coordinates of gridblock (15-17)	
On stream	From 61 to 91 years	

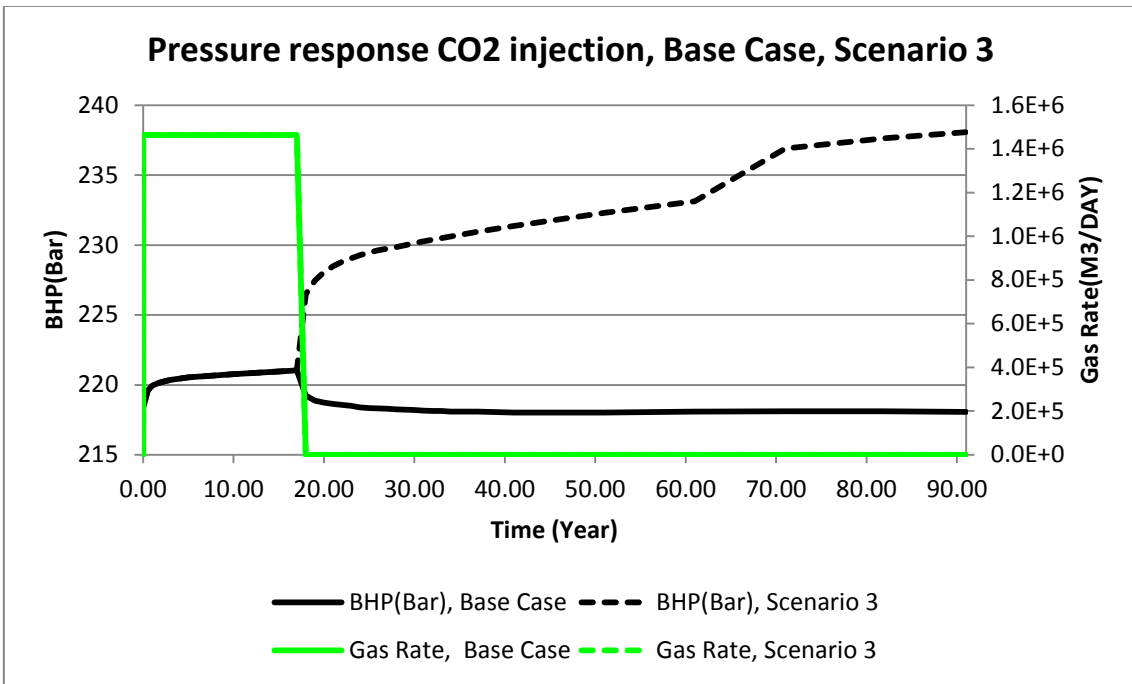


Figure 74. Gas injection rate and pressure response, compared to the base case (no remediation).

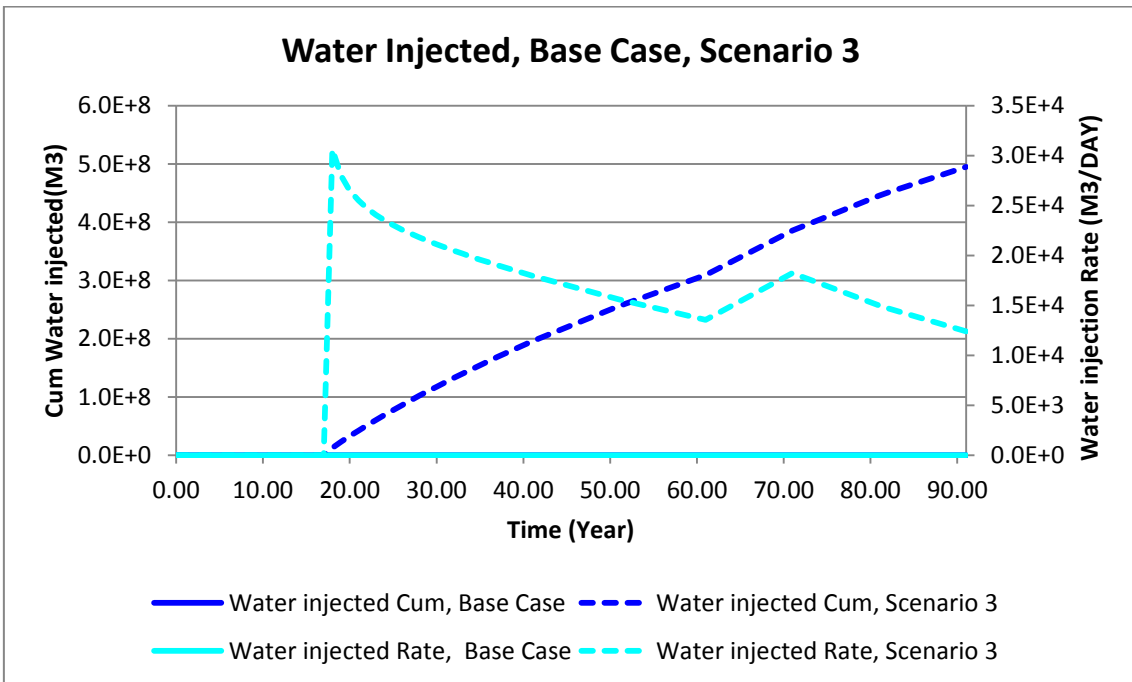


Figure 75. Water injection rates and cumulatives of well REM1, compared to the base case (no remediation) scenario.

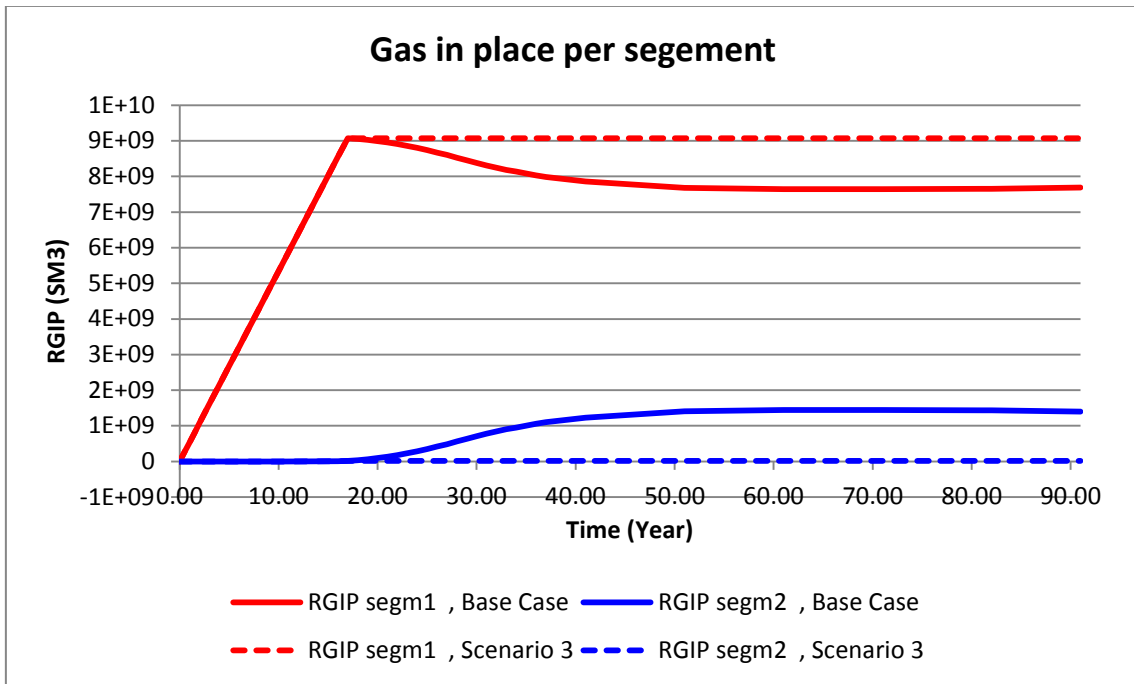


Figure 76. Unwanted migration to segment 2 compared to the base case (no remediation) scenario.

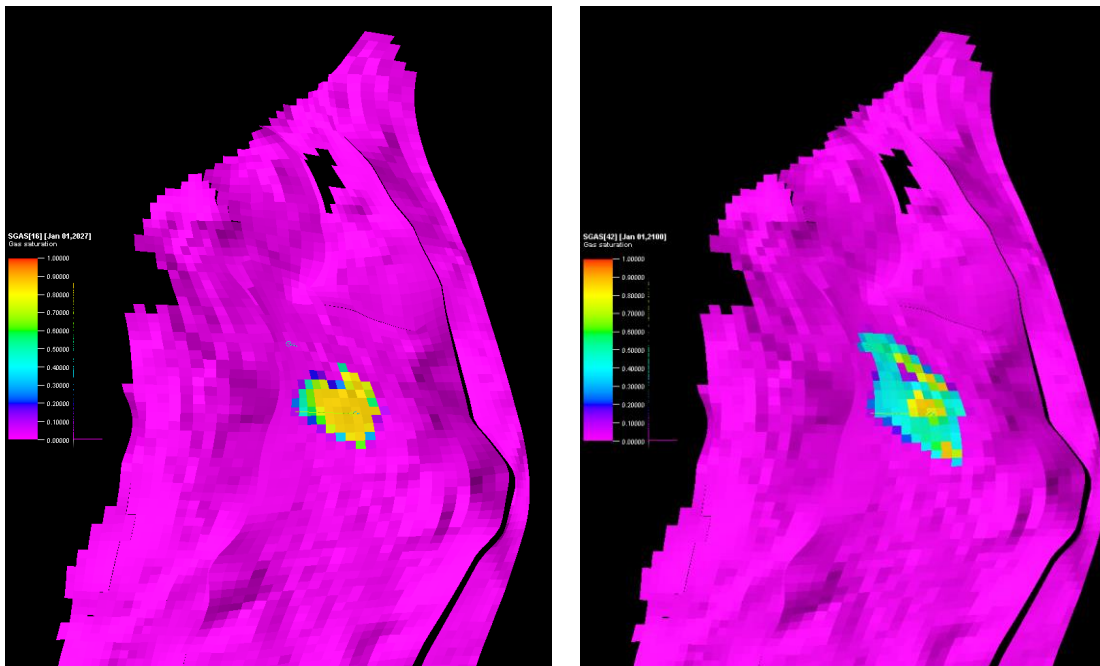


Figure 77. CO₂ plume after first detection of unwanted migration (left) and CO₂ plume after remediation at the end of simulation period of 93 years (right).

5.5.4 Remediation scenario 4

Table 23. Scenario description.

Scenario	Remediation 4
Description	After detection of unwanted migration of CO ₂ , CO ₂ injection stopped and injection of water for 5 years by one well

Table 24. Simulation settings.

General		Remarks
Begin simulation	0	(year)
End simulation	91	(year)
CO₂ Injection well	JOHAN1	
Constraints	Rate constraint: 1 Mton/yr BHP constraint 360*BAR	
Location	Vertical well in gridblock (x,y)→(45, 47)	
Perforation	Z-coordinates of gridblock (15-17)	
On stream	From 0 to 17 years	
Remediation well	REM 1	
Constraints	BHP constraint 234*BAR (10% above P initial)	
Location	Vertical well in gridblock (x,y)→(38, 47)	
Perforation	Z-coordinates of gridblock (15-17)	
On stream	From year 18 to year 23	

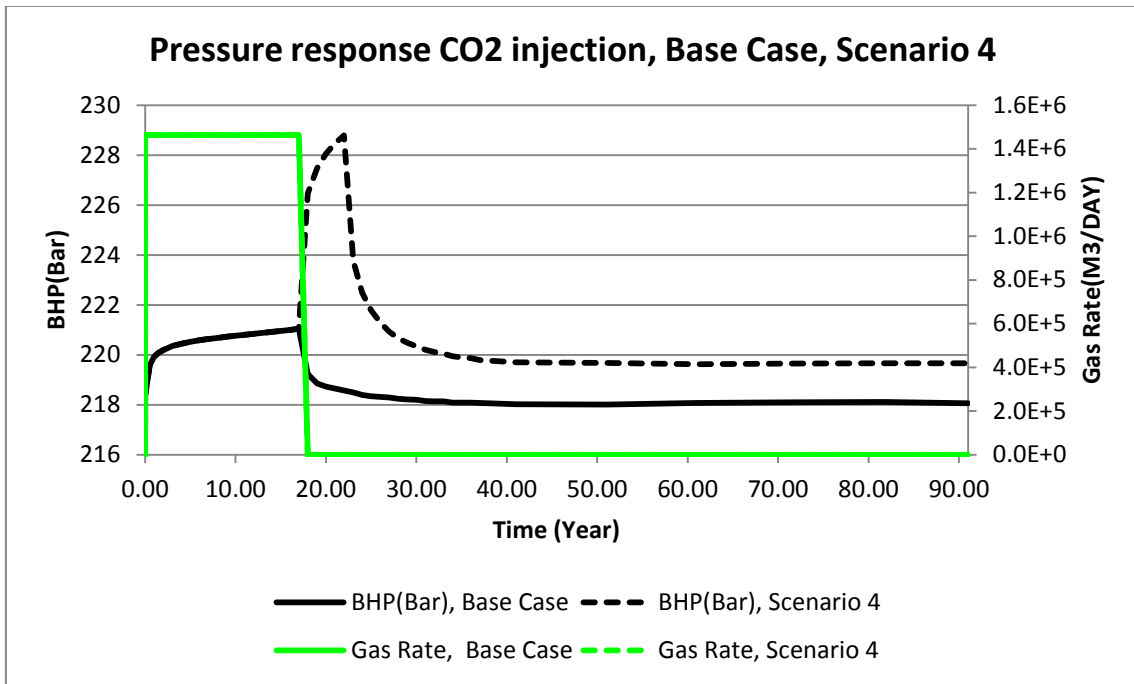


Figure 78. Gas injection rate and pressure response, compared to the base case (no remediation).

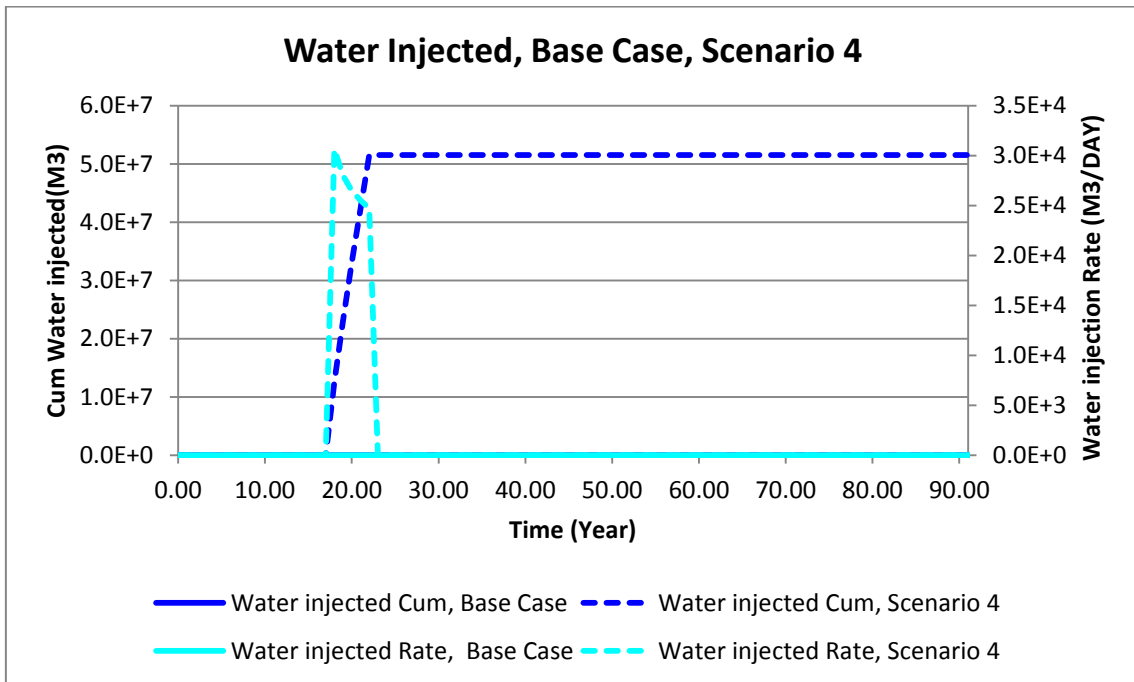


Figure 79. Water injection rates and cumulatives of well REM1, compared to the base case (no remediation) scenario.

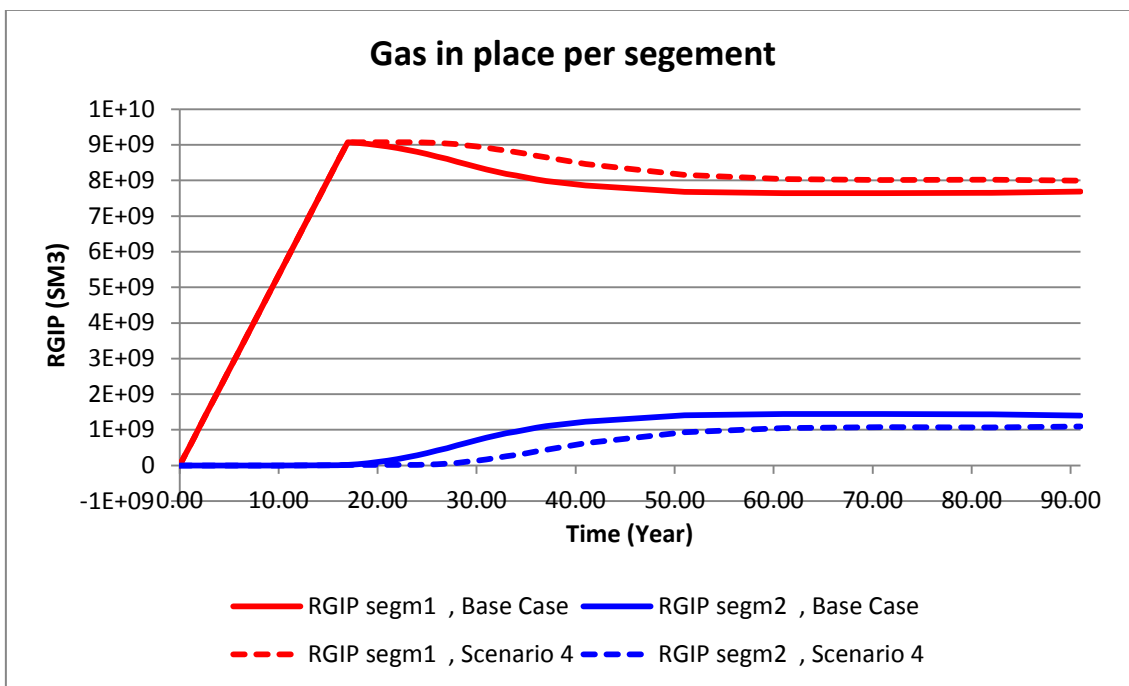


Figure 80. Unwanted migration to segment 2 compared to the base case (no remediation) scenario.

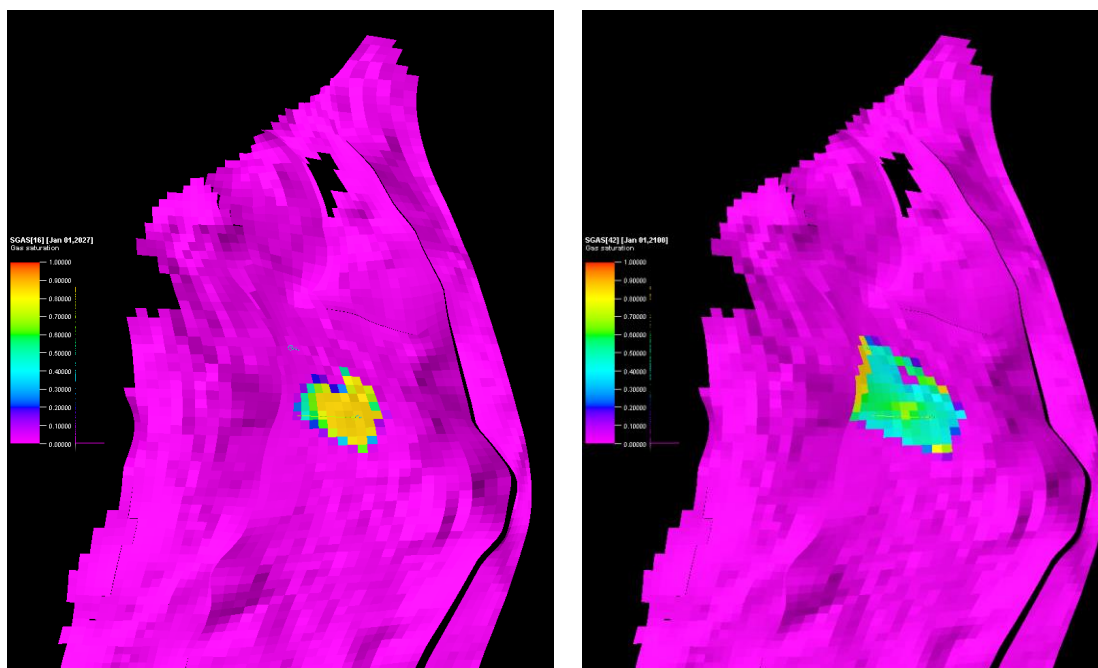


Figure 81. CO₂ plume after first detection of unwanted migration (left) and CO₂ plume after remediation at the end of simulation period of 93 years (right).

5.5.5 Remediation scenario 5

Table 25. Scenario description.

Scenario	Remediation 5
Description	After detection of unwanted migration of CO ₂ , Co ₂ injection stopped and injection of water for 10 years by one well

Table 26. Simulation settings.

General		Remarks
Begin simulation	0	(year)
End simulation	91	(year)
CO₂ Injection well	JOHAN1	
Constraints	Rate constraint: 1 Mton/yr BHP constraint 360*BAR	
Location	Vertical well in gridblock (x,y)→(45, 47)	
Perforation	Z-coordinates of gridblock (15-17)	
On stream	From 0 to 17 years	
Remediation well	REM 1	
Constraints	BHP constraint 234*BAR (10% above P initial)	
Location	Vertical well in gridblock (x,y)→(38, 47)	
Perforation	Z-coordinates of gridblock (15-17)	
On stream	From year 18 to year 23	

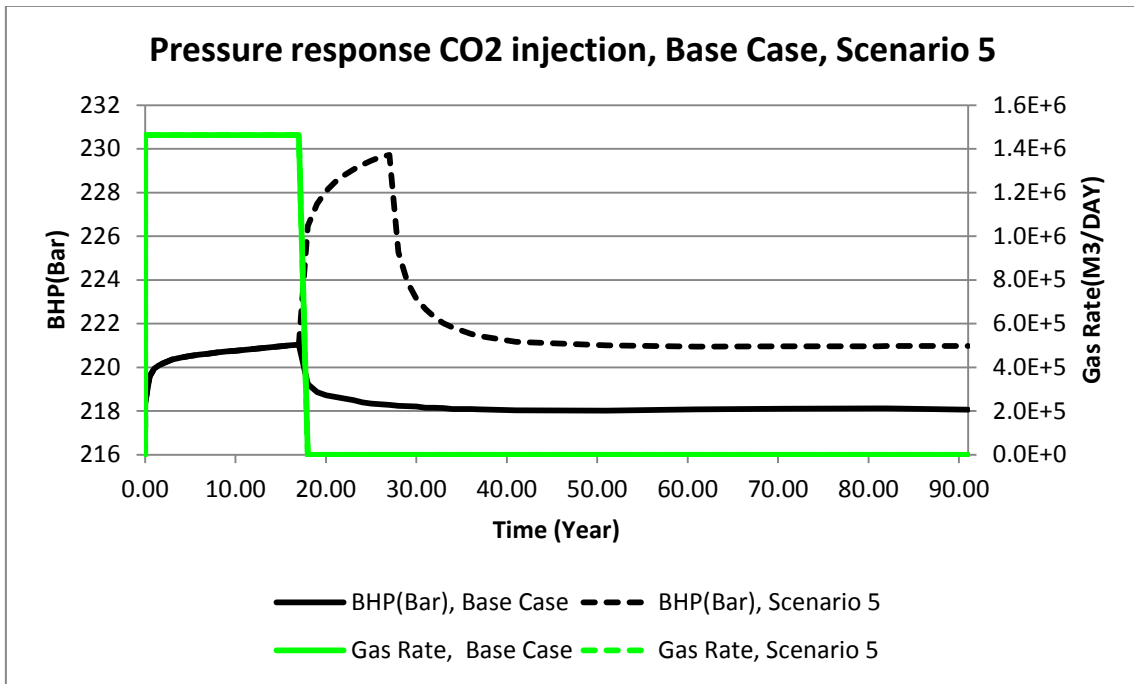


Figure 82. Gas injection rate and pressure response, compared to the base case (no remediation).

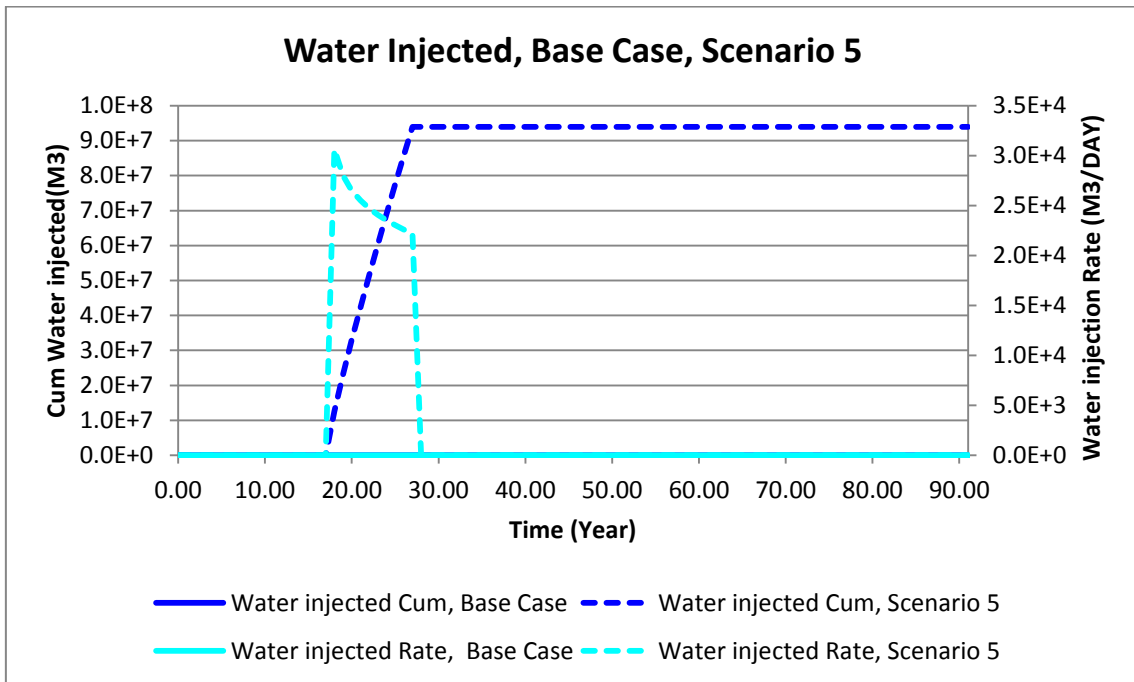


Figure 83. Water injection rates and cumulatives of well REM1, compared to the base case (no remediation) scenario.

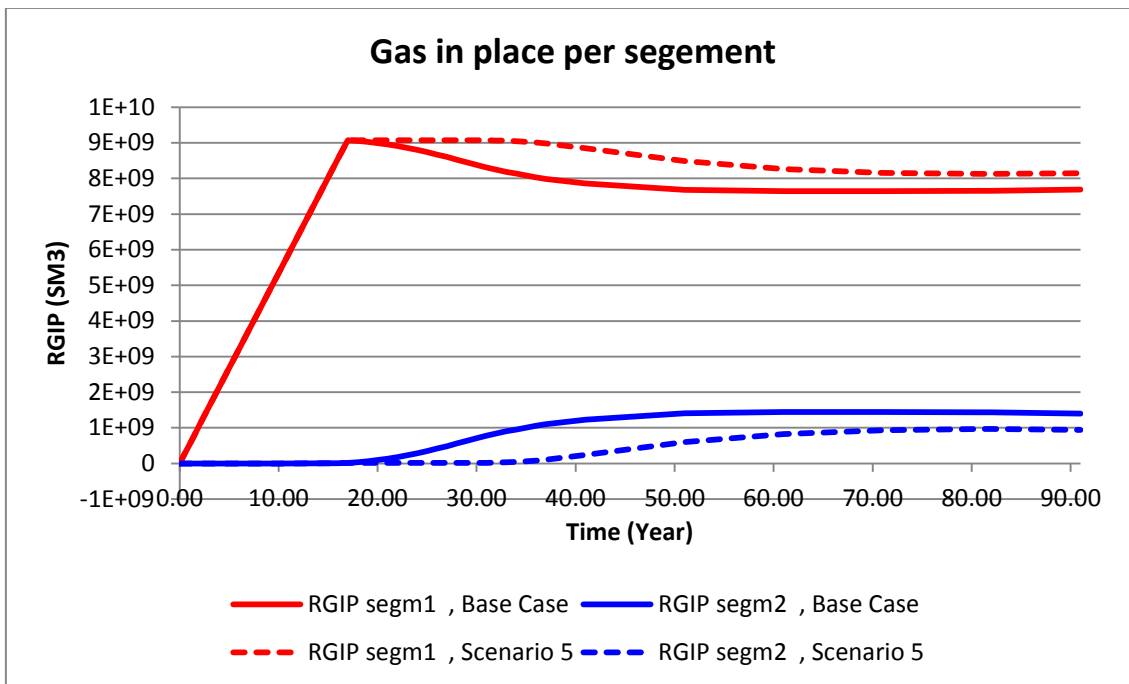


Figure 84. Unwanted migration to segment 2 compared to the base case (no remediation) scenario.

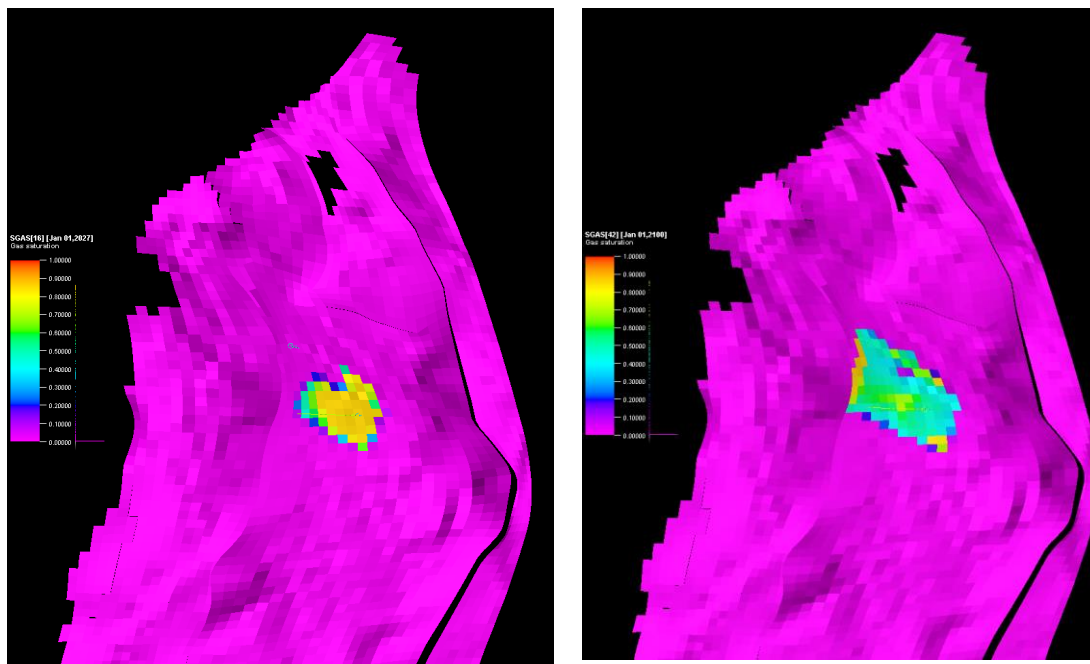


Figure 85. CO₂ plume after first detection of unwanted migration (left) and CO₂ plume after remediation at the end of simulation period of 93 years (right).

5.5.6 Remediation scenario 6

Table 27. Scenario description.

Scenario	Remediation 6
Description	After detection of unwanted migration of CO ₂ , Co ₂ injection stopped and injection of water for 17 years by one well (whole simulation period)

Table 28. Simulation settings.

General		Remarks
Begin simulation	0	(year)
End simulation	91	(year)
CO₂ Injection well	JOHAN1	
Constraints	Rate constraint: 1 Mton/yr BHP constraint 360*BAR	
Location	Vertical well in gridblock (x,y)→(45, 47)	
Perforation	Z-coordinates of gridblock (15-17)	
On stream	From 0 to 17 years	
Remediation well	REM 1	
Constraints	BHP constraint 234*BAR (10% above P initial)	
Location	Vertical well in gridblock (x,y)→(38, 47)	
Perforation	Z-coordinates of gridblock (15-17)	
On stream	From year 18 to year 23	

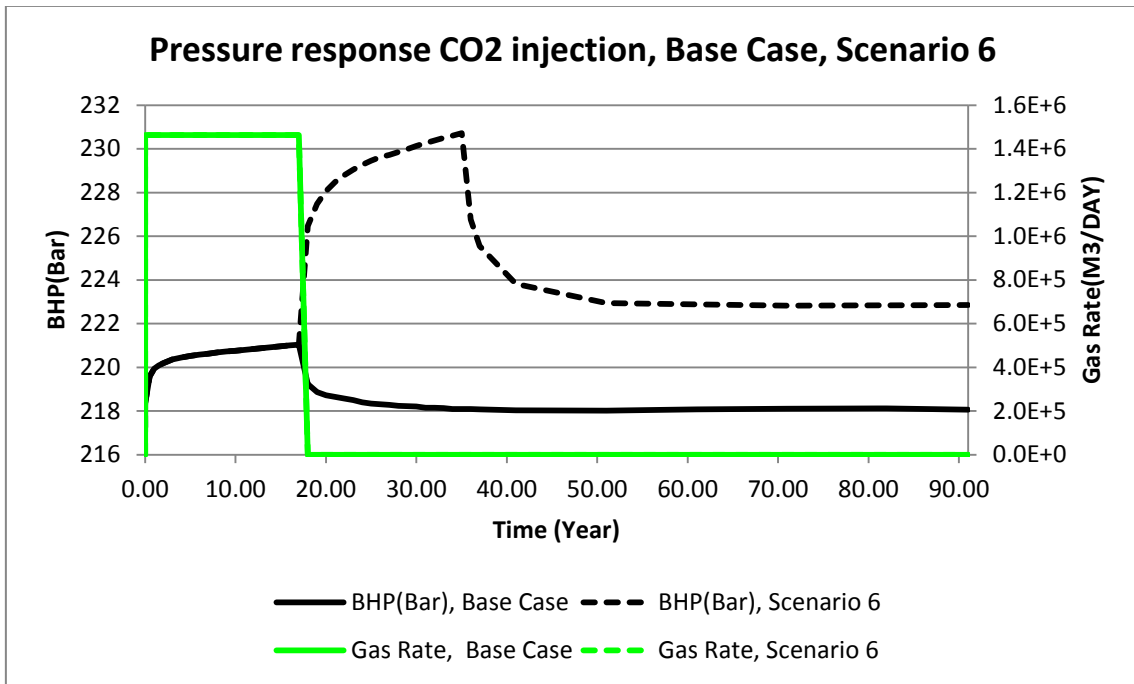


Figure 86. Gas injection rate and pressure response, compared to the base case (no remediation).

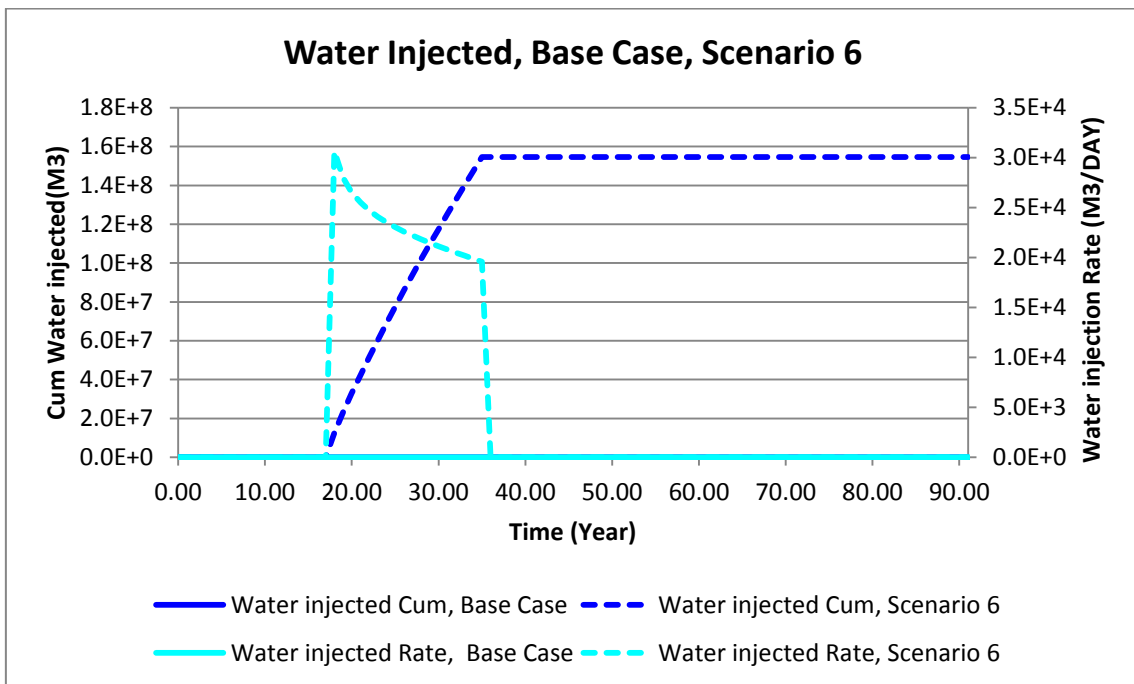


Figure 87. Water injection rates and cumulatives of well REM1, compared to the base case (no remediation) scenario.

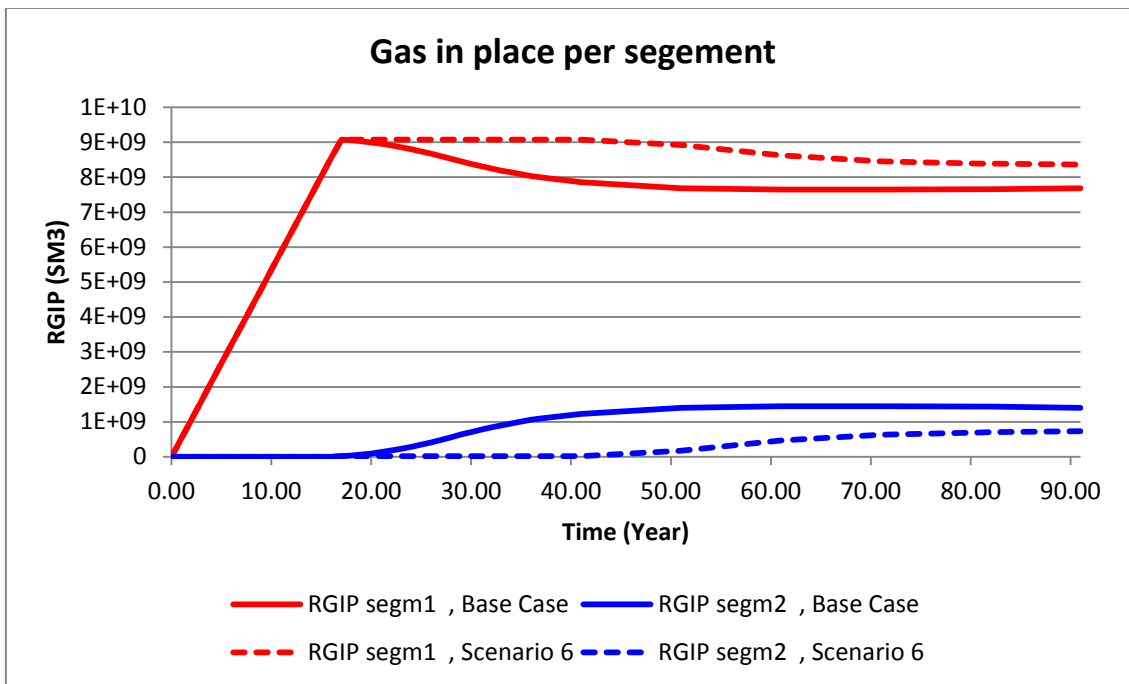


Figure 88. Unwanted migration to segment 2 compared to the base case (no remediation) scenario.

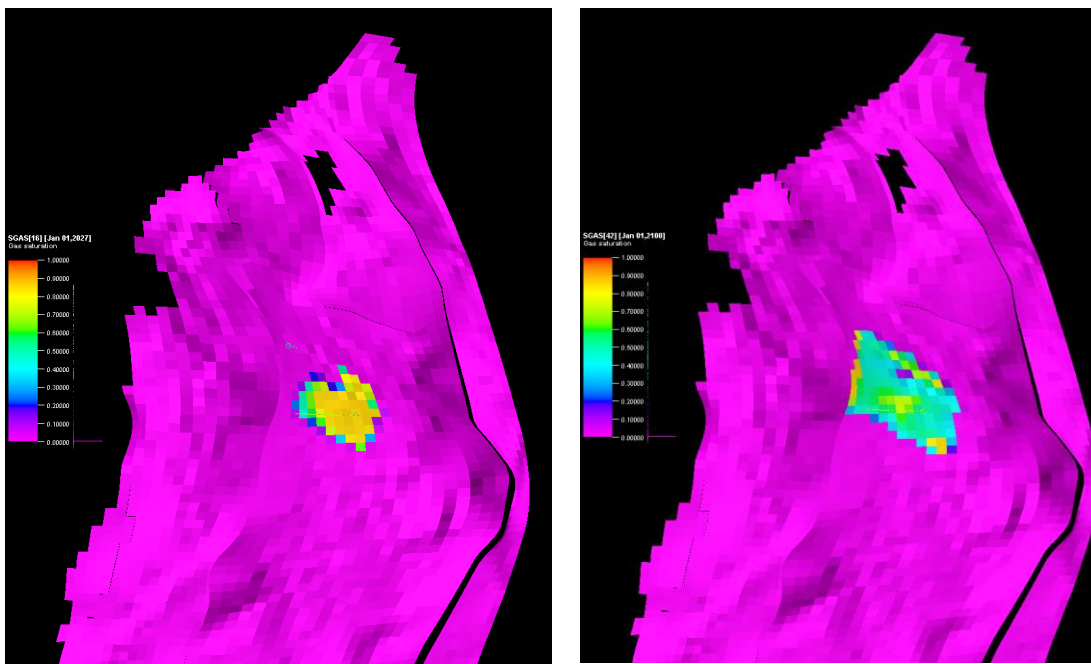


Figure 89. CO₂ plume after first detection of unwanted migration (left) and CO₂ plume after remediation at the end of simulation period of 93 years (right)

5.5.7 Remediation scenario 7

Table 29. Scenario description.

Scenario	Remediation 7
Description	After detection of unwanted migration of CO ₂ , CO ₂ injection stopped and back production started for a period of 50 years (gas rate constraint of 1 Mton/yr). Injection of water for 18 years by one well.

Table 30. Simulation settings.

General		Remarks
Begin simulation	0	(year)
End simulation	91	(year)
CO₂ Injection well	JOHAN1	
Constraints	Rate constraint: 1 Mton/yr BHP constraint 360*BAR	
Location	Vertical well in gridblock (x,y)→(45, 47)	
Perforation	Z-coordinates of gridblock (15-17)	
On stream	From 0 to 17 years	
Remediation well	REM 1	
Constraints	BHP constraint 234*BAR (10% above P initial)	
Location	Vertical well in gridblock (x,y)→(38, 47)	
Perforation	Z-coordinates of gridblock (15-17)	
On stream	From year 18 to year 36	
Back production	JOHAN1	
Constraints	Gas Rate constraint: 1.4 e6 m ³ /day	
Location	Vertical well in gridblock (x,y)→(45, 47)	
Perforation	Z-coordinates of gridblock (15-17)	
On stream	From year 18 to year 69	

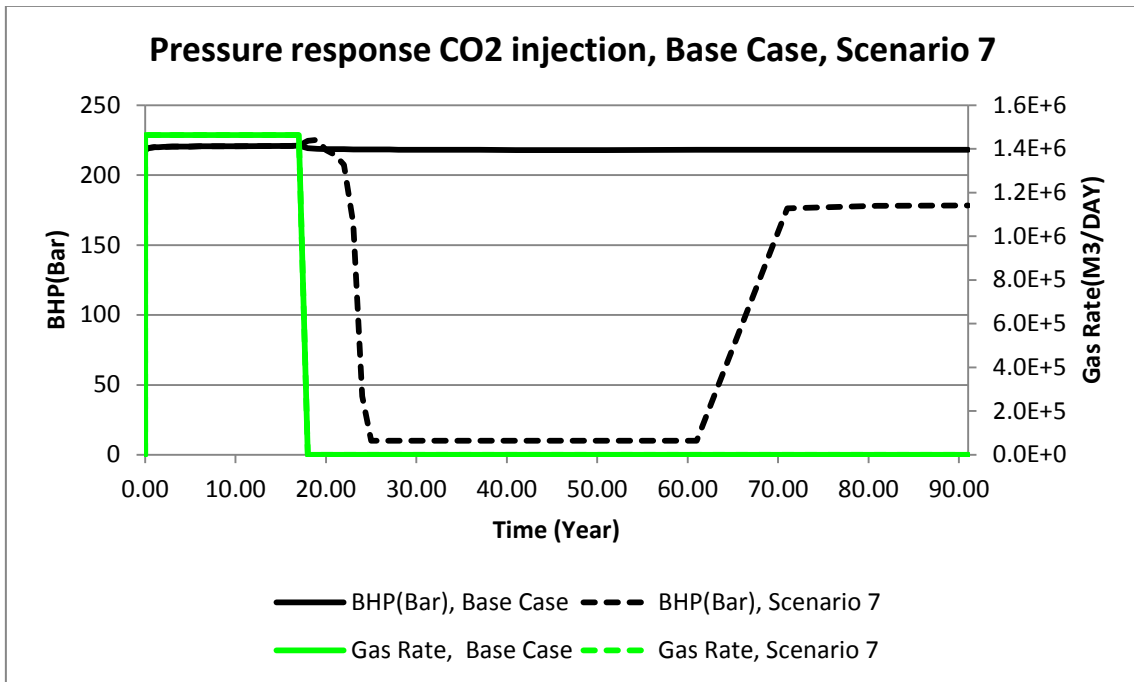


Figure 90. Gas injection rate and pressure response, compared to the base case (no remediation).

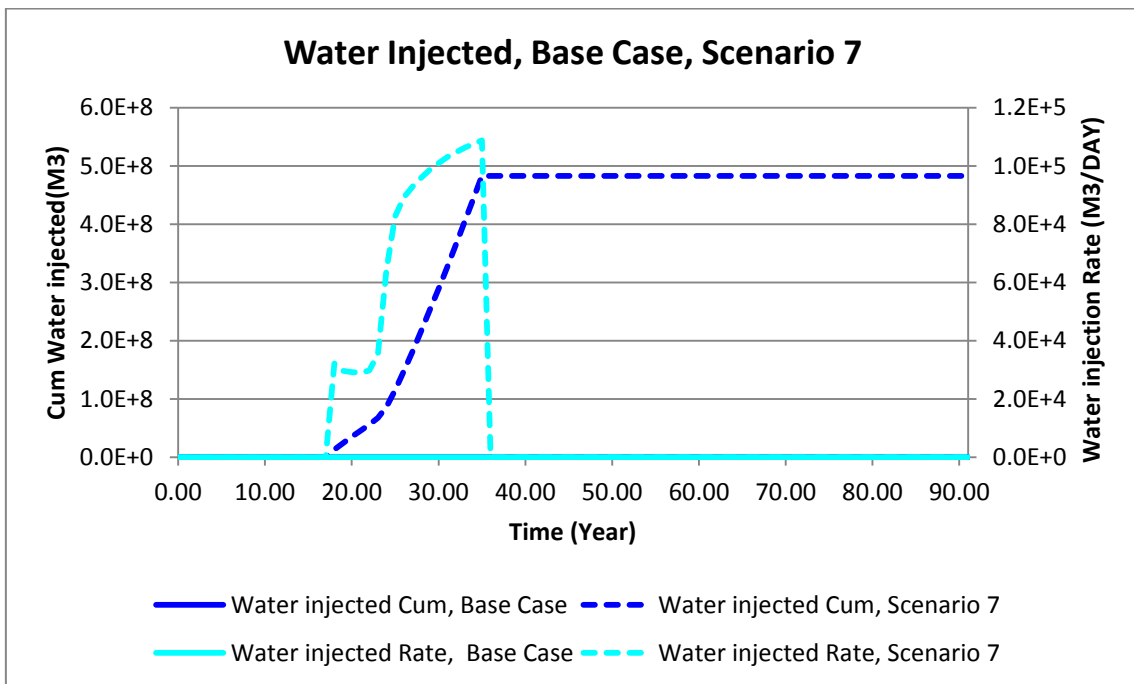


Figure 91. Water injection rates and cumulatives of well REM1, compared to the base case (no remediation) scenario.

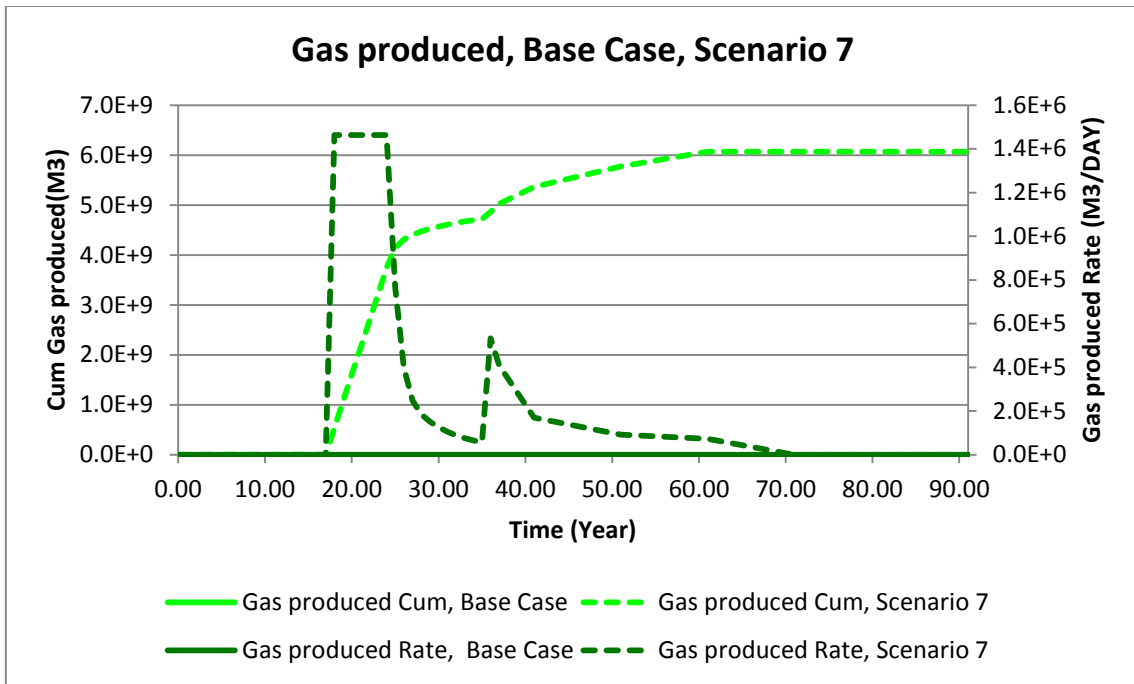


Figure 92. Gas back production rate and cumulatives of well JOHAN compared to the base case (no remediation) scenario.

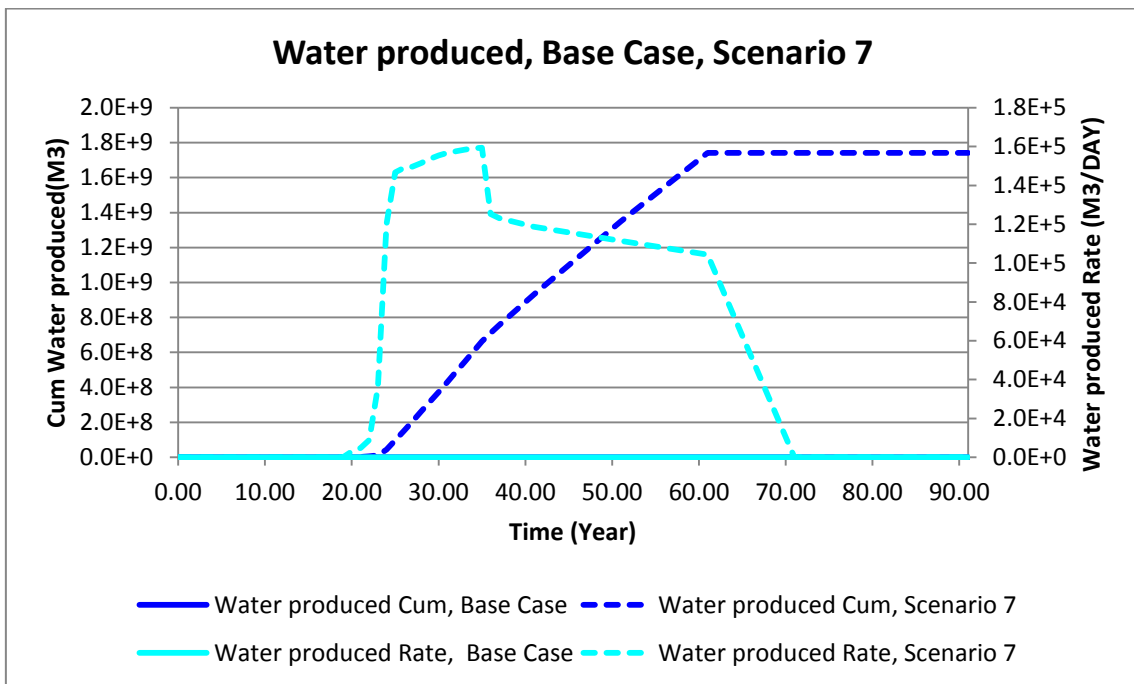


Figure 93. Water back production rate and cumulatives of well JOHAN compared to the base case (no remediation) scenario.

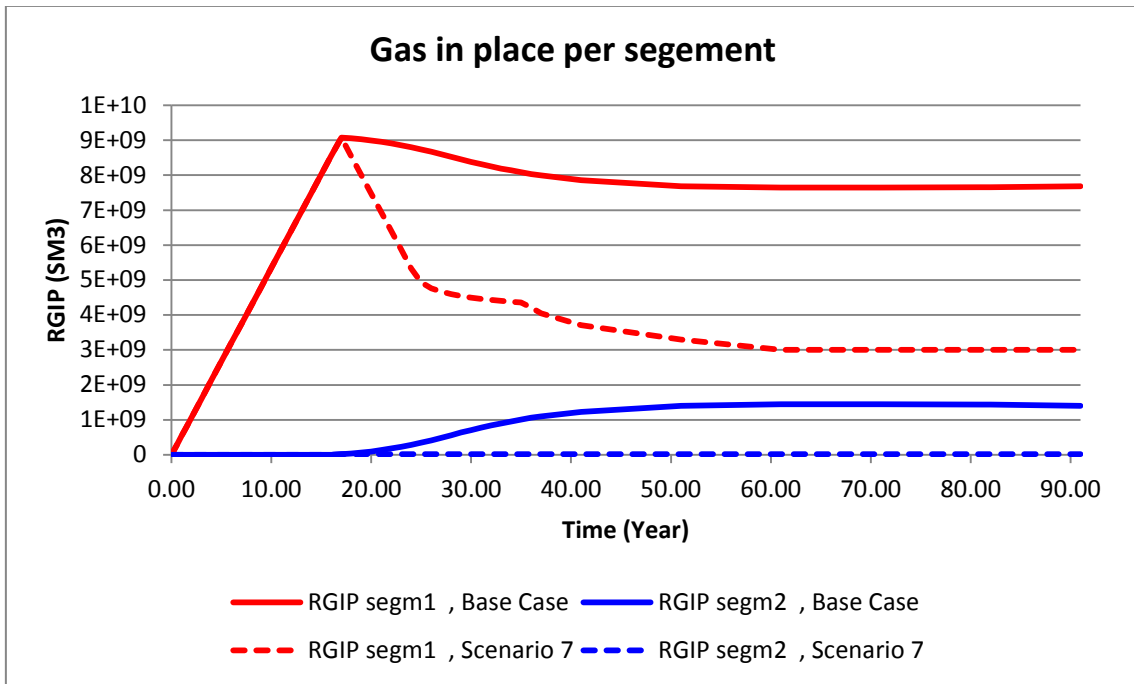


Figure 94. Unwanted migration to segment 2 compared to the base case (no remediation) scenario.

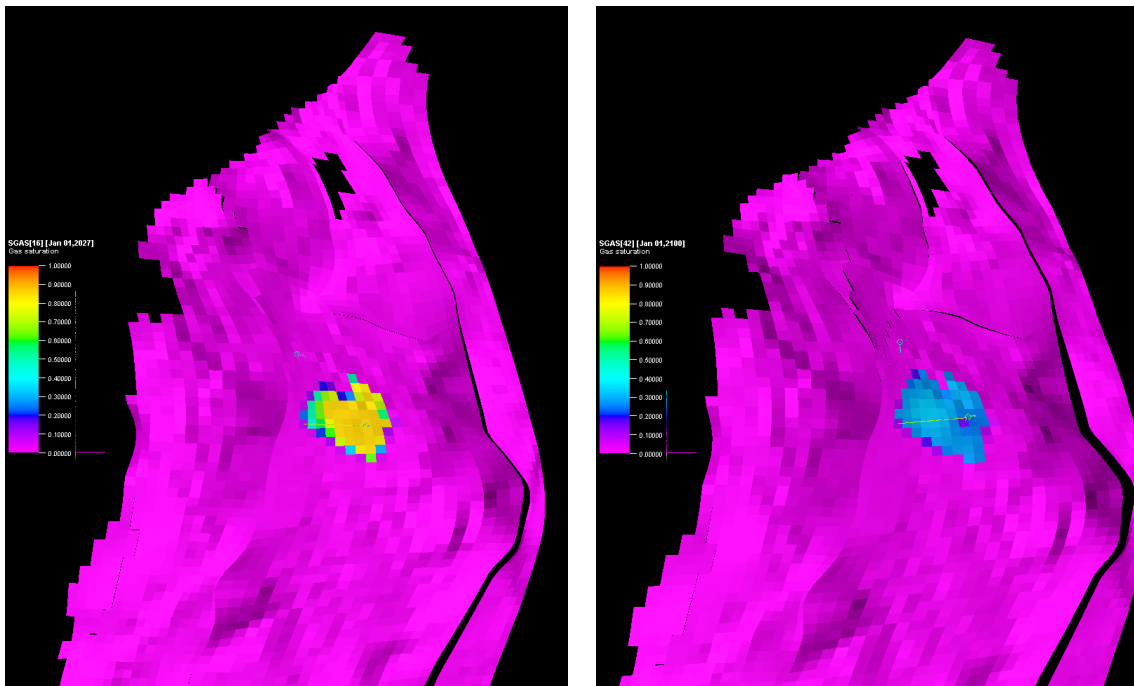


Figure 95. CO₂ plume after first detection of unwanted migration (left) and CO₂ plume after remediation at the end of simulation period of 93 years (right).

5.5.8 Remediation scenario 8

Table 31. Scenario description.

Scenario	Remediation 8
Description	After detection of unwanted migration of CO ₂ , CO ₂ injection stopped and back production started for a period of 50 years (gas rate constraint of 0.5 Mton/yr). Injection of water for 18 years by one well.

Table 32. Simulation settings.

General		Remarks
Begin simulation	0	(year)
End simulation	91	(year)
CO₂ Injection well	JOHAN1	
Constraints	Rate constraint: 1 Mton/yr BHP constraint 360*BAR	
Location	Vertical well in gridblock (x,y)→(45, 47)	
Perforation	Z-coordinates of gridblock (15-17)	
On stream	From 0 to 17 years	
Remediation well	REM 1	
Constraints	BHP constraint 234*BAR (10% above P initial)	
Location	Vertical well in gridblock (x,y)→(38, 47)	
Perforation	Z-coordinates of gridblock (15-17)	
On stream	From year 18 to year 36	
Back production	JOHAN1	
Constraints	Gas Rate constraint 234: 0.7 e6 m3/day	
Location	Vertical well in gridblock (x,y)→(45, 47)	
Perforation	Z-coordinates of gridblock (15-17)	
On stream	From year 18 to year 69	

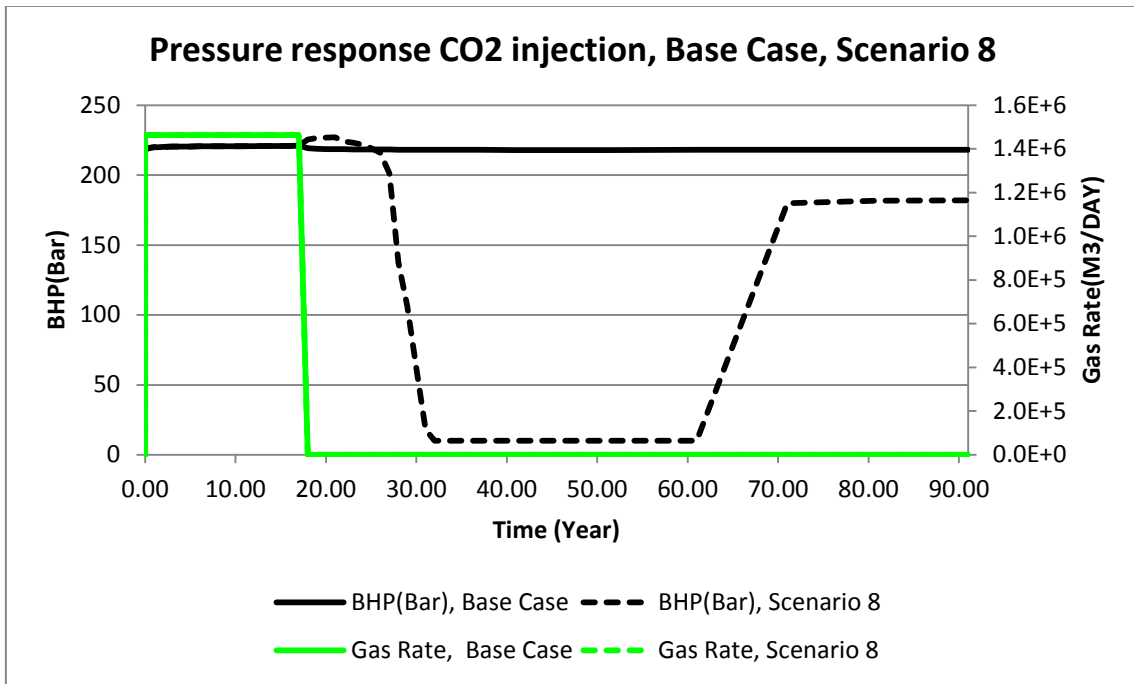


Figure 96. Gas injection rate and pressure response, compared to the base case (no remediation).

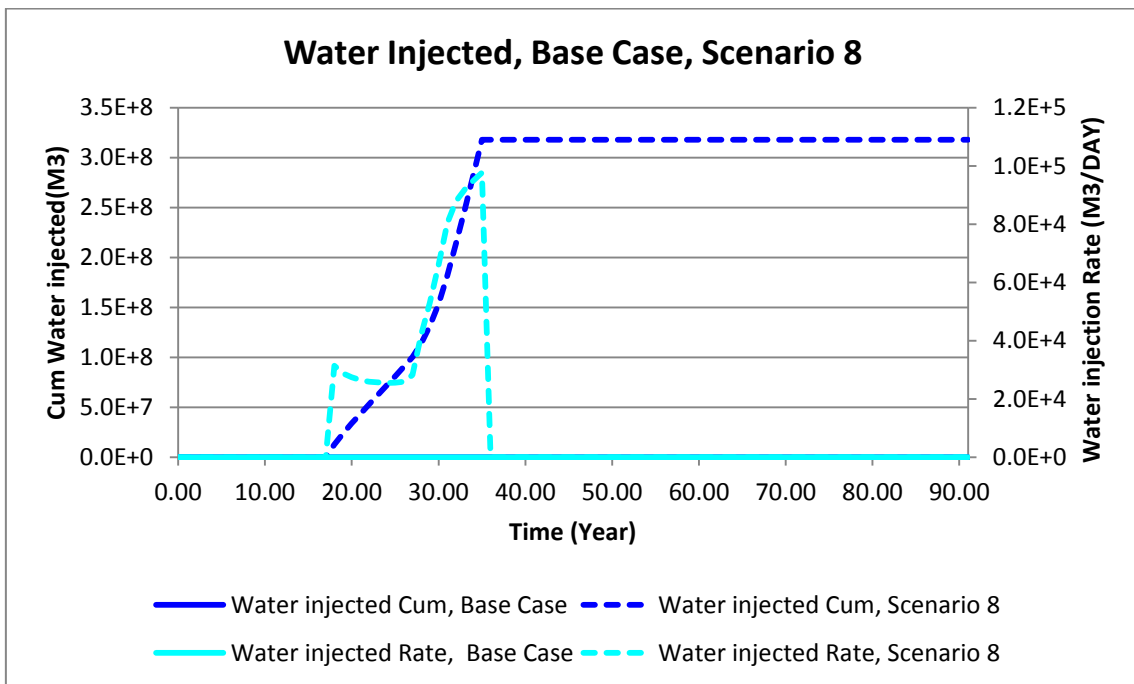


Figure 97. Water injection rates and cumulatives of well REM1, compared to the base case (no remediation) scenario.

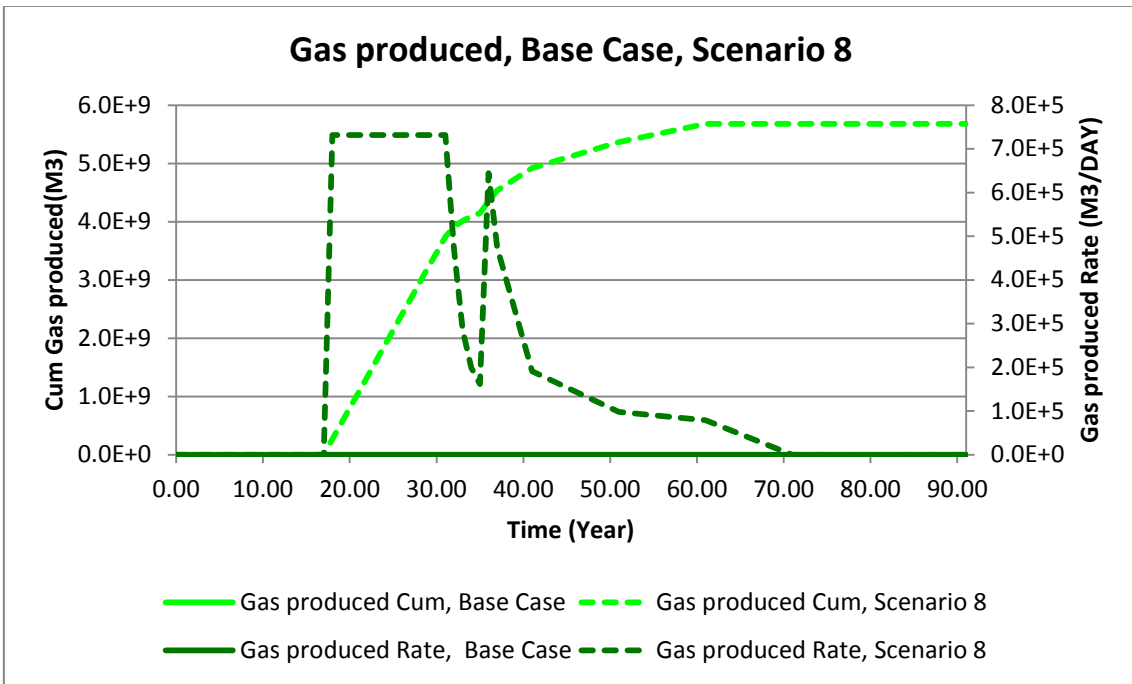


Figure 98. Gas back production rate and cumulatives of well JOHAN compared to the base case (no remediation) scenario.

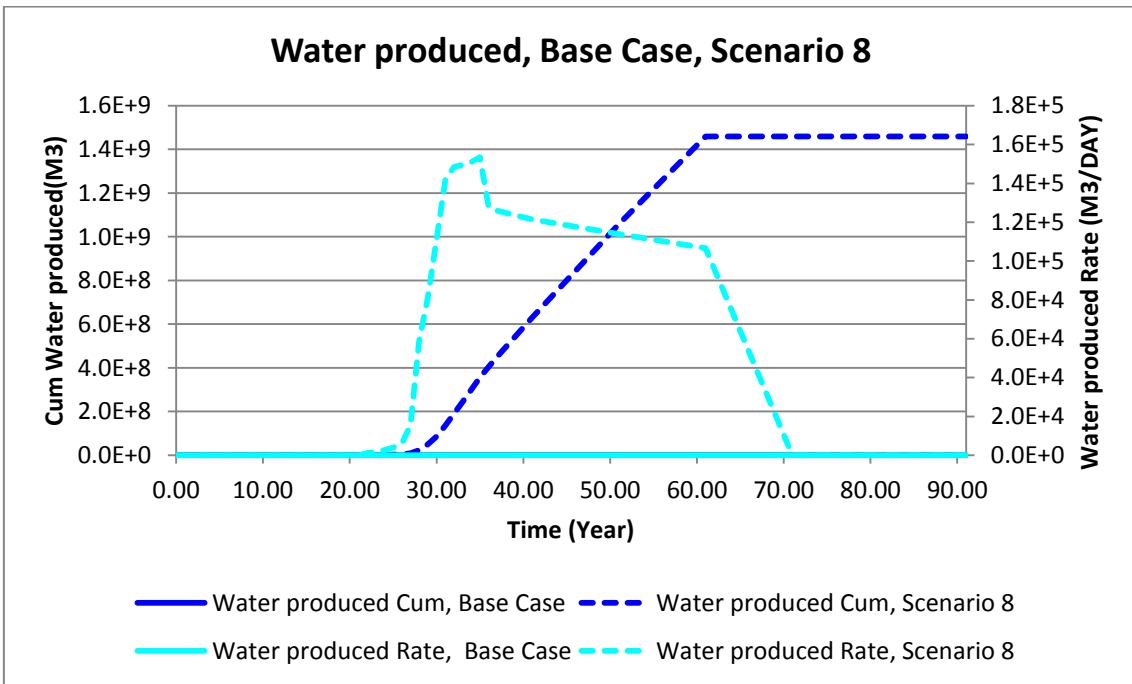


Figure 99. Water back production rate and cumulatives of well JOHAN compared to the base case (no remediation) scenario.

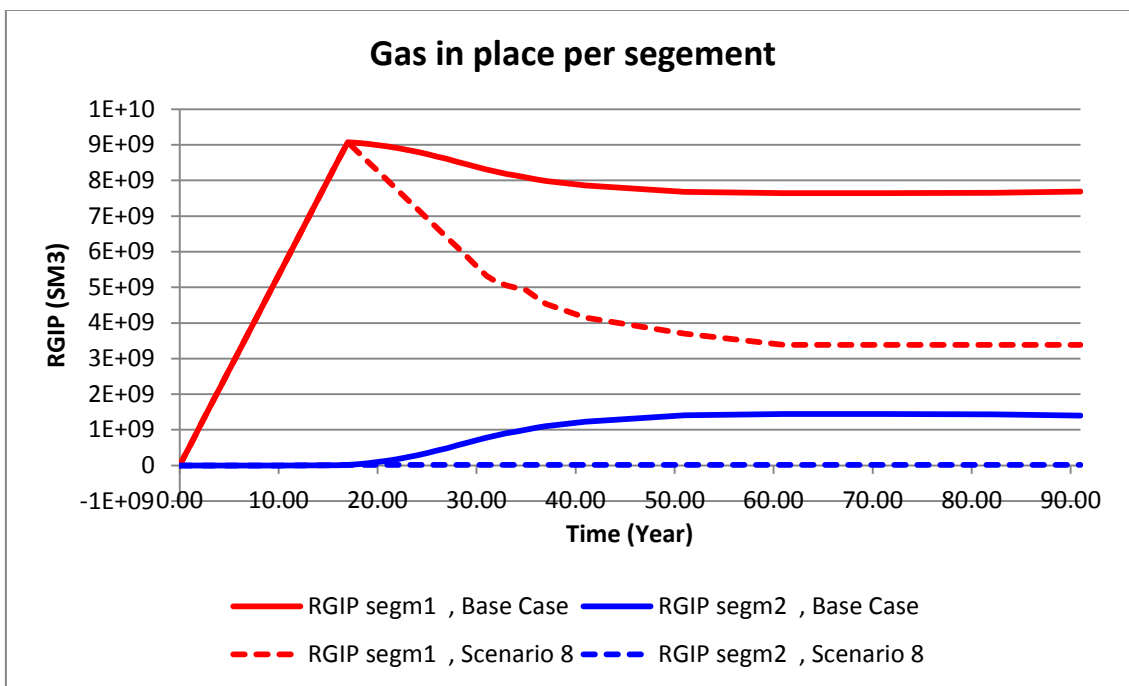


Figure 100. Unwanted migration to segment 2 compared to the base case (no remediation) scenario.

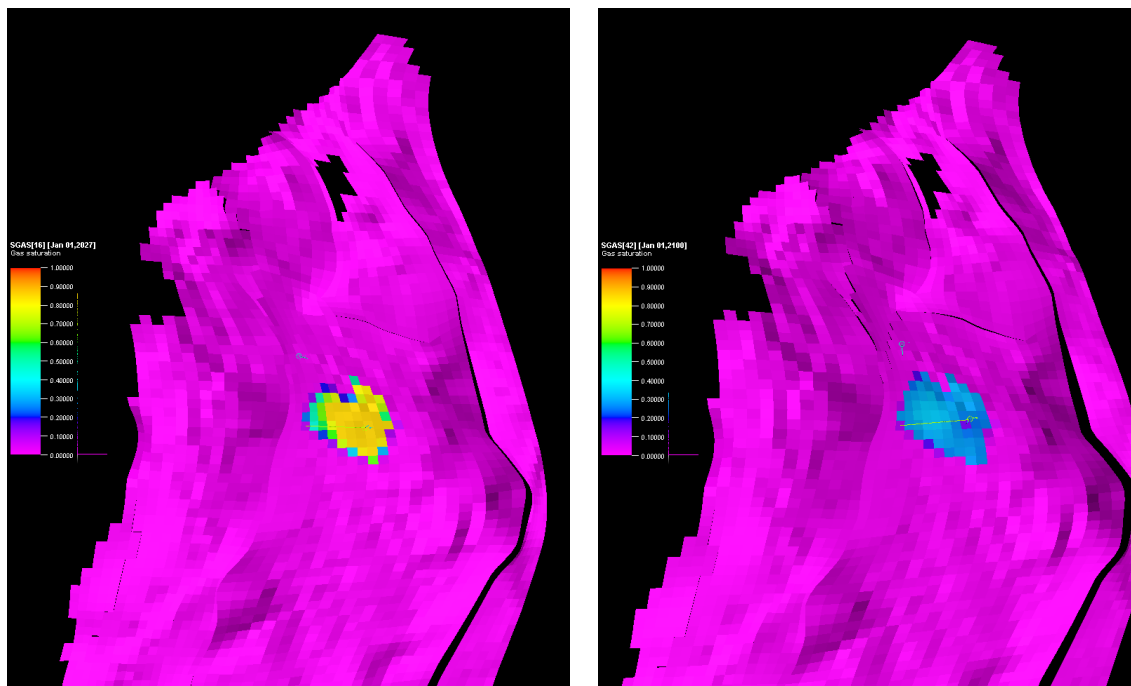


Figure 101. CO₂ plume after first detection of unwanted migration (left) and CO₂ plume after remediation at the end of simulation period of 93 years (right).

5.5.9 Remediation scenario 9

Table 33. Scenario description.

Scenario	Remediation 9
Description	After detection of unwanted migration of CO ₂ , CO ₂ injection stopped and back production started for a period of 50 years (gas rate constraint of 1 Mton/yr). Injection of water for 10 years by one well.

Table 34. Simulation settings.

General		Remarks
Begin simulation	0	(year)
End simulation	91	(year)
CO₂ Injection well	JOHAN1	
Constraints	Rate constraint: 1 Mton/yr BHP constraint 360*BAR	
Location	Vertical well in gridblock (x,y)→(45, 47)	
Perforation	Z-coordinates of gridblock (15-17)	
On stream	From 0 to 17 years	
Remediation well	REM 1	
Constraints	BHP constraint 234*BAR (10% above P initial)	
Location	Vertical well in gridblock (x,y)→(38, 47)	
Perforation	Z-coordinates of gridblock (15-17)	
On stream	From year 18 to year 27	
Back production	JOHAN1	
Constraints	Gas Rate constraint 234: 0.7 e6 m3/day	
Location	Vertical well in gridblock (x,y)→(45, 47)	
Perforation	Z-coordinates of gridblock (15-17)	
On stream	From year 18 to year 69	

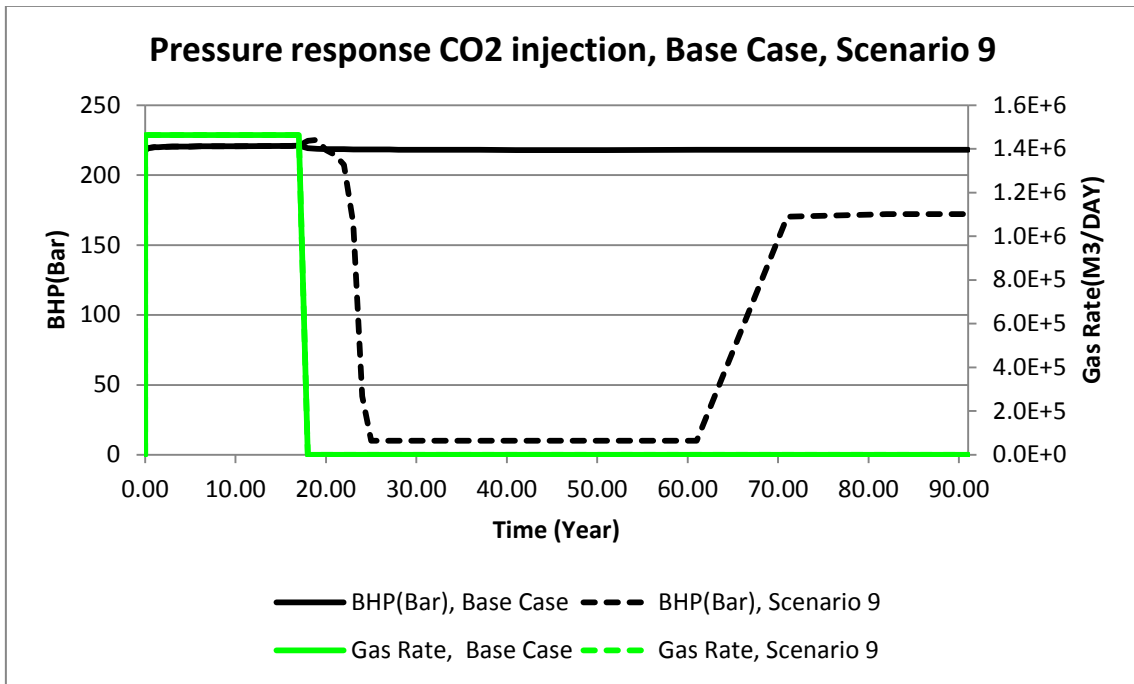


Figure 102. Gas injection rate and pressure response, compared to the base case (no remediation).

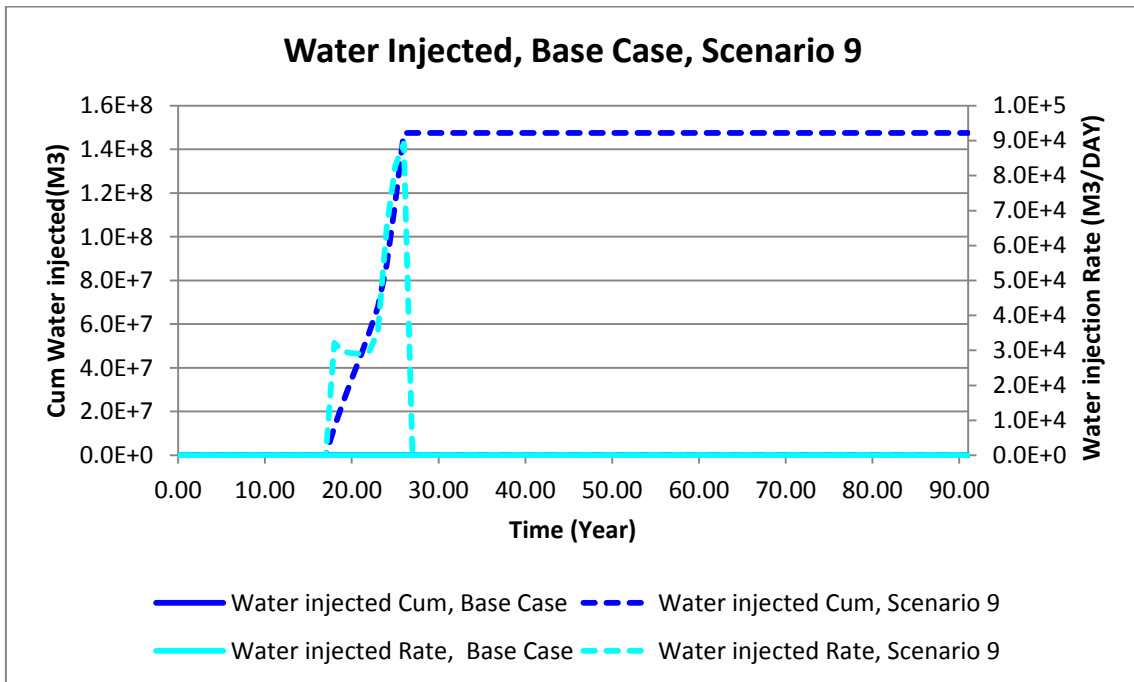


Figure 103. Water injection rates and cumulatives of well REM1, compared to the base case (no remediation) scenario.

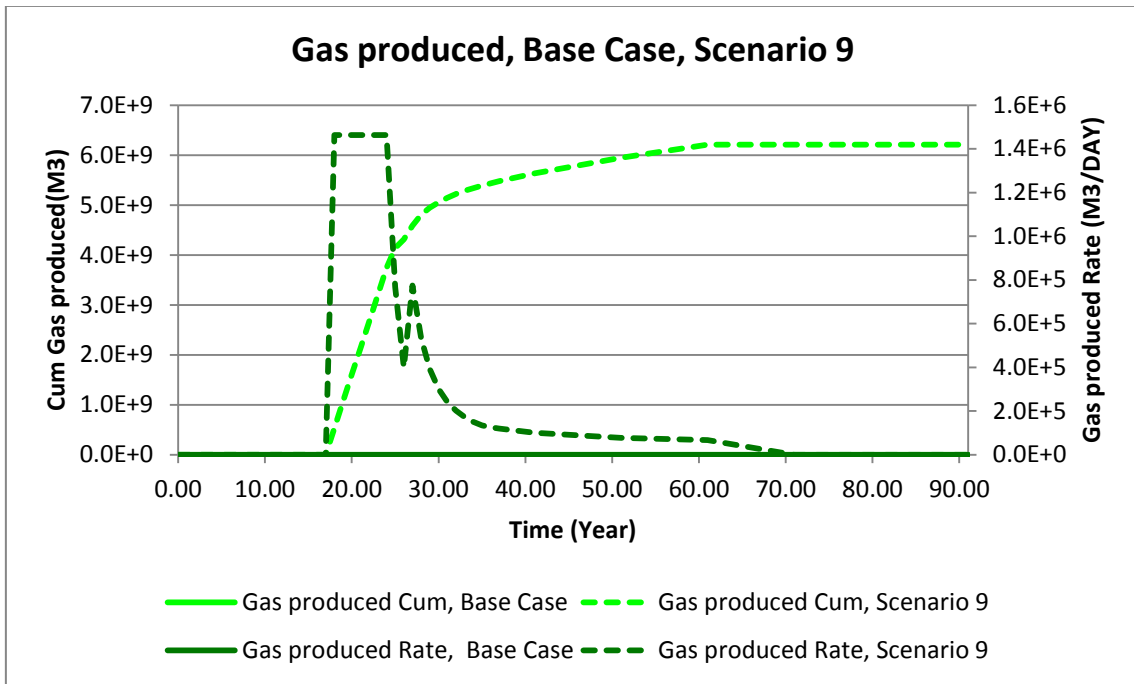


Figure 104. Gas back production rate and cumulatives of well JOHAN compared to the base case (no remediation) scenario.

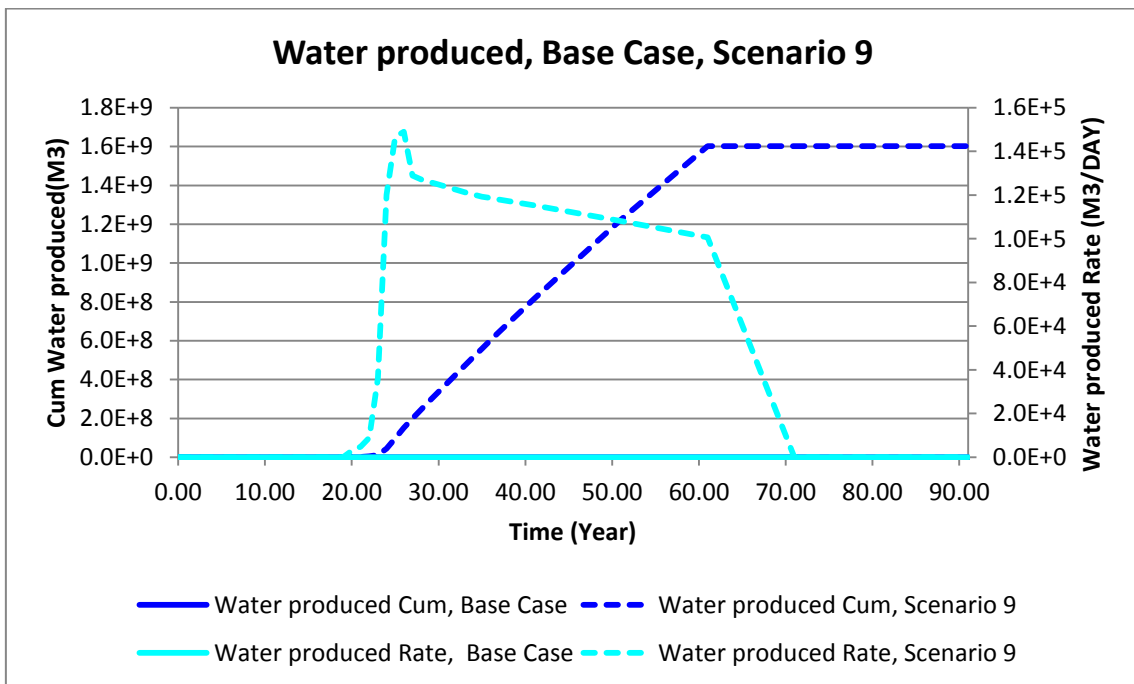


Figure 105. Water back production rate and cumulatives of well JOHAN compared to the base case (no remediation) scenario.

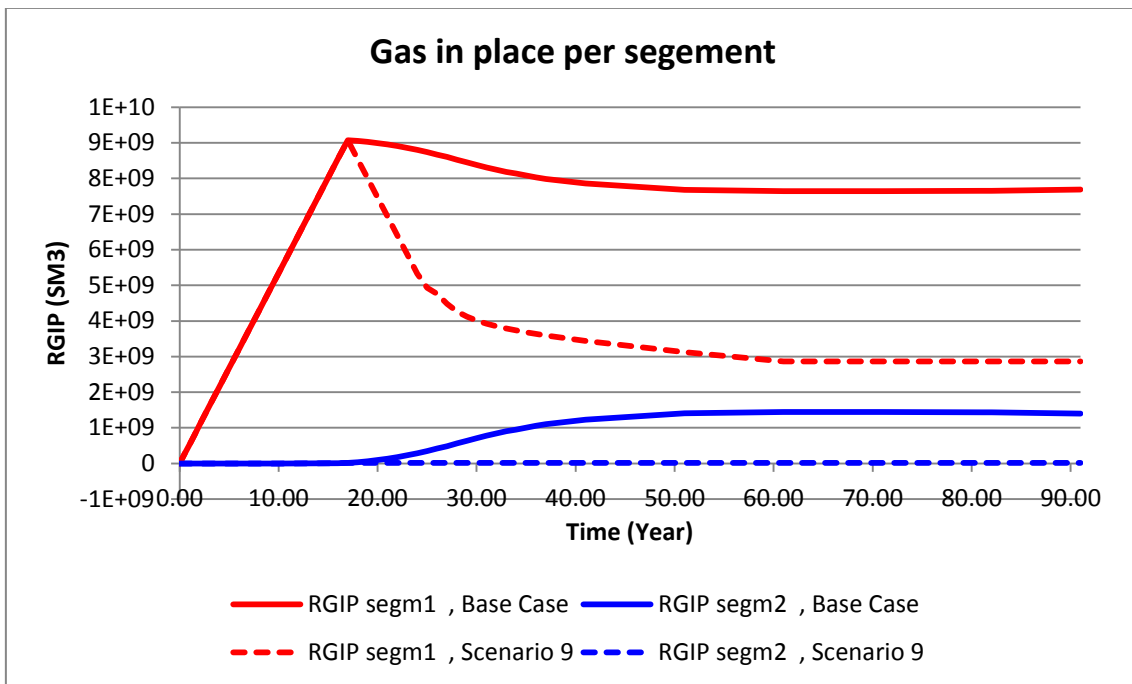


Figure 106. Unwanted migration to segment 2 compared to the base case (no remediation) scenario.

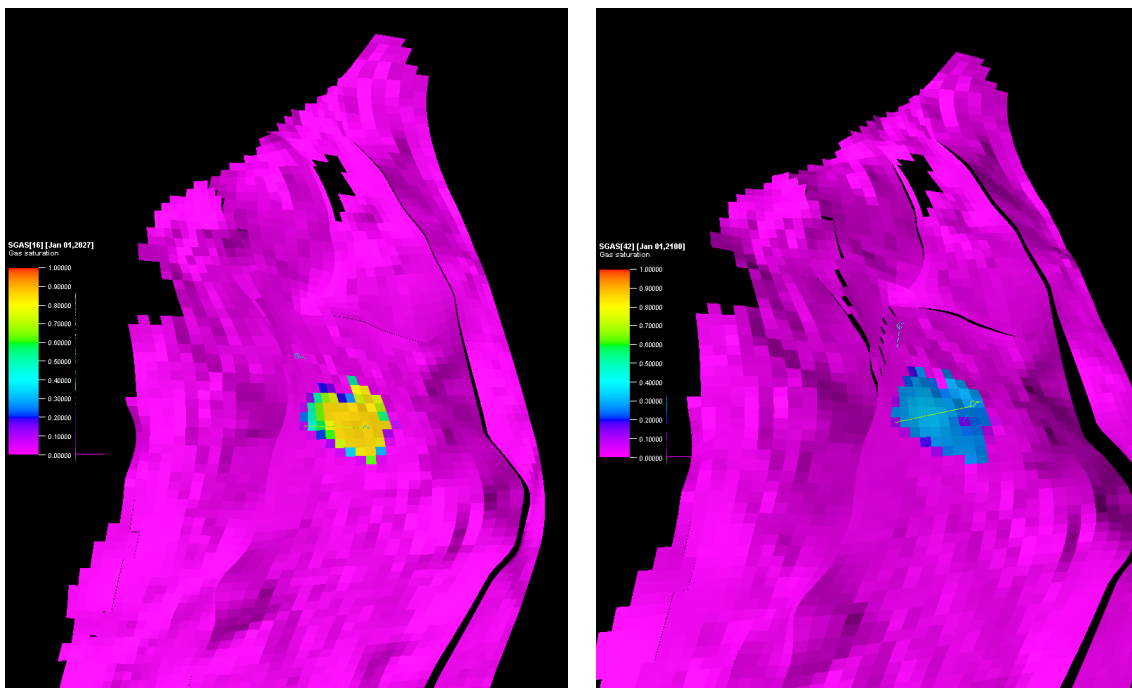


Figure 107. CO₂ plume after first detection of unwanted migration (left) and CO₂ plume after remediation at the end of simulation period of 93 years (right).

5.5.10 Remediation scenario 10

Table 35. Scenario description.

Scenario	Remediation 10
Description	After detection of unwanted migration of CO ₂ , Co ₂ injection stopped and injection of water for 10 years by one well (whole simulation period)

Table 36. Simulation settings.

General		Remarks
Begin simulation	0	(year)
End simulation	91	(year)
CO₂ Injection well	JOHAN1	
Constraints	Rate constraint: 1 Mton/yr BHP constraint 360*BAR	
Location	Vertical well in gridblock (x,y)→(45, 47)	
Perforation	Z-coordinates of gridblock (15-17)	
On stream	From 0 to 17 years	
Remediation well	REM 1	
Constraints	BHP constraint 234*BAR (10% above P initial)	
Location	Vertical well in gridblock (x,y)→(38, 47)	
Perforation	Z-coordinates of gridblock (15-17)	
On stream	From year 18 to year 23	
Back production	JOHAN1	
Constraints	Gas Rate constraint 234: 0.7 e6 m3/day	
Location	Vertical well in gridblock (x,y)→(45, 47)	
Perforation	Z-coordinates of gridblock (15-17)	
On stream	From year 18 to year 69	

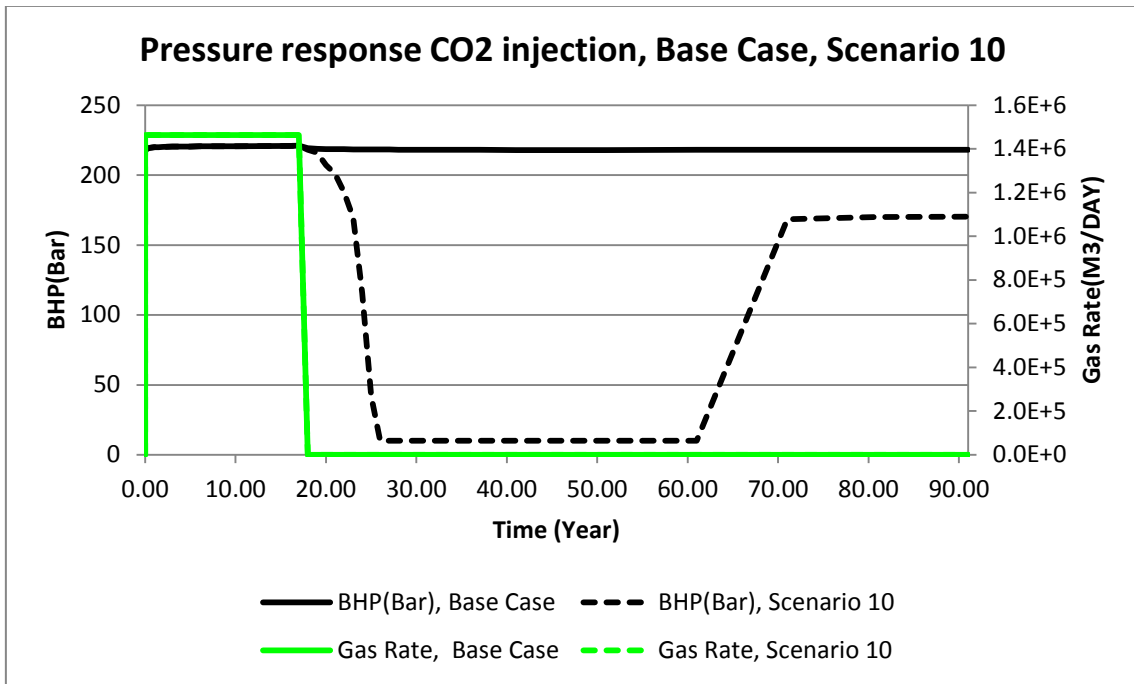


Figure 108. Gas injection rate and pressure response, compared to the base case (no remediation).

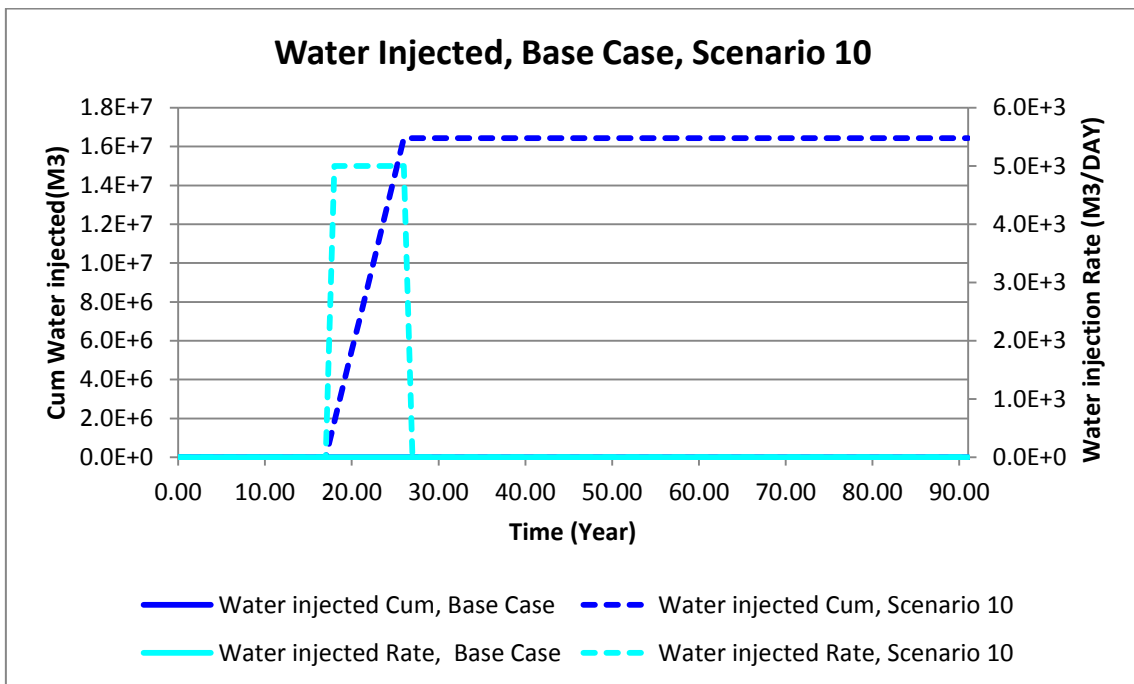


Figure 109. Water injection rates and cumulatives of well REM1, compared to the base case (no remediation) scenario.

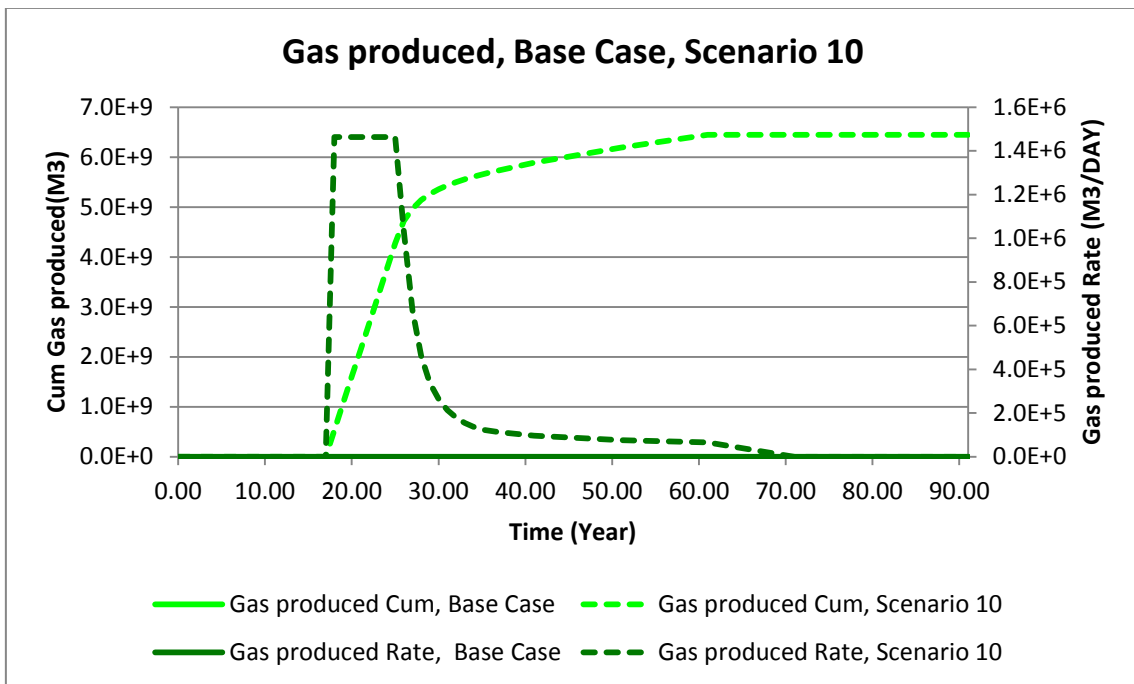


Figure 110. Gas back production rate and cumulatives of well JOHAN compared to the base case (no remediation) scenario.

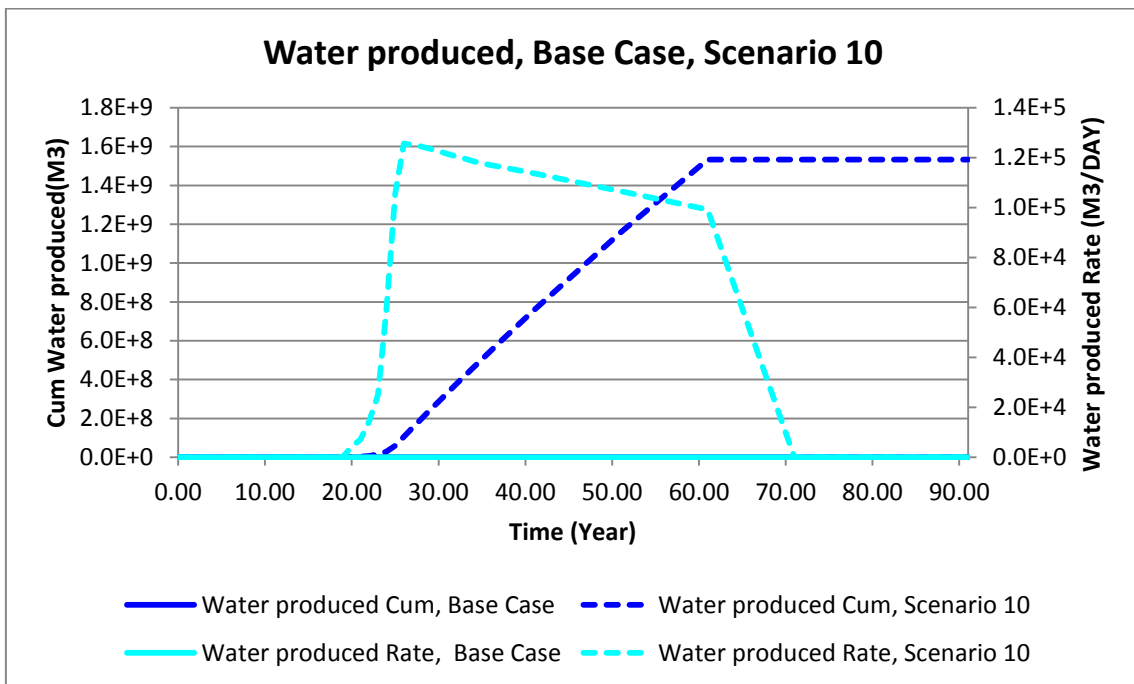


Figure 111. Water back production rate and cumulatives of well JOHAN compared to the base case (no remediation) scenario.

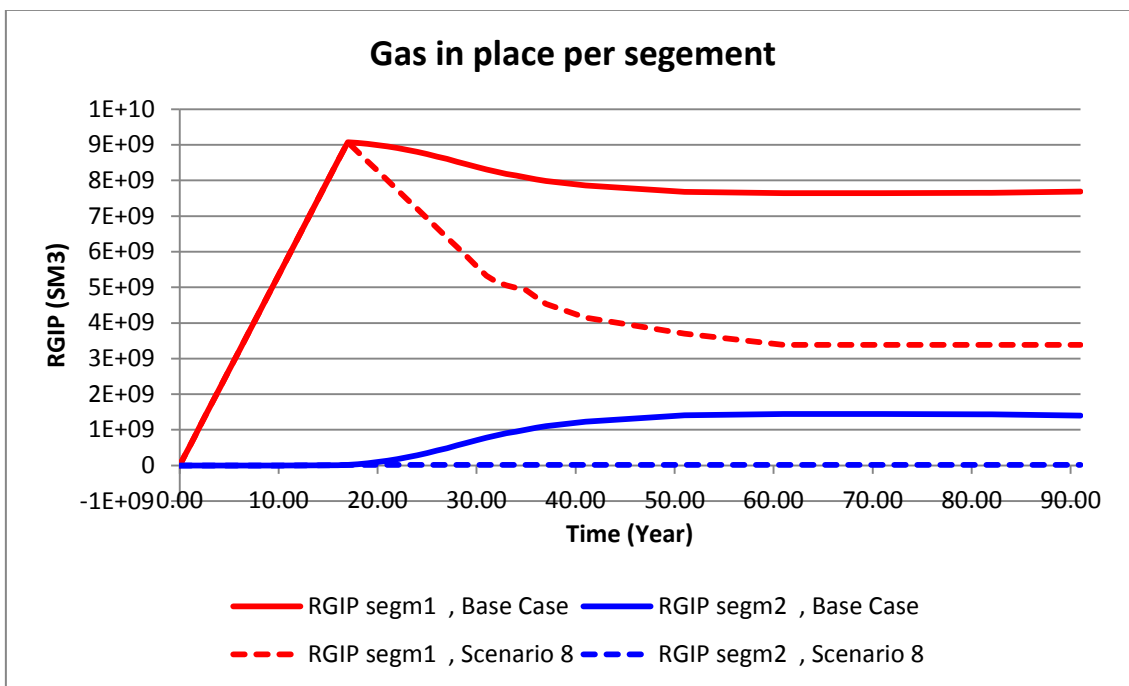


Figure 112. Unwanted migration to segment 2 compared to the base case (no remediation) scenario.

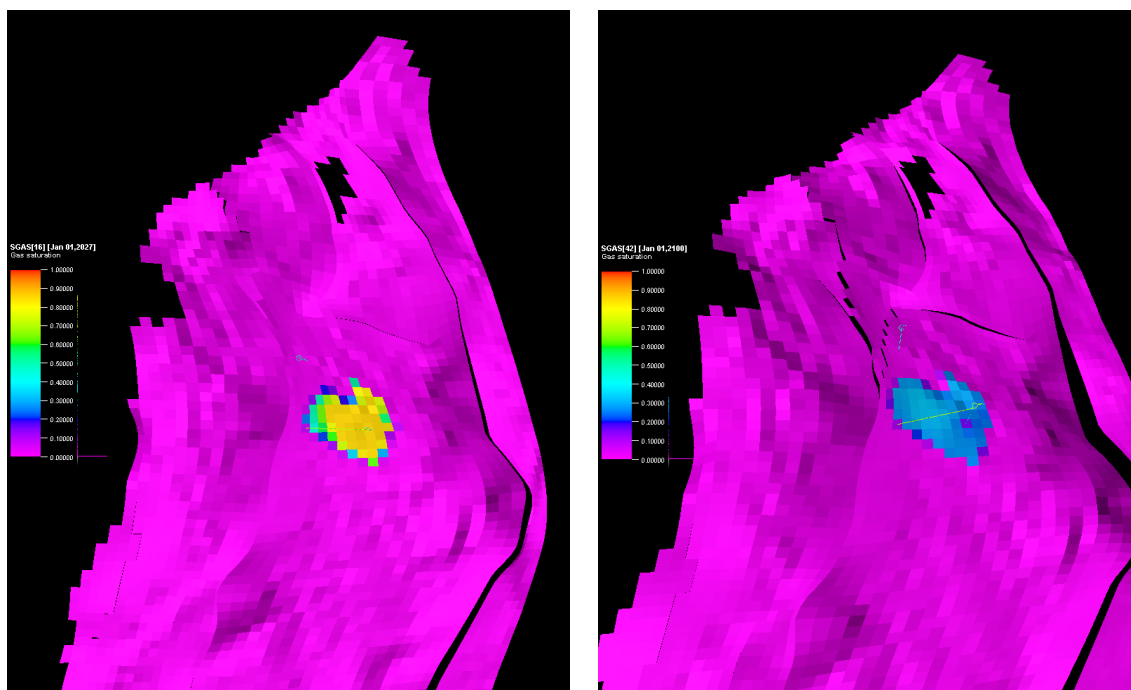


Figure 113. CO₂ plume after first detection of unwanted migration (left) and CO₂ plume after remediation at the end of simulation period of 93 years (right).

6 SUMMARY AND CONCLUSIONS

SINTEF

Simulations were performed of CO₂ migration along a ridge structure in the Johansen aquifer, with water injection as a mitigation measure. Twenty-one combinations of CO₂ injection rate, permeability and reservoir depth were simulated.

It was shown that water injection effectively stops CO₂ migration but does not provide a long-lasting effect, lasting only from 1.4 to 7 years. Since migration of injected CO₂ will continue over many hundred years, water injection cannot be considered a long-term solution.

Obviously lower permeability will reduce the migration rate, but in addition it was seen that low permeability, especially with high CO₂ injection rates cause the flow to become much more diffuse, thereby by-passing the water injector and potentially reducing its mitigating effect.

No consistent trend in leakage reduction was observed due to variations in reservoir depth.

Imperial College

Using a generic model, Imperial College have studied the reduction of CO₂ leakage through a sub-seismic fault by means of water injection via the well previously used for CO₂ injection.

The results have shown that brine injection causes an increase in CO₂ dissolution which consequently reduces the amount of mobile CO₂ available for leakage.

For distances of 1km and 2km between the injector and the fault it appears that brine injection effectively stops leakage of CO₂ via the sub-seismic fault. For the 3km fault scenario however, there is a reduction in the amount of CO₂ leakage but it is not stopped.

Brine injection has the effect of retaining higher CO₂ saturation in the reservoir.

Further investigation of the 3km fault scenario by changing the injection rate and the injection period suggested that there is only a limited benefit longer term brine injection.

GFZ

The results from an actual water injection test on a former injection well on the Ketzin field were modelled and analysed. Water injection for three months prevented CO₂ from re-entering the well for two months.

A numerical simulation was prepared and calibrated with the injection history, but while this matched the bottom-hole pressure response will during the previous CO₂ injection phase, it did not predict correctly the significant pressure increase and fluctuations during water injection. Further work on the model is required.

Geo-electrical monitoring was found to reproduce the general trend of higher electrical conductivity due to higher brine concentration and showed good correlation with the injection dynamics.

TNO

Four injection locations were chosen near a major fault or a spill point in the Johansen formation to investigate mitigation of CO₂ migration. Remediation wells were used to inject water for up to 64 years and back-production of CO₂ was also applied in some cases. A base case and 10 remediation scenarios were simulated.

It was concluded that after CO₂ leakage is observed, the remediation technique by water injection only is not efficient and the addition of back-production of CO₂ is the most effective option to avoid further migration of the CO₂ present in the aquifer near the spill point or fault.

7 REFERENCES

- Anchliya A., Ehlig-Economides C. and Jafarpour B., 2012. "Aquifer management to accelerate CO₂ dissolution and trapping", SPE 126688.
- Bachu, S. & Bennion, B. (2008), 'Effects of in-situ conditions on relative permeability characteristics of CO₂-brine systems', *Environmental Geology* **54**, 1707-1722.
- Element Energy, 2012. Economic impacts of CO₂-enhanced oil recovery for Scotland - Final report, <https://www.scottish-enterprise.com/knowledge-hub/articles/publication/co2-enhanced-oil-recovery>.
- IEAGHG, 2011. Global storage resources gap analysis for policy makers, Report 2011/10, September, 2011.
- Kuuskräa V., Gedec M., 2007, Remediation of leakage from CO₂ storage reservoirs, IEA GHG report 2997/11.
- Möller, F.; Liebscher, A. & Schmidt-Hattenberger, C. (2016), 'Report on the dataset of the Brine Injection at the CO₂ Storage Pilot Site Ketzin, Germany'(16/05), Technical report, GFZ German Research Centre for Geosciences.
- Norwegian Petroleum Directorate, 2014, "CO₂ Storage Atlas, Norwegian Continental Shelf", ISBN 978-82-7257-134-3.
- Omorgie Z.S., King G.R., Strang C., Hodgson P. & Pressney R.A, 1995, "Reservoir management in the Ninian field – a case history", SPE 30443.
- Qi R., LaForce T.C. and J. Blunt M.J., 2009. "Design of carbon dioxide storage in aquifers." *International Journal of Greenhouse Gas Control*, 3.2: 195-205.
- Rippe, D., Bergmann, P., Labitzke, T., Wagner, F. M., Schmidt-Hattenberger, C. (2016): Surface-downhole and crosshole geoelectrics for monitoring of brine injection at the Ketzin CO₂ storage site. *Geophysical Research Abstracts*, 18, EGU2016-15388, EGU General Assembly 2016.
- Schmidt-Hattenberger, C.; Bergmann, P.; Kießling, D.; Krüger, K.; Rucker, C. & Schütt, H. (2011). Application of a Vertical Electrical Resistivity Array (VERA) for monitoring CO₂ migration at the Ketzin site: First performance evaluation *Energy Procedia*, 2011, 4, 3363-3370.
- USEPA, 2010. Geologic CO₂ Sequestration Technology and Cost Analysis, technical support documents. https://www.epa.gov/sites/production/files/2015-07/documents/support_uic_co2_technologyandcostanalysis.pdf.
- Wiese, B.; Böhner, J.; Enachescu, C.; Würdemann, H. & Zimmermann, G. (2010), Hydraulic characterisation of the Stuttgart formation at the pilot test site for CO₂ storage, Ketzin, Germany, *International Journal of Greenhouse Gas Control* **4**, 960-971.
- Wiese, B.; Wagner, F.; Norden, B. & Schmidt-Hattenberger, C. (in short), Fully coupled hydrogeophysical inversion of hydraulics, gas pressure and geoelectric, *Energy Procedia*, GHGT Lausanne.